EFFECTIVE INTERACTION

EFFECTIVE INTERACTIONS DERIVED FROM REALISTIC FORCES IN NUCLEAR MATTER

By

PRASID KUMAR BANERJEE, B.Sc., M.Sc.

A Thesis

Submitted to the Faculty of Graduate Studies

in Partial Fulfilment of the Requirements

for the Degree

Doctor of Philosophy

McMaster University

October 1969

DOCTOR OF PHILOSOPHY (1969) McMASTER UNIVERSITY
(Physics) Hamilton, Ontario.

TITLE: Effective interactions derived from realistic forces in Nuclear Matter

AUTHOR: Prasid Kumar Banerjee
B.Sc. (Calcutta University)
M.Sc. (Calcutta University)

SUPERVISOR: Professor D. W. L. Sprung

NUMBER OF PAGES: xvi, 116

SCOPE AND CONTENTS:

Nuclear matter calculations have been performed using two modern phenomenological potentials. The results have been used to derive effective forces for finite nuclei, which are well behaved and can be used for Hartree-Fock calculations. A study of the density dependence of these forces has also been made. The forces have been defined in such a way as to reproduce the binding energy of nuclear matter.

ACKNOWLEDGEMENTS

The author is greatly indebted to his supervisor Dr. D. W. L. Sprung for initiating him into the problem and supervising throughout the entire period of this work. He also expresses his gratitude to Dr. R. K. Bhaduri for his encouragement and many valuable discussions. He thanks Dr. A. B. Volkov and Dr. Y. Nogami for their kind interest in this work. He thanks his friends Mr. P. C. Yip and Mr. M. K. Srivastava who helped him in various ways and cleared up many points of confusion. He is particularly thankful to Mr. A. M. Jopko for his help in fitting gaussians to the effective potentials. The financial support of the Physics Department in the form of a teaching assistantship is gratefully acknowledged. Finally, he thanks Miss C. Wivell for typing the thesis so patiently and efficiently.

TABLE OF CONTENTS

LIST OF SYMBOLS

A: the mass number of a nucleus, Chapter I.

A: the constant term in the quadratic expression for $E^R(k)$, Chapter II.

A: abbreviation for the expression $\sum_{\text{odd } L} \{(L+1)\ \alpha_L^{L+1} - (2L+1)\ \alpha_L^L + L\ \alpha_L^{L+1}\}$, Chapter III.

a: denotes a particle above the Fermi sea, Chapter II.

a: when put inside a ket vector 'a' means a plane wave with momentum k_a, Chapter II.

a: the spin independent part in the most general expression for the reaction matrix, Chapter III.

a_1: the coefficient in the volume energy term of the semi-empirical mass formula, Chapter I.

a_2: the coefficient in the surface energy term of the semi-empirical mass formula.

a_3: the coefficient in the Coulomb energy term in the semi-empirical mass formula.

a_4: the coefficient in the symmetry energy term of the semi-empirical mass formula.

a_i (i=1,5): the ranges of the Gaussians fitted to the effective potential, Chapters IV and V.

α: S-1/2ik, Chapter III.

α_L^J: the diagonal matrix element of α where the superscript gives the total angular momentum and the subscript the orbital angular momentum.

α^J: the off-diagonal matrix element of α with the superscript denoting the total angular momentum.

α^l: the off diagonal matrix element of α when the total angular momentum is l.

α_l: same as α^l, p. 63, last line.

b: denotes a particle above the Fermi sea, Chapter II.

b: when put inside a ket vector, 'b' means a plane wave of momentum k_b, Chapter II.

c: the radius of the hard core in the two-nucleon potential, Chapter II.

c: the symbol multiplied by $i(=\sqrt{-1})$ stands for the coefficient of the vector-like term $(\underset{\sim}{\sigma}^1+\underset{\sim}{\sigma}^2).\underset{\sim}{n}$ in the most general expression for the reaction matrix, Chapter III.

$c_i (i=1,5)$: the strengths of the Gaussians fitted to the effective potential.

χ: the radial part of the wave defect $\phi-\psi$.

$\chi_L(k_0,r)$: the radial part of the wave defect $\xi^R(r)$, Chapter II.

$\chi^J_{L'L}$: the radial part of the wave defect corresponding to an unperturbed wave of angular momentum L and a correlated wave function of angular momentum L'. J is the total angular momentum, Chapter II.

$\chi^S_{m_s}$: the spin wavefunction of total spin S and projection m_s.

D: an abbreviation for $\underset{\sim}{\sigma}^1.\underset{\sim}{r}\ \underset{\sim}{\sigma}^2.\underset{\sim}{r} + \underset{\sim}{\sigma}^1.\underset{\sim}{r}'\ \underset{\sim}{\sigma}^2.\underset{\sim}{r}'$, Chapter III.

d: the cut-off distance beyond which the potential is assumed to be zero.

Δ: a parameter which defines the energy gap between a particle of momentum $\sqrt{.6}\ k_F$ in the Fermi sea and a particle of the same momentum above the Fermi sea.

Δ': similar to Δ except that the momentum is zero in this case.

δ: the Dirac delta function, Chapter I, p. 9.

$\delta_{JJ''}$ $\delta_{L'L'''}$,

δ_{M+m_s',m_s}: Knoecker δ-symbol with $\delta_{rs}=0$ if $r \neq s$
$=1$ if $r = s$.

$\delta(r-r')$: the Dirac delta function, Chapter III.

E: generic name for the energy of a particle either above or below the Fermi sea, Chapter II.

E: abbreviation for $\underset{\sim}{\sigma}^1.\underset{\sim}{r}'\ \underset{\sim}{\sigma}^2.\underset{\sim}{r} + \underset{\sim}{\sigma}^1.\underset{\sim}{r}\ \underset{\sim}{\sigma}^2.\underset{\sim}{r}'$, Chapter III.

$E_\ell, E_{\ell''}, E_m, E_n$: the energy of a particle in state ℓ, ℓ'', m, n ..., Chapters I and II.

E(k): the energy of a particle of momentum k.

$E(k_a)$, $E(k_b)$: the energy of a particle in a state of momentum k_a, k_b.

$E^R(k)$: the reference spectrum approximation to E(k).

e: the energy denominator.

e: the exponential function, Chapter II, p. 21.

exp: the exponential function

e_{eff}: the effective energy denominator in Kuo and Brown's sense (Ref. 60).

e_N: the energy denominator using nuclear spectrum.

e^N: same as e_N.

e^R: the energy denominator in the reference approximation.

$\varepsilon(k')$: $(1-Q)e^R$, Chapter II, section B.

$\varepsilon(\rho)$: the energy density of nuclear matter, Chapter I.

F_L: the Bessel Fourier transform of the radial part of the wave defect χ_L, Chapter II, section A.

$F^J_{L'L}$: the Bessel Fourier transform of $\chi^J_{L'L}$, Chapter II, section A.

$\mathcal{J}^M_{ST}$: the Bessel Fourier transform of the wave defect with spin S, isospin T and projection M.

$\mathcal{J}_{av}$: the average of $\mathcal{J}^M_{ST}$ over sixteen spin and isospin state.

$F^{JS}_{LL'}(r)$: the radial part in the partial wave expansion of $(1-Q)v\,\psi_{Sm_s}(k_0,r)$.

fm: femtometer; 1×10^{-13} cm.

G: the reaction matrix in Brueckner theory.

G_s: the reaction matrix corresponding to the short range part of the two-nucleon potential.

G^F_s: G_s for the case of free scattering.

G^N_s: G_s for a system of bound nucleons.

G^N: the complete reaction matrix in the case of a system of bound nucleons.

G^R: the reaction matrix in the reference approximation.

$G^{JS}_{LL'}(k,k_0)$: the partial G matrix element for total angular momentum J and total spin S but off-diagonal in orbital angular momenta L,L' and also in momenta k,k_0.

G_{Sm_s}: the components of the G matrix in Sm_s representation G_{ss} for singlet, G_{11} for $S=1$ $m_s=1$ and so on.

g: this symbol in combination with h forms the coefficient of the tensor-like terms $\underset{\sim}{\sigma}^1 \cdot \underset{\sim}{X}\ \underset{\sim}{\sigma}^2 \cdot \underset{\sim}{X}$ and $\underset{\sim}{\sigma}^1 \cdot \underset{\sim}{x}\ \underset{\sim}{\sigma}^2 \cdot \underset{\sim}{x}$ in the most general expression for the reaction matrix, Chapter III.

g(r): abbreviation for $-\gamma^2 - m^* v_L(r) - L(L+1)/r^2$, Chapter II, p. 41.

g': that part of g which contains diagonal elements of α in the expression for g in terms of matrix elements of α, Chapter III.

g": that part of g which contains nondiagonal elements of α in the expression for g, Chapter III.

Γ_L: $-\frac{d}{dr} \log \mathcal{H}_L(r)$.

γ: defined by the relation $\gamma^2 = P^2 + m^*(2A - W)$. γ^2 is an effective energy, Chapter II.

$H_L^-(x)$: $i^{L+1}(ix)\ h_L^+(ix)$, Chapter II.

$\mathcal{H}_L(r)$: $\mathcal{J}_L(k_0 c)\ H_L^-(\gamma r)/H_L^-(\gamma c)$, Chapter II.

h: this symbol in combination with g forms the coefficient of the tensor-like terms $\underset{\sim}{\sigma}^1 \cdot \underset{\sim}{X}\ \underset{\sim}{\sigma}^2 \cdot \underset{\sim}{X}$ and $\underset{\sim}{\sigma}^1 \cdot \underset{\sim}{x}\ \underset{\sim}{\sigma}^2 \cdot \underset{\sim}{x}$ in the most general expression for the reaction matrix, Chapter III.

h': that part of h which contains only the diagonal elements of α in the expression for h, Chapter III.

h": that part of h which contains only the nondiagonal elements of α in the expression for h, Chapter III.

$h(r)$: $-m^* v_L(r) \mathcal{J}_L(k_0 r)$, Chapter II.

$h_L^+(x)$: the out going spherical Hankel function, Chapter II.

i: $\sqrt{-1}$.

J, J': total angular momentum quantum number.

$\mathcal{J}_L(x)$: the Ricatti spherical Bessel function of order L and argument x. $\mathcal{J}_L(x) = x\, j_L(x)$

$j_L(x)$: the spherical Bessel function of order L and argument x.

J_Z: the z component of the total angular momentum.

j_0: the spherical Bessel function of order zero. The argument has been suppressed, Chapter III.

j_2: the spherical Bessel function of order 2. The argument has been suppressed, Chapter III.

K: the centre of mass momentum, Chapter II.

k: the relative momentum of the scattering particles, Chapter III.

k: the momentum of a particle

k_a, k_b..: the momenta of particles in states a, b..

k_F: the Fermi momentum.

k_0: the relative momentum of a pair below the Fermi sea, Chapter II.

k': the relative momentum of a pair above the Fermi sea, Chapter II.

$\hat{k}_0$: unit vector in the direction of k_0.

κ: density x wound integral (wound integral = $\int \chi^2(r) d^3r$).

L: the orbital angular momentum quantum number.

L',L",L''': the orbital angular momentum quantum numbers, Chapter II.

ℓ: denotes a particle below Fermi sea, Chapter II.

M: the projection of the total spin S.

m: denotes a particle below the Fermi sea, Chapter II.

m: the coefficient of the tensor-like term $\underset{\sim}{\sigma}^1.\underset{\sim}{n}\ \underset{\sim}{\sigma}^2.\underset{\sim}{n}$ in the most general expression for the reaction matrix, Chapter III.

m': that part of m which contains only diagonal terms of α in the expression for m.

m": that part of m which contains only diagonal terms of α in the expression for m nondiagonal.

m^*: the effective mass, Chapter II.

m_h^*: the effective mass for hole states, Chapter II.

m_s: the projection of the spin S.

μ: cos θ; θ is the scattering angle.

N: the neutron number of the nucleus, Chapter I.

N: normalization constant, Chapter II.

n: denotes a particle below the Fermi sea, Chapter II.

$\underset{\sim}{n}$: denotes a unit vector perpendicular to the scattering plane, Chapter III.

Ω: volume of the box in which the normalization is carried out.

$\omega(k_0)$: normalized probability of occurrence of a pair of particles with relative momentum k_0 in the Fermi sea.

ω: frequency such that $\hbar\omega$ = oscillator strength, p. 80.

ω: auxiliary function in the Ridley method, Chapter II.

P: the average momentum of a pair of particles, Chapter II.

P_{av}: the average value of P for a given value of the relative momentum k_0.

P': 1 - Q; Q is the Pauli operator.

$P_L(\mu)$: the Legendre Polynomial of order L and argument μ.

$P'_L(\mu)$: the derivative of $P_L(\mu)$.

$P_L^M(\mu)$: the associated Legendre Polynomial of order L and projection M and argument μ.

Φ: the uncorrelated wavefunction.

ϕ: that part of Φ which describes the relative motion.

ϕ_{ST}^M: the uncorrelated wavefunction with total spin S, total isospin T and projection M.

ϕ: the azimuthal angle, Chapter III.

π^t: the projector which choose only the triplet state.

Ψ: the correlated wavefunction.

Ψ_N: the true nuclear correlated wavefunction.

Ψ^R: Ψ in the reference approximation.

$\psi(r)$: that part of Ψ which describes the relative motion.

$\psi^R(r)$: that part of Ψ^R which describes the relative motion.

ψ_{Sm_s}: the correlated wavefunction with spin S and spin projection m_s.

Q: the Pauli operator.

Q_{12}: the quadratic spin orbit operator.

$\underset{\sim}{R}$: the coordinate of the centre of mass.

r: the relative coordinate of a pair of particles.

$\hat{\underset{\sim}{r}}$: unit vector in the direction of $\underset{\sim}{r}$, Chapter II.

$\hat{\underset{\sim}{r}}$: unit vector in the incoming direction in the scattering plane, Chapter III.

$\hat{\underset{\sim}{r}}'$: unit vector in the outgoing direction in the scattering plane, Chapter III.

ρ: the density, Chapter I.

S: the total spin, Chapter II.

S: the scattering matrix, Chapter III.

S_{12}: the tensor operator.

s: the auxiliary function in the Ridley method, Chapter II.

σ^1: spin of particle 1.

σ^2: spin of particle 2.

T: total isospin.

T_3: the third component or projection of T.

θ: the scattering angle, Chapter III.

$\theta_{rr'}$: angle between $\underset{\sim}{r}$ and $\underset{\sim}{r}'$, Chapter III.

U: general name for potential energy, Chapter V.

$\bar{U}$: average potential energy, Chapter II.

$U(k)$: the potential energy of a particle with momentum k.

$U(b)$: the potential energy of a particle in the intermediate state above the Fermi sea, Chapter II.

$U^{JS}_{LL'}$: the radial part of the correlated wavefunction for the case with total angular momentum J, total spin S. L' indicated that the unperturbed was of angular momentum L' and L is the orbital angular momentum of the correlated wave.

$U(k_0,r)$: the correlated wavefunction for relative momentum k_0 and the relative separation r, Chapter III.

$U_L(k_0,r)$: the Lth partial wave of the correlated wavefunction. k_0 = relative momentum, r = relative separation.

$U_{00}, U_{20}, U_{02}, U_{22}$: same as $U^{JS}_{LL'}$, with J=1, S=1 (the deuteron state).

$U^J_{LL''}$: same as $U^{JS}_{LL'}$. S has been suppressed, Chapter III.

$u_L(k_0,r)$: the radial part of the correlated wavefunction in the reference approximation, Chapter II.

u_L: same as $u_L(k_0,r)$, the arguments have been suppressed.

u: abbreviation for $\sqrt{(L+1)\ (L+2)}\ \alpha^{L+1} + \sqrt{L(L-1)}\ \alpha^{L-1}$, Chapter III.

V: the two-nucleon potential, Chapter III.

V: abbreviation for $\sqrt{(L+2)\,(L+1)}\ \alpha^{L+1} - \sqrt{(L-1)/L}\ \alpha^{L-1}$, Chapter III, p. 54.

$V_c(r)$: the central part of the potential, Chapter III.

V_{LS}: the strength of the spin-orbit part of the potential.

V_L: the two-nucleon potential in the angular momentum state L.

V_T: the strength of the tensor part of the potential.

$V_{00}, V_{02}, V_{20}, V_{22}$: the matrix elements of the potential for total angular momentum 1, the subscripts give the two orbital angular momenta involved.

$V^J_{LL'}$: general term for the matrix element of the potential for total angular momentum J. L and L' are the orbital angular momenta involved.

$V(k_F)$: the effective potential as a function of k_F, Chapter IV.

V_0: the same as above at $k_F = 1.36$ fm^{-1}, Chapter IV.

V_{TL}: the strength of the tensor force, Chapters IV and V.

v: the two-nucleon potential, Chapters I, II and III.

v_s: the short-range part of the nucleon-nucleon potential in Moszkowski-Scott separation method.

v_ℓ: the long-range part of the nucleon-nucleon potential in Moszkowski-Scott separation method.

V^{eff}: the effective potential.

$V^{eff}_{00}, V^{eff}_{20}, V^{eff}_{02}, V^{eff}_{22}$: the matrix elements of the effective potential for the total angular momentum J=1, the subscripts denote the orbital angular momenta involved.

W: the starting energy.

$\underset{\sim}{X}$: unit vector in the direction of $\hat{\underset{\sim}{r}} + \hat{\underset{\sim}{r}}'$, Chapter III.

$\underset{\sim}{x}$: unit vector in the direction of $\hat{\underset{\sim}{r}} - \hat{\underset{\sim}{r}}'$, Chapter III.

x: k_0/k_F, Chapter II.

ξ: wave defect

ξ^R: that part of the reference wave defect which describes the relative motion.

Y_{LM}: the associated Legendre Polynomial of order L and projection M.

$\mathcal{Y}^{m_s}_{JLS}$: the eigenfunction for the total angular momentum, the orbital angular momentum and total spin operators, also the total projection $J_Z = m_s$ (the spin projection).

Z: the proton number, Chapter I.

Z^R: the wave defect $\Phi - \Psi^R$, Chapter II.

CHAPTER I

INTRODUCTION

The concept of a potential has been very successful in explaining the behaviour and interaction of two charged particles and also in the field of gravitation. This idea was, therefore, carried forth to explain the interaction between two nucleons when the interactions were specifically of nuclear origin (i.e. not of the electric or gravitational type or for that matter, not the so-called "weak" interaction). It seemed doubtful whether this idea would work in the high energy region where the nucleons are moving with relativistic velocities, but at low energies the concept may be quite valid. The experimental basis on which one constructs such a potential is the two-body scattering data. In a typical experiment one shoots a proton beam at a target containing neutrons or protons and looks for the deviation of the projectile. These data could then be used to extract phase shifts, which in turn can be fitted by a potential. The two-nucleon potential turns out to be pretty complicated and there could be more than one potential which would fit the known data. To make things worse it was found that the phase shifts from the state $^1S_0$ changed sign around 250 MeV. It was shown by Jastrow[1] that to make the $^1S_0$ phase shift

change sign one needs strong short-range repulsion e.g. a hard core.

It is known that to calculate nuclear structure or various other nuclear properties one ideally should solve the N-body Schrödinger equation with a potential acting between the various pairs of nucleons. This is mathematically unmanageable and also, this procedure does not give too much physical insight. On the other hand, one might use a well known procedure. One assumes that the various pairs of nucleons in a nucleus interact amongst themselves in such a way that the interactions average out to form a one-body potential. This one-body potential resembles a harmonic oscillator potential at short distances. However, it is clear that some "residual" interaction will also be left. One generally considers this residual interaction only between the "valence" particles. This procedure can give a good description of the nucleus and is, in fact, the shell model of the nucleus. The residual interaction that one uses is, however, a well behaved potential and generally one constructs these in such a way that a good fit to energy levels and other experimental data can be obtained.

At the basis of the shell model is the Hartree-Fock method of nuclear structure calculations. This method is well known and is given in many places[2]. In this method the particles move in a "self consistent" field generated

by the interaction of other neighbouring particles on it. Here also one must use a two-body force through which the particles would interact. But we have seen that the scattering data seem to indicate infinite repulsion at short distances. In the shell model and so also in the Hartree-Fock method the particles move independently of each other except for the fact that they have to obey the Pauli principle. This means that at times one nucleon may find itself at a very close distance from another. This sort of uncorrelated motion would make the matrix elements involved in the calculation become infinite if one uses two-body interactions with hard core. Thus, it must be recognized that at short distances the motion of the nucleons becomes highly correlated. This was first done by K. A. Brueckner and his coworkers[3]. They started with a perturbation-theoretical approach and showed that if a certain class of diagrams corresponding to the various terms in the perturbation series could be summed to all orders then this would incorporate short-range correlations. One would then be able to handle even singular potentials. If one uses the technique of Feynmann diagrams then in this summation one encounters the so-called "unlinked" diagrams in addition to the linked ones. There appears a convergence problem in the theory if one has to consider these unlinked diagrams. Brueckner showed by explicit evaluation to fourth and sixth order that these diagrams need not be considered. He could

not, however, generalise the result. This was done by Goldstone[4] who used the technique of second quantization and showed that only the linked diagrams need be considered. The details of the Brueckner theory has been given in several places[5] and we do not wish to repeat it here. Essentially, this method is similar to the Hartree-Fock method but the strong short-range forces are taken care of by allowing the two interacting particles to scatter any number of times before they finally return to the sea of occupied levels. The resulting effective interaction is a sum of matrix elements of the interaction potential v which alternate in sign. This resultant effective interaction is called the G matrix and its matrix elements between states of two particles of initial momentum ℓm and final momentum $\ell' m'$ are written as

$$\langle \ell' m' | G | \ell m - m \ell \rangle$$

$$= \langle \ell' m' | v | \ell m - m \ell \rangle$$

$$- \frac{1}{2} \sum_{\ell'' m''}{}' \langle \ell' m' | v | \ell'' m'' - m'' \ell'' \rangle \frac{1}{E_{\ell''} + E_{m''} - E_{\ell} - E_{m}}$$

$$\langle \ell'' m'' | G | \ell m - m \ell \rangle \qquad \text{(I-1)}$$

where the prime on the summation indicates that $|\ell'' m''\rangle$ must be some unoccupied intermediate state so as to satisfy the Pauli principle. More formally,

$$G = v - v \frac{Q}{e} G \qquad \text{(I-2)}$$

where Q is the Pauli operator which forbids scattering into states which are occupied. The structure of the G matrix is similar to that of the t or K matrix in the theory of scattering of two free particles. It differs only through the presence of the operator Q and also the fact that the energy denominator contains the binding effects of the nuclear medium.

The G matrix is very hard to calculate in the case of a finite nucleus because the system is finite and has surface effects. In other words one has to keep track not only of the relative coordinate r of the interacting pair but also of their centre of mass coordinate R. Furthermore the operator Q will be very complicated in this case. So the earlier attempts were devoted to a hypothetical system called nuclear matter. This system is infinite in extension and contains an equal number of neutrons and protons. All states up to a certain momentum k_F called the Fermi momentum are filled up. Moreover the Coulomb interaction between protons is neglected. Such a system will have a binding energy per particle equal to the first term in the semi-empirical mass formula[6] which may be written as follows

$$B.E. = - a_1 A + a_2 A^{2/3} + a_3 Z^2 A^{-1/3} + \frac{1}{4} a_4 (N-Z)^2/A + ... \quad .(I-3)$$

Also the system should saturate and the saturation density should correspond to the central density of a heavy nucleus.

Nuclear matter has a great advantage that as the system is translationally invariant the wavefunctions are plane waves and the Hartree-Fock self consistency problem is simple. The first numerical calculation of the binding energy of nuclear matter was done by Brueckner and Gammel[7] who directly solved the integral equation. This procedure was capable of great accuracy but complicated to carry out in practice. So there was a search for simpler methods. An important step in this direction was made by Moszkowski and Scott[8] who showed that the theory is greatly simplified if the nucleon-nucleon interaction is separated into a short-range part v_s and a long-range part v_ℓ. They set up a criterion for this separation and showed that the short-range part could then be represented by a reaction matrix G_s. This reaction matrix G_s is not very different for nuclear matter from that for free nucleons. The long-range part v_ℓ could be treated by Born approximation in nuclear matter but this is not possible for free nucleons and a very different result is obtained. The criterion for separation mentioned above was that the short-range reaction matrix G_s^F for free nucleons should vanish so that one has to treat v_ℓ in the Born approximation and also to calculate the difference $G_s^N - G_s^F$. Moszkowski and Scott showed how to do this but further studies by Köhler[9] showed that their method of calculation for $G_s^N - G_s^F$ might not be sufficiently accurate. In 1963, Bethe, Brandow and Petschek[10] came up with the

idea of reference spectrum method which provided a simple but quite accurate approximation to G^N. This approximate G, generally written as G^R could be improved to the desired degree of accuracy by adding correction terms which are easy to calculate.

The application of Brueckner theory to finite nuclei was first made by Brueckner, Gammel and Weitzner[11]. They observed that the theory gets highly complicated when one directly uses it for finite nuclei. In a Hartree-Fock calculation as one goes from one iteration to another, one is faced with the self consistency problem because the wavefunctions used in producing the non-local H-F potential should be the same as one obtains after the calculation. In other words, when the self consistency is achieved one gets back the same wavefunction as one starts with. In nuclear matter, this problem is trivial because one knows before hand that these are plane waves. In finite nuclei, however, as one goes from one iteration $\phi_n \rightarrow \phi_{n+1}$ the energy denominator in (I-2) gets changed. This is the double self consistency problem encountered in finite nuclei.

Brueckner, Gammel and Weitzner circumvented this difficulty by an approximation. They found that the short-range correlation structures contained in G involve distances of the order of 1 fm and made a prescription that if the density density does not vary appreciably over this distance one can take the G matrix from nuclear matter at that density

and treat this as the effective interaction for doing Hartree-Fock calculations.

Another approach is to start directly from the oscillator basis and to do Brueckner theoretic calculations with them. This was done by Kohler and McCarthy[12] and also somewhat differently by Becker, MacKeller and Morris[13]. One is thus left with two choices. Either one should derive some effective interactions from a fundamental basis and use them in Hartree-Fock calculations or use the Brueckner theory in its full glory following the footsteps of Kohler and McCarthy.

Side by side with the Brueckner Hartree-Fock theory other simple theories of the Thomas Fermi type have been developed on similar ideas. Berg and Wilets[14] developed a phenomenological theory which used some fundamental ideas of nuclear matter theory. They defined an energy density of nuclear matter $\varepsilon(\rho)$ which is a function of the density ρ. This function contained an attractive and a repulsive part in addition to the kinetic energy. Each of these functions were represented by suitable powers of density. These were multiplied by some coefficients which were chosen to give the correct binding and equilibrium density. In addition to these a term was introduced to allow the variation of the energy density as the nuclear density changed with position. Thus an idea of the "local energy density" was introduced. There were many other attempts made in this line by various

workers and mention may be made of the work by Hara[15] and of Kumar, LeCouteur and Roy[16]. Hara used nuclear matter theory extensively. He used a long-range attractive potential with a δ-function repulsion at the surface of the core. This repulsion was dependent on the density as $\rho^{1/3}$ while the attractive part was independent of density. He fixed parameters to give correct binding energy and density for nuclear matter. He determined the surface thickness by a variational calculation and obtained a value which was 10 - 20% too large. He obtained the surface energy to be about 23 - 28 MeV compared to the empirical value of 18 MeV. Kumar et al. used an expression for energy density similar to that of Berg and Wilets but attempted to connect the parameters with the work of Brueckner, Gammel and Weitzner. But they found that the attractive force used in the work of Brueckner's group did not have enough density dependence and they fixed their own parameters. They found good agreement with experimental data. Recently, Bethe[17] worked on the Thomas Fermi theory and made maximum use of the information obtained from nuclear matter calculations. He found that the local density approximation would be good even at the nuclear surface with certain corrections.

Thus the current practice is to make extensive use of nuclear matter results in calculating the properties of finite nuclei. It will, therefore, not be out of place to give a brief review of the present status of nuclear matter

calculations. After the first calculation by Brueckner and Gammel numerical calculations were made by Brueckner and Masterson[18] and by Razavy[19]. Brueckner and Masterson used the integral equation method and used the Yale potential[20]. Razavy, on the other hand, used the reference spectrum method and used the Hamada-Johnston potential[21]. Both of these calculations yielded a value of about 8 MeV per particle for binding energy of nuclear matter which is half the empirical value of about 16 MeV. Their saturation density was also too low compared to observed data. Further Brown, Schappert and Wong[22] pointed out corrections to these calculations which reduced the binding energy further. At this stage it was pointed out by Rajaraman[23] that the Brueckner-Goldstone series does not converge order by order and that a rearrangement in terms of the number of hole-lines was necessary. It was Bethe[24] who succeeded in summing three-body cluster diagrams to all orders in the interaction and when the calculations were done by Bhargava and Sprung[25] a further gain of about 5 MeV in binding was obtained. This treatment of three-body energy and also that in the work of Kirson[26] were not correct. It was later found by Bethe[27] that the three-body clusters had a rather small contribution to the binding energy so that one could put the potential energy of the intermediate states equal to zero and later add the three-body contribution to that from the two-body clusters. This method was advocated by

Brown and used by Azziz[28] but Azziz did not include the p states in his calculations. A calculation using this prescription of putting only kinetic energy in the intermediate state was performed by Dahlblom[29] and by Sprung and Banerjee[30]. The reference spectrum method was used in these calculations. The authors used both the Reid soft core and hard core potentials[31] which are given state by state. For higher partial waves ($J > 2$) they used OPEP. It was found that some amount of attraction could be obtained from some of the higher partial waves whereas OPEP gave repulsion. So an improvement on this point was necessary. Finally Kallio and Day[32] put forward a method of solving the Bethe-Goldstone equation directly and calculated the binding energy for Reid soft core and Reid hard core potentials. But they worked only at normal density and used OPEP for states with angular momentum $J > 2$. Their results were very nearly self consistent and provided a good check on the reference spectrum results of Sprung and Banerjee. These results confirmed the convergence of the reference spectrum method. Kallio and Day used an angle averaged Pauli operator and used only the kinetic energy in the intermediate states. The angle averaged Pauli operator is a good approximation for the operator Q as observed by Brown, Schappert and Wong and also investigated by Köhler[33]. Köhler finds that the angle average approximation is quite accurate and uses the matrix inversion method in his cal-

culations. He also finds that the averaging of the centre of mass momentum used in the Pauli operator is also quite accurate and may give only an error of .1 MeV in binding.

The motivation for the present work was that although a lot of information obtained from nuclear matter calculations is being used particularly in Thomas Fermi theory, an effective interaction derived from such calculations has not been extensively used in Hartree-Fock calculations. The aim is therefore to give a clear prescription of constructing such effective interaction and to actually construct one from the most accurate nuclear matter calculations. As there are still no nuclear matter results available using the exact methods like those of Kallio and Day for modern phenomenological potentials like Reid's over a range of densities and also resolving some of the ambiguities of the higher partial wave contributions there is a need for one more calculation incorporating all these. Such a calculation will also enable one to know the binding energy of nuclear matter as exactly as possible under the present state of the theory. In Chapter II we have described the formalism and results of our nuclear matter calculations for the Reid soft core potential and for the potential of Bressel, Kerman and Rouben[34]. In Chapter III, the idea of a density dependent effective interaction has been introduced and a clear prescription of obtaining these has been given. In Chapter IV we have discussed the results obtained from

these calculations and a simple study of the density dependence has been made. In Chapter V we have been led to the conclusion that the tensor force is the main mechanism of density dependence in these effective forces. While dealing with the remnant tensor force a qualitative agreement with the Kuo-Brown prescription of using effective energy denominators has also been found.

CHAPTER II

NUCLEAR MATTER CALCULATIONS

The main objective of a nuclear matter calculation is to obtain the reaction matrix defined by the equation

$$G = v - v\frac{Q}{e_N} G \qquad \text{(II-1)}$$

where v is the potential, Q is the Pauli operator and e_N is the energy denominator which is chosen with a negative sign so as to make it positive-definite. Equivalently, one can interest oneself in calculating the correlated wavefunction Ψ_N. An equation for Ψ_N can be developed by noting that

$$G\Phi = v\,\Psi_N \qquad \text{(II-2)}$$

where Φ denotes an uncorrelated wavefunction which, in the nuclear matter case, is a plane wave.

Using (II-1) and (II-2) one obtains

$$\Psi_N = \Phi - \frac{Q}{e_N} v\,\Psi_N \qquad \text{(II-3)}$$

This is the Bethe-Goldstone equation. Once Ψ is known it can be used in various calculations. We have calculated the reaction matrix G by two standard methods - the reference spectrum method and the integro-differential method of Kallio and Day. In principle the latter method is the same as that

of Brueckner and as such is of greater accuracy. It also gives the true correlated nuclear wavefunction $\psi_N(r)$ which we used in finding the effective interactions. These methods will now be described.

A. REFERENCE SPECTRUM METHOD:

This method was developed in 1963 by Bethe, Brandow and Petschek. The original paper and its authors are often quoted in literature as BBP and we shall also use this. The motivation for this method[35,36] was simple. Although the method of Brueckner and Gammel was, in principle, capable of very great accuracy it did not give much physical insight. It also did not provide any simple approximation where the full accuracy of the method was not required. The reference spectrum method gives a first approximation which is very easy to compute and quite accurate and also can be improved upon to any desired degree of accuracy. Because of this advantage it permits a quantitative study of higher order diagrams[37] so that the convergence of the Brueckner-Goldstone series could be investigated.

We go back to equation (II-3). In terms of the coordinates of the interacting pair of particles it can be written as

$$\Psi(\underset{\sim}{r}_1,\underset{\sim}{r}_2) = \Phi(\underset{\sim}{r}_1,\underset{\sim}{r}_2) - \frac{Q}{e}\, v\, \Psi(\underset{\sim}{r}_1,\underset{\sim}{r}_2) \qquad \text{.(II-a-1)}$$

The basic idea in the reference spectrum method is to replace

the operator $\frac{Q}{e}$ by a simpler one because it is the operator $\frac{Q}{e}$ which presents the main difficulty in calculating $\psi(r)$ - the relative part of the wavefunction Ψ_N. The operator e has the property

$$e|ab\rangle = [E(k_a) + E(k_b) - W] \ |ab\rangle$$

where $|ab\rangle$ is the product of two plane waves. W is called the starting energy and represents the energy $E_m + E_n$ of two interacting particles inside the Fermi sea. a, b represent two particles above the Fermi sea. W is introduced as a parameter so that for a fixed W the G matrix is hermitian[38]. The main approximations in the reference spectrum method are (i) to approximate the energy denominator e by a quadratic function of momentum k and (ii) to replace Q by 1. One can now examine the implications of these approximations. If E(k) is replaced by $E^R(k)$ such that

$$E^R(k) = \frac{k^2}{2m^*} + A \qquad \text{(II-a-2)}$$

where A is a constant and also m is a constant called the effective mass, then the energy denominator e will be approximately

$$e^R = -\frac{1}{2m^*}(\nabla_1^2 + \nabla_2^2) + 2A - W \qquad \text{(II-a-3)}$$

This expression for e along with Q=1 allows one to write a differential equation for Ψ instead of an integral equation. The solution of an integral equation is definitely much more

difficult than this differential equation. Now whether this approximation for E(k) is a good one or not depends on our choice of the potential energy U(k). The choice of U(k) is, however, at our disposal and it should be chosen in such a way as to make the convergence of Brueckner-Goldstone expansion as rapid as possible. At the time the Sprung-Bhargava[25] calculations were being done it was shown by Bethe[24] that a good choice of U(k) should cancel all the three-body cluster diagrams. The procedure was reasonable because it was shown by Rajaraman[23] that the Brueckner-Goldstone expansion does not converge order by order. (This was first pointed out by Hugenholtz[39].) Good convergence can be obtained by summing diagrams with the same number of hole lines, or in other words different many body clusters. So the idea was to sum all two-body diagrams, then all three-body diagrams and so on. An estimate of these showed that as the number of whole lines increased i.e., the number of particles in a particular type of cluster increased the contribution of that sum to the binding energy fell off rapidly. Bethe solved the three-body equations following the work of Faddeev[40]. Improved solutions to the Bethe-Faddeev equations were given by Day[41]. Following his solution of the three-body equations Bethe gave a prescription for calculating U(k). It was seen that with a quadratic approximation the reference spectrum could be fitted well with U(k) obtained by the above method over a restricted momentum

range of about 2.5 fm^{-1} to 5 fm^{-1}. Of course, when the BBP paper came out these ideas were not known but arguments were put forward which showed why in some high momentum region the quadratic approximation should be good. It was also argued by BBP that due to the presence of the hard core in the nucleon-nucleon interaction the states of typical momenta to which two nucleons in nuclear matter would scatter were also in the above region. Another very important fact that should be noted is that the energy spectrum of states in the Fermi sea is completely irrelevant to the purpose of computing the G matrix, once the choice for the starting energy W is made. The reason for this fact will be found from the equation for the correlated wavefunction. The presence of the operator Q allows the operator $\frac{Q}{e}$ to act only on states outside the Fermi sea. Thus, for a given value of W the behaviour of $\frac{Q}{e}$ depends only on $E(k_b)$ such that $k_b > k_F$. Brueckner's work showed that the energy of the states within the Fermi sea could be represented by a quadratic function. As a matter of fact, W should then be calculated from the actual nuclear spectrum. For a given pair of particles W is then just a number and should not be approximated in any way. In our calculations we put in a quadratic function determined by two parameters Δ and m*. Of course, the self consistency question will naturally arise and we will describe that later.

We now look into the question why putting Q=1 will

not be a very bad approximation. The number of states into which the operator Q will forbid scattering, is a small fraction of the total number of states of importance in calculating the correlated wavefunction Ψ. In other words, Q prohibits scattering into states of momentum up to $k = k_F$ (~ 1.36 fm^{-1}) whereas states up to 5 fm^{-1} play an important role in determining ψ. Thus, the important region of phase space is about 40 times bigger than the Fermi sphere which is affected by Q.

Secondly, if one applies the operator $\frac{1}{e^R}$ to states forbidden by Q, one generally gets a small result. The reference energy denominator e^R gives the difference between the reference energy of the forbidden state and the actual energy of the initial state. Typically this comes to about 100 MeV giving a small result. Even in the worst case of $k = k_F$ this is of the order of 50 MeV. Thus, $\frac{1}{e^R}$ is always reasonably small and has the remarkable property of having no singularity. It is well known that the correlated wave-function in nuclear matter heals whereas in a free scattering there is a non-zero phase shift. The reason for this may be traced to the absence of any singularity in the operator $\frac{Q}{e}$. As there is no singularity in the operator $\frac{1}{e^R}$ the healing property is retained. Counting all these advantages of the reference approximation, we now see why G^R should be a good first order approximation to G. We can write an equation

for G^R as

$$G^R = v - v\frac{1}{e^R} G^R \qquad .(II\text{-}a\text{-}4)$$

Once G^R has been calculated, it can be improved upon by solving the exact equation

$$G = G^R + G^R[\frac{1}{e^R} - \frac{Q}{e}]G \qquad .(II\text{-}a\text{-}5)$$

This is a special case of an equation given in Appendix A of BBP. Note that G^R is a first approximation in a systematic expansion of G. This expansion is very useful because G^R is simple and accurate.

From (II-a-4) we can write

$$\Psi^R = \Phi - \frac{1}{e^R} v\Psi^R \qquad .(II\text{-}a\text{-}6)$$

If we write $Z^R = \Phi - \Psi^R$, then

$$e^R Z^R = v\Psi^R \qquad .(II\text{-}a\text{-}7)$$

At this point it is useful to make the separation of the centre-of-mass part and the relative part of the two-body wavefunction. So we write

$$\left.\begin{matrix}\Phi \\ \Psi^R \\ Z^R\end{matrix}\right\} = \Omega^{-1} \exp(i2\underset{\sim}{P}.\underset{\sim}{R}) \left\{\begin{matrix}\phi\ (\underset{\sim}{r}) \\ \psi^R(\underset{\sim}{r}) \\ \xi^R(\underset{\sim}{r})\end{matrix}\right\} \qquad (II\text{-}a\text{-}8)$$

where Ω is the volume. BBP in their paper used the symbol P as the average momentum so that the centre-of-mass momentum was 2P.

We have used the same convention as theirs.

In view of the quadratic dependence of e^R on the relative momentum k', in coordinate-space k'^2 can be written as $-\nabla^2$. So one introduces the abbreviation

$$\gamma^2 = p^2 + m^*(2A-W) \qquad .(II\text{-}a\text{-}9)$$

Then one at once obtains the differential equation

$$(\nabla^2-\gamma^2)\ \xi^R(\underset{\sim}{r}) = -\ m^*\ v\psi^R(\underset{\sim}{r}) \qquad .(II\text{-}a\text{-}10)$$

The last equation is known as the reference wave equation. The constant γ^2 turns out to be positive and, therefore, as $r\to\infty$ ξ^R falls off as $e^{-\gamma r}$. Thus healing of the wavefunction is ensured. ξ is called the wave defect because it gives the deviation of the correlated wavefunction from the plane wave. To proceed further, one has to make the usual partial-wave expansion so that equation (II-a-10) can be split into several uncoupled differential equations, each for a particular angular momentum. This is true for central, spin orbit and quadratic spin orbit forces only. Whenever a tensor force is present, one will have to solve a coupled differential equation corresponding to a fixed value of the total angular momentum J. We write

$$\left.\begin{matrix}\phi\ (\underset{\sim}{r})\\ \psi^R(\underset{\sim}{r})\\ \xi^R(\underset{\sim}{r})\end{matrix}\right\} = \sum_L i^L[4\pi(2L+1)]^{\frac{1}{2}}\ (k_0 r)^{-1} \qquad .(II\text{-}a\text{-}11)$$

$$\times\ Y_{L0}(\hat{k}_0,\hat{r})\begin{cases}\mathcal{A}_L(k_0,r)\\ u_L(k_0,r)\\ \chi_L(k_0,r)\end{cases}$$

Here we have introduced

$$\mathcal{J}_L(x) = x\, j_L(x) \qquad .$$

Using equation (II-a-11) we now get

$$\left[\frac{d^2}{dr^2} - \frac{L(L+1)}{r^2} - \gamma^2\right] \chi_L(r) = - m^* v u_L(r) \qquad .(II\text{-}a\text{-}12)$$

The modern phenomenological two-nucleon potentials are generally distinct for each partial wave. So one starts with equation (II-a-12) as the first step in any numerical work. If a hard core is present then the boundary condition for χ will be

$$\chi_L(r) = \mathcal{J}_L(k_0 r) \qquad \text{for } r<c$$

$$= 0 \qquad \text{as } r\to\infty \qquad .$$

The differential equation (II-a-12) will give the reference wave function which can be used to write G^R in terms of partial waves,

$$\langle k_0|G|k_0\rangle = 4\pi \sum_L (2L+1)\, \frac{1}{k_0^2} \int_0^\infty \mathcal{J}_L v u_L dr \qquad .(II\text{-}a\text{-}13)$$

If we are dealing with a potential with an infinite hard core then in the core region $v=\infty$ and $u=0$. So the product $vu=\infty \times 0$ is an indeterminate form. However, this can be made tractable by comparing the following three equations

$$\left\{\frac{d^2}{dr^2} - \frac{L(L+1)}{r^2} + k_0^2\right\} \mathcal{J}_L(k_0 r) = 0 \qquad (II\text{-}a\text{-}14)$$

$$\{\frac{d^2}{dr^2} - \frac{L(L+1)}{r^2} - \gamma^2\}\ \chi_L(k_0,r) = -\ m^*vu_L(k_0,r) \qquad \text{(II-a-12)}$$

$$\{\frac{d^2}{dr^2} - \frac{L(L+1)}{r^2} - \gamma^2\}\mathcal{H}_L = 0 \qquad \text{(II-a-15)}$$

$\mathcal{H}_L$ is the solution for the case of a pure hard core. The equation (II-a-15) is used only for values of r such that r>c where c = core radius of the potential. Multiplying (II-a-14) by χ_L and (II-a-12) by $\mathcal{J}_L$ we subtract one from the other to get

$$\frac{d}{dr}\ (\chi_L \frac{d\mathcal{J}_L}{dr} - \mathcal{J}_L \frac{d\chi_L}{dr}) + (\gamma^2+k_0^2)\ \mathcal{J}_L\chi_L = m^*\ \mathcal{J}_L vu_L \qquad \text{(II-a-16)}$$

This gives

$$\int_0^{c+} \mathcal{J}_L vu_L dr = \frac{\gamma^2+k_0^2}{m^*} \int_0^c \mathcal{J}_L^2\ dr + \frac{\mathcal{J}_L(c)}{m^*}\ (\frac{d\mathcal{J}_L}{dr} - \frac{d\chi_L}{dr})_{r=c+} \qquad \text{(II-a-17)}$$

From equations (II-a-12) and (II-a-15) $\left.\frac{d\chi_L}{dr}\right|_{r=c+}$ can be written as

$$\frac{\mathcal{J}_L(c)}{m^*}\ \left.\frac{d\chi_L}{dr}\right|_{c+} = \frac{\mathcal{J}_L(c)}{m^*}\ \left.\frac{d\mathcal{H}_L}{dr}\right|_{c+} + \int_{c+}^{\infty} \mathcal{H}_L vu_L dr \qquad \text{(II-a-18)}$$

Thus the reference G matrix can be written as

$$\langle k_0|G^R|k_0\rangle = \frac{4\pi}{k_0^2} \sum_L (2L+1)\ \{\frac{\gamma^2+k_0^2}{m^*} \int_0^c \mathcal{J}_L^2\ dr$$

$$+ \frac{\mathcal{J}_L(c)}{m^*}\ (\frac{d\mathcal{J}_L}{dr} - \frac{d\mathcal{H}_L}{dr})_{r=c} + \int_0^{\infty} (\mathcal{J}_L - \mathcal{H}_L) vu_L dr\} \qquad \text{(II-a-19)}$$

Comparing (II-a-12) and (II-a-15) it could also be written in the form

$$\langle k_0|G^R|k_0\rangle_L = \frac{4\pi(k_0^2+\gamma^2)}{m^* k_0^2}\left[\int_0^c \mathcal{J}_L^2(k_0 r)\,dr + \int_c^\infty \mathcal{J}_L(k_0 r)\;\chi_L^R(k_0,r)\,dr\right] \qquad \text{(II-a-20)}$$

$$\mathcal{H}_L(r) = \mathcal{J}_L(k_0 c)\; H_L^{(-)}(\gamma r)/H_L^{(-)}(\gamma c)$$

$$H_L^{(-)} = i^{L+1}(ix)\; h_L^{(+)}(ix)$$

$h_L^+(x)$ is the outgoing spherical Hankel function. The three terms in equation (II-a-19) are known as the core volume, the core surface and the outer contributions respectively. The reason for introducing this separation is to show that the complete effect of the outer potential can be isolated in the integral term. The form is not very convenient and is seldom used in an actual calculation.

To calculate the binding energy of nuclear matter one requires the diagonal G matrix averaged over sixteen spin and isospin states of the interacting pair. When proper statistical weights and exchange contributions are taken into account one writes

$$\frac{1}{16}\sum_{S,M,T,T_3} \langle\phi^M_{S,T}|G^R|\phi^M_{S,T}\rangle$$

$$= \frac{\pi}{2} \frac{(\gamma^2+k_0^2)}{m^*k_0^2} \Big[\sum_{\text{odd } L} (2L+1) \int_0^\infty \mathcal{J}_L(k_0r)\ \chi_L(k_0,r)\ (S=0,\ T=0)dr$$

$$+ 3 \sum_{\text{even } L} (2L+1) \int_0^\infty \mathcal{J}_L(k_0r)\ \chi_L(k_0,r)\ (S=0,\ T=1)dr$$

$$+ \sum_{\text{even } L} \sum_{J} (2J+1) \int_0^\infty \mathcal{J}_L(k_0r)\ \chi^J_{LL}(k_0,r)\ (S=1,\ T=0)dr$$

$$+ 3 \sum_{\text{odd } L} \sum_{J} (2J+1) \int_0^\infty \mathcal{J}_L(k_0r)\ \chi^J_{LL}(k_0,r)\ (S=1,\ T=1)dr\Big] \quad .(II\text{-}a\text{-}21)$$

At this point we should interest ourselves as to how one goes about determining γ^2. BBP estimated

$$\gamma^2 = 2\Delta k_F^2 - k_0^2 \qquad \text{(occupied initial state)} \quad .$$

The parameter Δ represents the gap in energy between an average interacting pair in the Fermi sea and a pair of the same relative momentum in the reference spectrum (figure 1). In all the previous equations m* represented the curvature of the particle spectrum in the reference spectrum. In his recent studies, Bethe[27] estimated the three-body energies and found them quite small. This has led to the conclusion that it is best to put U(b)=0 when calculating the two-body G matrix and add the three-body energy as a perturbation at the end of the calculation. The above prescription leads to tremendous simplification in calculations because e^R is now exact. So there will be no "spectral correction". In this case, however, the expression for γ will be a little

complicated. m* will now be 1 but we can still introduce a m_h^* for hole states where there will still be a quadratic dependence. Defining a Δ' as shown in figure 2, we can now write

$$e = E_a+E_b - E_m-E_n$$

$$= (k'^2+P^2) - \frac{1}{2m_h^*}(k_0^2+P^2) + 2\Delta' k_F^2$$

$$= k'^2+\gamma^2$$

So $$\gamma^2 = P^2(1 - \frac{1}{m_h^*}) + 2\Delta' k_F^2 - \frac{k_0^2}{m_h^*} \qquad \text{(II-a-22)}$$

$$\Delta' = \Delta + .3(1/m^*_h - 1)$$

It may be recalled that P is the average momentum and is half the centre-of-mass momentum. We made a further approximation by replacing P by its average value for a given k_0:

$$P_{av} = .6\, k_F^2(1-x)\ [1 + \frac{x^2}{3(2+x)}] \qquad \text{(II-a-23)}$$

where $$x = k_0/k_F$$.

We have now a definite prescription for calculating G^R. It may be seen that in calculating G^R we are really calculating the off-energy shell matrix elements of the free reaction matrix. In particular we are calculating the K-matrix of scattering theory with $-\gamma^2$ thus avoiding singularities and ensuring healing. So these G^R matrix elements can be calculated as a function of γ^2 and k_0. Later

these can be used by choosing a suitable γ at a particular density. The problem was attacked in this fashion by Köhler[33].

In our approach and also in that of Bhargava, a value for k_F and also one value for k_0 was chosen. These were then used to compute a value of γ and G^R was then calculated. But in Köhler's approach one calculates G^R as a function of γ at a small number of well spread out values. As the variation of G with γ is smooth one can get G at other γ values by interpolation. So all one needs to do is to choose a value for k_F and for k_0 to get the corresponding γ and interpolate in the table of G matrices. Obviously this saves much of computing time and is definitely an improvement. The reference G matrix must be corrected for Pauli principle and energy denominators. One recalls

$$G^N - G^R = G^{R^+}\left(\frac{1}{e^R} - \frac{Q}{e^N}\right)G^N$$

$$= G^{R^+}\left(\frac{1}{e^R} - \frac{Q}{e^N}\right)G^R + G^{R^+}\left(\frac{1}{e^R} - \frac{Q}{e^N}\right)G^{R^+}\left(\frac{1}{e^R} - \frac{Q}{e^N}\right)G^R$$

$$+ \ldots . \qquad \text{.(II-a-24)}$$

As mentioned before, in our calculation $e^R = e^N$ because the intermediate states are plane waves. We have only the Pauli correction given by

$$G^N - G^R = G^{R^+}\frac{1-Q}{e^R}G^R + \ldots . \qquad .$$

Except in the case of $^3S_1$-$^3D_1$ partial wave, the first term in the correction was considered to be sufficient. In the mentioned case, it was necessary to go to the second term. This was done by Bhargava and Sprung and they called it third order correction term

The matrix element of the second order correction term can be written as

$$\langle \phi^M_{ST} | G^{R^+} \frac{1-Q}{e^R} G^R | \phi^M_{ST} \rangle = \int_0^\infty \varepsilon(k') \mathcal{F}^M_{ST}(k') dk' \qquad \text{(II-a-25)}$$

where $$\varepsilon(k') = (1-Q)e^R \qquad \text{(II-a-26)}$$

The average value of $\mathcal{F}^M_{ST}$ over the spin and isospin states is

$$\mathcal{F}_{av} = \frac{1}{16} \sum_{S,M,T,T_3} \mathcal{F}^M_{ST}(k') = \left(\sum_{\text{odd } L} + 3 \sum_{\text{even } L} \right) (2L+1) F_L^2(k')$$

$$+ \left(\sum_{\text{even } LL'} + 3 \sum_{\text{odd } LL'} \right) \sum_J (2J+1) F^J_{L'L}(k')^2 \qquad \text{(II-a-27)}$$

$$F^J_{L'L}(k') = \frac{1}{k_0} \int_0^\infty \mathcal{J}_{L'}(k'r) \chi^J_{L'L}(k_0, r) dr \qquad \text{(II-a-28)}$$

As before, $\chi^J_{L'L}(k_0, r)$ is the wave function distortion in the coupled state of total angular momentum J, taking the solution with dominant orbital angular momentum L and looking at the L' component.

One might now ask oneself as how to handle the operator Q. This operator presents the main difficulty in the reaction matrix calculation. It was, however, observed

by Brown, Schappert and Wong[22] that an angle average approximation to Q is quite good. BBP, however, used Q as a step function which is true only when P=0. The angle-averaged Pauli operator is given as

$$Q(P,k') = 0 \qquad , \quad k' < (k_F^2 - P^2)^{\frac{1}{2}}$$

$$= (k'^2 + P^2 - k_F^2)/2k'P, \quad (k_F^2 - P^2)^{\frac{1}{2}} < k' < k_F + P$$

$$= 1 \qquad , \quad k' > k_F + P \qquad \text{.(II-a-29)}$$

The same prescription has been used by other authors.

To carry out the third order corrections one goes one step further. This has been discussed in detail by Bhargava and Sprung[25]. In this calculation the same procedure was adopted.

B. KALLIO-DAY METHOD:

This is a more exact method than the one just described. One great advantage of this method is that it gives the true correlated wavefunction ψ (rather than ψ^R) which we wish to use to get the effective interaction. The physical insight into the method was definitely provided by the reference spectrum method and by Bethe's treatment of three-body clusters[27]. Briefly speaking, the method is a direct solution of the Bethe-Goldstone equation under two approximations: (i) the Pauli operator is treated in the angle average approximation and (ii) the intermediate states have

zero potential energy which implies that the energy denominator e can be written as $e = k'^2+\gamma^2$. So one starts by writing the Bethe-Goldstone equation

$$\psi = \phi - \frac{Q}{e} v\psi \qquad .(II-b-1)$$

The unperturbed wave ϕ can be written as

$$\phi = \exp(i\underset{\sim}{k}_0 \cdot \underset{\sim}{r})\ \chi^S_{m_s} = \langle \underset{\sim}{r} | \underset{\sim}{k}_0\ S\ m_s \rangle \qquad .(II-b-2)$$

Here $\chi^S_{m_s}$ is the spin part of the wavefunction, S is the total spin of the two nucleons and m_s is the projection on the polar axis.

As mentioned, the assumption of zero potential energy in the intermediate states will mean

$$e = k'^2+\gamma^2$$

$$= \nabla^2-\gamma^2 \qquad (II-b-3)$$

where γ^2 will be given by (II-a-22).

Using (II-b-2), and (II-b-3) we get from (II-b-1)

$$(\nabla^2-\gamma^2-v)\psi = -(\gamma^2+k_0^2)\phi - (1-Q)v\psi \qquad .(II-b-4)$$

The procedure to solve this equation is by the method of iteration. In the first iteration $(1-Q)v\psi$ is neglected. The equation (II-b-4) then corresponds to the reference wave equation. But as the reference reaction matrix G^R gives a good approximation to G one can expect the iteration procedure to converge fairly well. In the second iteration, the wave-

function ψ obtained from the first iteration is used to calculate $(1-Q)v\psi$ and in the n^{th} iteration, results from the $(n-1)^{st}$ iteration are used. To proceed further one has to use the usual method of decomposition into partial waves

$$\left.\begin{matrix}\phi(\underset{\sim}{k}_0,\underset{\sim}{r})\\ \psi(\underset{\sim}{k}_0,\underset{\sim}{r})\end{matrix}\right\} = \sum_{JL} i^L\,[4\pi(2L+1)]^{\frac{1}{2}}\,\langle LSOm_s|Jm_s\rangle \times \begin{cases} j_L(k_0r)\,\mathcal{Y}^{m_s}_{JLS}(\hat{\underset{\sim}{k}}_0,\hat{\underset{\sim}{r}}) \\ \sum_{L'} r^{-1}\,U^{JS}_{LL'}(k_0,r)\,\mathcal{Y}^{m_s}_{JL'S}(\hat{\underset{\sim}{k}}_0,\hat{\underset{\sim}{r}}) \end{cases} \qquad .(II\text{-}b\text{-}5)$$

The curly $\mathcal{Y}$'s are eigenfunctions of J L S and $J_Z=m_s$ and have been obtained by coupling Y_{LO} to $\chi^{m_s}_S$. It can be seen from equation (II-b-5), whereas ϕ will have the quantum numbers $LSJJ_Z$, ψ will have the same JSJ_Z but different values of L because of the presence of the tensor force. Using the "language of nuclear reaction theory", the correlated wavefunction $U^{JS}_{LL'}$ in channel L' comes from an unperturbed wavefunction L. In order to treat the term $(1-Q)v\psi$ one needs a partial wave expansion for

$$\langle \underset{\sim}{k}Sm_s'|G|\underset{\sim}{k}_0Sm_s\rangle = \langle \exp(i\underset{\sim}{k}.\underset{\sim}{r})\chi^S_{m_s'}|v|\psi_{Sm_s}(\underset{\sim}{k}_0,\underset{\sim}{r})\rangle \qquad .(II\text{-}b\text{-}6)$$

It should be noted that although the total spin S is conserved the projection m_s is not. The polar axis chosen for defining m_s and m_s' is in the direction of $\hat{\underset{\sim}{k}}_0$. The symbol

$\wedge$ on a vector is used here and also elsewhere to denote a unit vector in that direction. Now in the expansion of $\exp(i\underset{\sim}{k}.\underset{\sim}{r})$ there will occur the function $Y_{LO}(\hat{\underset{\sim}{k}}_0, \hat{\underset{\sim}{r}})$. This has to be expressed as product of $Y^*_{LM}(\hat{\underset{\sim}{k}}, \hat{\underset{\sim}{k}}_0)$ and $Y_{LM}(\hat{\underset{\sim}{k}}_0, \hat{\underset{\sim}{r}})$ in order to carry out the integration over angles.

Using the addition theorem for spherical harmonics

$$\langle \exp(i\underset{\sim}{k}.\underset{\sim}{r}) | = \sum_{L'} i^{-L'} [4\pi(2L'+1)]^{\frac{1}{2}} Y_{L'O}(\hat{\underset{\sim}{k}}, \hat{\underset{\sim}{r}})\, j_{L'}(kr)$$

$$= 4\pi \sum_{L'} \sum_{M} i^{-L'} j_{L'}(kr)\, Y^*_{L'M}(\hat{\underset{\sim}{k}}_0, \hat{\underset{\sim}{r}})\, Y_{L'M}(\hat{\underset{\sim}{k}}, \hat{\underset{\sim}{k}}_0)$$

so that

$$\langle \exp(ik.r)\, \chi^S_{m_s'} | = 4\pi \sum_{L'} \sum_{M} i^{-L'} j_{L'}(kr)\, Y^*_{L'M}(\hat{\underset{\sim}{k}}_0, \hat{\underset{\sim}{r}})\, Y_{L'M}(\hat{\underset{\sim}{k}}, \hat{\underset{\sim}{k}}_0) \times \chi^S_{m_s'} \quad \text{.(II-b-7)}$$

Also

$$v|U^{JS}_{LL'}, \mathcal{Y}^{m_s}_{JL'S}\rangle = \sum_{L''} \langle JL''S|V(r)|JL'S\rangle\, |U^{JS}_{LL'}, \mathcal{Y}^{m_s}_{JL''S}\rangle \quad \text{.(II-b-8)}$$

L" can be different from L' only when a tensor force is present. So one gets

$$v|\psi_{Sm_s}(k_0, r)\rangle = \sum_{JLL''} i^L [4\pi(2L+1)]^{\frac{1}{2}} \langle LSOm_s|Jm_s\rangle \times r^{-1} \sum_{L'''} \langle JL'''S|V|JL''S\rangle\, |U^{JS}_{LL''}(k_0, r) \times \mathcal{Y}^{m_s}_{JL'''S}(\hat{\underset{\sim}{k}}_0, \hat{\underset{\sim}{r}}) \quad \text{.(II-b-9)}$$

We can rewrite equation (II-b-7) as

$$4\pi \sum_{L'} \sum_{M} \sum_{J'} i^{-L'} j_{L'}(kr) \langle L'SMm_s' | J'M+m_s' \rangle \mathcal{Y}^{M+m_s'*}_{J'L'S}(\hat{k}_0, \hat{r})$$

$$\times Y_{L'M}(\hat{k}, \hat{k}_0) \qquad \text{.(II-b-10)}$$

Using equations (II-b-10) and (II-b-9) we have

$$\langle kSm_s' | G | k_0 Sm_s \rangle$$

$$= \sum_{L'MJ'} i^{L-L'} \langle L'SMm_s' | J'M+m_s' \rangle Y_{L'M}(\hat{k}, \hat{k}_0)$$

$$\times \sum_{JLL''} [4\pi(2L+1)]^{\frac{1}{2}} \langle LSOm_s | Jm_s \rangle \sum_{L'''} \int \mathcal{Y}^{M+m_s'*}_{J'L'S} \mathcal{Y}^{m_s}_{JL'''S} \, d\Omega$$

$$\times \int \langle JL'''S | V(r) | JL''S \rangle \, 4\pi \, r j_{L'}(kr) \, U^{JS}_{LL''}(k_0, r) dr$$

$$= \sum_{L'MJ'} \sum_{JLL''} \sum_{L'''} i^{L-L'} \langle L'SMm_s' | J'M+m_s' \rangle Y_{L'M}(\hat{k}, \hat{k}_0)$$

$$\times [4\pi (2L+1)]^{\frac{1}{2}} \langle LSOm_s | Jm_s \rangle \delta_{JJ'} \delta_{L'L'''} \delta_{M+m_s', m_s}$$

$$\times 4\pi \int r j_{L'}(kr) \langle JL'''S | V(r) | JL''S \rangle U^{JS}_{LL''}(k_0, r) dr$$

$$= \sum_{JLL'} i^{L-L'} [4\pi (2L+1)]^{\frac{1}{2}} \langle L'Sm_s - m_s' m_s' | Jm_s \rangle$$

$$\times \langle LSOm_s | Jm_s \rangle Y_{L'm_s - m_s'}(\hat{k}', \hat{k}_0) \times G^{JS}_{LL'}(k, k_0) \qquad \text{(II-b-11)}$$

where

$$G^{JS}_{LL'}(k, k_0) = 4\pi \sum_{L''} \int_0^\infty r j_{L'}(kr) \langle JL'S | V(r) | JL''S \rangle U^{JS}_{LL''}(k_0, r) dr$$

$$\text{.(II-b-12)}$$

The operator (1-Q) may be abbreviated as P′ and its eigenvalues in the angle-average approximation may be written as follows:

$$P'(k,K) = 1 \quad \text{for } k < \sqrt{k_F^2 - \frac{1}{4}K^2}$$

$$= 0 \quad \text{for } k > k_F + \frac{K}{2} \qquad \text{.(II-b-13)}$$

$$= 1 - (k^2 + \frac{K^2}{4} - k_F^2)/kK \quad \text{otherwise}$$

Here K is the total momentum, and not the average momentum, and k is the relative momentum. We have worked in momentum space here because P′ is diagonal in that representation. The above values follow trivially from equation (II-a-29). We now see how to handle $(1-Q)v\psi_{Sm_s}(k_0,r)$. If we expand $v\psi$ in terms of the complete set of states $|kSm_s'>$ then we have

$$(1-Q)v\psi_{Sm_s}(\underset{\sim}{k}_0,\underset{\sim}{r}) = \sum_{m_s'} \int \frac{d^3k}{(2\pi)^3} e^{i\underset{\sim}{k}\cdot\underset{\sim}{r}} |\chi^S_{m_s'}> P'(k,K) \cdot$$

$$x <\chi^S_{m_s'} e^{i\underset{\sim}{k}\cdot\underset{\sim}{r}}|v|\psi_{Sm_s}(\underset{\sim}{k}_0,\underset{\sim}{r})> \qquad \text{.(II-b-14)}$$

We have now to use equations (II-b-6) and (II-b-11) in equation (II-b-14). If we then expand the remaining $e^{ik.r}$ (which is now a ket) in the fashion of equation (II-b-7) then integration over the angle $(\hat{\underset{\sim}{k}},\hat{\underset{\sim}{k}}_0)$ will eliminate the corresponding Y_{LM}'s leaving $Y_{L'm_s-m_s'}(\hat{\underset{\sim}{k}}_0,\hat{\underset{\sim}{r}})$. Also note that if L" is the symbol for angular momentum in the expansion of $e^{i\underset{\sim}{k}\cdot\underset{\sim}{r}}$, then the above integration will produce $\delta_{L'L"}\ \delta_{M,m_s-m_s'}$

which takes care of the sum over L" and M. Carrying out the algebra as used in obtaining equation (II-b-11) one finally obtains

$$(1-Q)v\psi_{Sm_s}(\underset{\sim}{k}_0,\underset{\sim}{r}) = \sum_{JLL'} i^L [4\pi (2L+1)]^{\frac{1}{2}} \langle LSOm_s|Jm_s\rangle r^{-1} \times F^{JS}_{LL'}(r)\, \mathcal{Y}^{m_s}_{JL'S}(\hat{\underset{\sim}{k}}_0,\hat{\underset{\sim}{r}}) \qquad \text{(II-b-15)}$$

where

$$F^{JS}_{LL'}(r) = \frac{1}{2\pi^2}\int rj_{L'}(kr)\, P'(k',K)\, G^{JS}_{LL'}(k,k_0)k^2dk \qquad \text{(II-b-16)}$$

We are now in a position to write down the equation (II-b-4) in its partial wave form. We substitute (II-b-5), (II-b-8) and (II-b-15) in (II-b-4). To eliminate $\mathcal{Y}^{m_s}_{JLS}$ part of the wavefunction, we take scalar product with $\langle \mathcal{Y}^{m_s}_{JL'S}(\hat{k}_0,\hat{r})|$ and multiply throughout by $\langle LSOm_s|Jm_s\rangle$ and sum over m_s. It then at once follows

$$\left[\frac{d^2}{dr^2} - \frac{L'(L'+1)}{r^2} - \gamma^2\right] U^{JS}_{LL'}(r) - \sum_{L"} \langle JL"S|v(r)|JL'S\rangle\, U^{JS}_{LL"}(r) = -\delta_{LL'}(\gamma^2 + k_0^2) rj_L(k_0r) - F^{JS}_{LL'}(r) \qquad \text{(II-b-17)}$$

This equation is perfectly general; it applies in the case of coupled states as well as uncoupled ones. If one is using a potential with a hard core then the most obvious boundary conditions are

$$U^{JS}_{LL'}(r) = 0 \qquad \text{for } r<c$$
$$U^{JS}_{LL'}(r) \to \delta_{LL'} rj_L(k_0r) \qquad \text{as } r\to\infty \qquad \text{(II-b-18)}$$

where c is the core radius.

It is clear that equation (II-b-12) can not be used to get $G^{JS}_{LL'}(k,k_0)$ when the potential has a hard core. One has to use the same method as BBP did. One manipulates the following equation to get a practical form for $G^{JS}_{LL'}$,

$$\left[\frac{d^2}{dr^2} - \frac{L'(L'+1)}{r^2} + k^2\right] rj_{L'}(kr) = 0 \qquad .(II\text{-}b\text{-}19)$$

We multiply equation (II-b-17) by $rj_{L'}(kr)$, equation (II-b-19) by $U^{JS}_{LL'}(r)$, and subtract one from the other to get

$$U^{JS}_{LL'}(r) \frac{d^2}{dr^2}\{rj_{L'}(kr)\} - \frac{d^2}{dr^2}\{U^{JS}_{LL'}(r)\} \; rj_L(kr)$$

$$+ (k^2+\gamma^2)\, rj_{L'}(kr)\, U^{JS}_{LL}(kr) + \sum_{L''} rj_{L'}(kr) \langle JL'S|v(r)|JL''S\rangle$$

$$\times U^{JS}_{LL''}(r)$$

$$= \delta_{LL'}(\gamma^2+k_0^2)\, rj_{L'}(kr)\, rj_L(k_0r) + rj_L(k_0r)\, F^{JS}_{LL'}(r) \; .$$

Integrating from 0 to c+0 and remembering that $U^{JS}_{LL}(r)=0$ for $r<c$

$$\int_0^c rj_{L'}(kr) \langle JL'S|v(r)|JL''S\rangle U^{JS}_{LL''}(r)dr$$

$$= cj_{L'}(kc) \left[\frac{dU^{JS}_{LL'}}{dr}\right]_{r=c} + \int_0^c rj_{L'}(kr) \left[\delta_{LL'}(\gamma^2+k_0^2)\right.$$

$$\left.\times rj_L(k_0r) + F^{JS}_{LL'}(r)\right]dr \qquad .(II\text{-}b\text{-}20)$$

This integral in equation (II-b-12) can be split into two regions 0 to c and c to ∞. For the region 0 to c (II-b-20) can be used.

As mentioned, the equation (II-b-17) has to be solved by the method of successive iterations. In a typical iteration $U^{JS}_{LL'}(r)$ is obtained and the result is used to calculate $G^{JS}_{LL'}(k,k_0)$ as a function of k. $G^{JS}_{LL'}(k,k_0)$ can then be put into (II-b-16) to get $F^{JS}_{LL'}(r)$ which will be used in the next iteration. When the numbers $G^{JS}_{LL'}(k,k_0)$ do not differ appreciably from those obtained in the previous iteration one has obtained the desired solution.

To solve equation (II-b-17) one has to solve the homogeneous equation as well as the inhomogeneous one. At each iteration, the general solution of the full equation is obtained by adding a particular solution to the general solution of the homogeneous equation. This has to be done numerically by starting with asymptotic solutions for large r and integrating inwards. The asymptotic solution to the homogeneous equation will be $h_{L'}(i\gamma r)$ where h is the spherical Hankel function and that for the full inhomogeneous equation will be

$$U^{JS}_{LL'}(r) \sim \delta_{LL'}\, rj_L(kr) + \frac{1}{2\pi^2}\int rj_{L'}(kr)\; P(k,K)$$

$$\times\; G^{JS}_{LL'}(k,k_0)\; \frac{k^2 dk}{\gamma^2+k^2} \qquad \text{.(II-b-20)}$$

The asymptotic solutions are valid for such large distances of r so that v(r) can be neglected.

C. THE SELF CONSISTENCY PROBLEM AND NUMERICAL RESULTS:

It is obvious that in a numerical calculation of the binding energy of nuclear matter, a self consistency question is implied. The energy spectrum of the hole states is put in the calculation through the starting energy W. At the end of the calculation one should obtain the same spectrum as one started with. Obviously one has to do this by trial and error. However, it was shown in Brueckner's work that the hole spectrum could be represented by a formula of the type

$$E(k) = - A + \frac{h^2 k^2}{2m_h^*} \qquad .(II\text{-}c\text{-}1)$$

In our notation this will be represented by two parameters Δ and m* which are assumed to be dependent on k. As mentioned, Δ will specify the depth of the potential below zero for the average pair while m_h^* will give the shape of the spectrum. The use of Δ and m_h^* is simply a matter of convenience and simplicity. One might read in a table of values for the nuclear spectrum and attempt to recover those at the end of the calculation.

In our work, we repeated the calculation until the output value and input value of Δ were close to each other within a desired limit. The same was true for the parameter

m_h^*.

Another problem associated with this study is to observe the variation of the binding energy per particle with Δ. Let us illustrate this point. When one does a binding energy calculation with plane waves in intermediate states, one considers only the two-body clusters. A self consistent calculation done in this manner assumes that other contributions, like those from higher order clusters, three-body forces etc., are zero. This can hardly be true. If there is some contribution to the binding energy from the latter sources, then the single particle spectrum will be deeper than that obtained in a "pure two-body" calculation. This means that the energy denominators will now be larger and a self consistent calculation will give a slightly lower value for the two-body contribution. We illustrate this by an example. The binding energy per particle at k_F=1.36 using Reid's potential was found to be 11.08 MeV with no potential energy in the intermediate states. Then the input spectrum for a pair was made deeper so that the output spectrum was shallower than the corresponding input by 5 MeV. The binding energy in this case was 10.56 MeV. If one assumes that higher order clusters and other sources gave an additional binding of 2.5 MeV, then this value of 10.56 MeV would be the contribution of the two-body clusters in a self consistent calculation. We know that the binding energy per particle is given as sum

of the kinetic energy T and half of the potential energy U. That is why we considered 2.5 MeV as the contribution to binding while the spectrum was made deeper by 5 MeV. We see a contribution of 2.5 MeV in binding reduces the two-body contribution by (11.08 - 10.56)=.52 MeV. Thus the total binding energy instead of being (11.08 + 2.5) MeV is now (10.56 + 2.5) MeV. Thus we can make a rule that instead of adding the contribution of other terms to the pure two-body contribution one must first subtract about 20% of this additional contribution and later add it to the pure two-body contribution. In our example, we subtract 20% of 2.5 MeV from it and then add it to 11.08 MeV. Of course, this is a rough method of estimation but it should be good when the contribution from higher order terms is small.

The reference spectrum calculations were done following the well-known method of Bhargava and Sprung[25]. It is assumed that beyond a certain distance d, v(r) is negligible so that one can write

$$\chi_L(r) = \mathcal{H}_L(r) \quad N \qquad \text{for } r>d \qquad .$$

$\mathcal{H}_L(r)$ is the decaying Hankel function and N is a constant. Using the abbreviation

$$\Gamma_L = -\frac{d}{dr}\log\mathcal{H}_L(r), \qquad \Gamma_0 = \gamma$$

one can write down the boundary condition as

$$\chi_L(c) = \mathcal{J}_L(k_0 c) \qquad \text{for r=c=hard core radius}$$

$$\chi_L'(d) + \Gamma_L \chi_L(d) = 0 \qquad \text{for } r=d \quad .$$

In this work d was about 9.85 fm. The two point boundary value problem is solved by the Ridley method[42]. One introduces the auxiliary functions s and ω to factorise the equation

$$\left[\frac{d^2}{dr^2} - \gamma^2 - L(L+1) - m^*v(r)\right] \chi_L(r) = - m^*v(r) \mathcal{J}_L(k_0 r) \qquad \text{(II-c-2)}$$

obtained by rewriting the equation (II-a-12). The three equations obtained are

$$\frac{ds}{dr} - s^2 = g$$

$$\frac{d\omega}{dr} - s\omega = h \qquad \text{(II-c-3)}$$

$$\frac{d\chi}{dr} + s\chi = \omega$$

where $g(r) = - \gamma^2 - m^*v_L(r) - L(L+1)/r^2$

$$h(r) = - m^*v_L(r) \mathcal{J}_L(k_0 r) \quad .$$

Boundary conditions are satisfied if $s(d)=\Gamma$ and $\omega(d)=0$. The mesh set up in r-space consisted of 5 blocks having 24 steps each. At each of these points $\chi(r)$ was calculated. The steplength is doubled between blocks as one moved outward. For the auxiliary functions s and ω, the steplength was half that of χ, making these available at midpoints

for integration by Runge-Kutta-Gill method. For the potential, the steplength was half of that used for s and ω. The smallest steplength for the potential was $H=.0033$ fm. The hard core and soft core potentials of Reid were used. For the soft core potential, a fictitious hard core of radius .03 fm was put to start the integration. The Bessel-Fourier transforms of $\chi(r)$ were obtained by the method of Filon[42]. The hard core potential of Reid had three different hard cores: one for $^1S_0$, one for $^3S_1$-$^3D_1$ and one for other states. Second order corrections were applied to all states and to the $^3S_1$-$^3D_1$ states third order corrections were also applied. These results were sent in detail to B. D. Day when he was debugging his programmes for the Kallio-Day method. In his calculations, he found good agreement with our results.

For comparison, we show in Table 1 the G matrix elements for the "average pair" at various densities and for various states. The results from the Kallio-Day method and the reference spectrum method have been collected in the same table. The agreement is very good for the S states where the divergences are within 1%. For the $^3D_1$ state, the improvement in agreement comes from our inclusion of the third order correction.

The calculations by the Kallio-Day method were performed by using programmes obtained from B. D. Day. Kallio and Day calculated the binding energy only at normal density. Their calculations are very nearly self consistent.

We have done self consistent calculations for densities corresponding to k_F=.7 fm^{-1} to k_F=1.6 fm^{-1} and also for k_F=1.8 fm^{-1} and k_F=2.0 fm^{-1}. These were done for the Reid potential. Also we have done a new calculation for the Bressel potential[34] which has a finite step core. Bhargava and Sprung's calculation showed that this potential gave a larger binding but the saturation density was also high. Since this calculation was done, Bressel, Kerman and Rouben changed the core heights and meson masses. Further the calculations of Bhargava were based on the incorrect treatment of three-body energy. So it was interesting to see what information a new calculation would reveal.

In the Kallio-Day method (also abbreviated as KD method) a mesh is set up in the r-space. A fictitious hard core of radius c=0.04 fm is used for starting the integration. The region from c to c+6.0 fm is divided into three parts of length 0.4 fm, 0.8 fm and 4.8 fm. One divides the entire range into a number of points, the step lengths being .01 fm, .025 fm, and .05 fm respectively in those three regions. The potential is calculated at those points and the integration is done by a fourth order Runge-Kutta formula. The correlated wavefunctions are available at steplengths of .02 fm, .05 fm, and .1 fm for those three regions. From c to c+6.0 fm, the wavefunction is calculated at 85 points. These are integrated by Simpson's rule to construct $G^{JS}_{LL'}(k,k_0)$. For construction of $F^{JS}_{LL'}(r)$ one uses

the fact that $(1-Q)'=P(k,K)$ is zero beyond $k=k_F+\frac{1}{2}K$. The centre of mass momentum K is set to its r.m.s. value. The step size in k-space integration has a maximum allowable value of .1 fm^{-1}. This integration is also done by Simpson's rule. The homogeneous equation is solved by starting with an asymptotic value of $h_L(i\gamma r)$ multiplied by a normalization constant at r=c+6 fm and integrating inwards up to c+1.2 fm. Also some small value of U' at r=c is put and outward integration is carried up to r=c+1.2 fm. The same thing is repeated for the inhomogeneous equation by starting with asymptotic solution (II-b-20). At the very beginning the G's are set equal to zero so that in the first iteration one is doing just the reference spectrum method. The slopes and the values of this set of inward and outward solutions are matched at r=c+1.2 fm. For a hard core, the core volume and core surface terms can be added. For region beyond c+6.0 fm, the correlated wavefunction is assumed to be $\sim rj_L(k_0r)$ and corrections to G are calculated by evaluating the integral (II-b-12) using rj_L in place of U and integrating up to a further distance of $\sim$ 9.6 fm where v will be definitely very very small. The G matrices calculated in one iteration are compared with those from the previous one. If the difference is more than the tolerance limit, the new G's are stored in place of old ones and one goes for a new cycle. When the desired accuracy is obtained, the calculations are stopped. The convergence can be stepped

up by assuming that at each iteration the error decreased by a constant fraction. Using the results for previous three iterations one can make an improved estimate to use in the next iteration. This speeds up the convergence.

For the Bressel potential there are some additional complications. First of all, the potential is soft having a square core so that at the core edge the potential is double-valued. This requires care in numerical integration. Secondly, the core radius is not the same for T=0 states and T=1 states. Again for T=1 states the meson mass for pp or nn states is not the same as that for the np state. It was decided that an average pion mass for T=1 state would not be bad. This was justified by noting that the G matrix elements obtained by using average pion mass were in good agreement with the average of G matrix elements obtained by using different pion masses. These are shown in Table 2. The first difficulty was removed by setting a counter such that as soon as the integration reached the core edge, the deep attractive value was replaced by the core value. In the next step the deep attraction was used to move outwards. The same procedure was used by Bhargava and Sprung (hereafter abbreviated as BS) in their calculations. The calculations were done exactly for the following partial waves for both potentials

$$^1S_0,\ ^1P_1,\ ^1D_2,\ ^3P_0,\ ^3P_1,\ ^3D_2,\ ^3S_1\text{-}^3D_1,\ ^3P_2\text{-}^3F_2\ .$$

For higher partial waves we used a combination of phase shift approximation and OPEP. The states treated in phase shift approximation were

$$T = 1, \qquad {}^1G_4,\ {}^3F_3,\ {}^3F_4$$

$$T = 0, \qquad {}^3D_3,\ {}^1F_3$$

The rest of the higher partial waves were treated using OPEP. The binding energies per particle for these two potentials at different densities are shown in Table 3. It is seen that Bressel potential gives more binding but saturates at a higher density. The same characteristic was found by BS. In figure 3 we show Δ at different densities. It is seen that for Bressel potential Δ is always bigger than that for Reid. This merely reflects the binding energy results. In figure 4 we plotted m* against k_F. Here, however, there was no definite distinctive feature and, in fact, the two curves cross each other. In figure 5 we show the variation of the average potential energy $\bar{U}$ for various states against density. The ${}^1S_0$ contribution goes on increasing with k_F but that from ${}^3S_1+{}^3D_1$ shows saturation as the density increases. The mechanism of this saturation may be traced to the presence of the tensor force. The contribution from ${}^1P_1$ always remains positive but is not large. The ${}^3P$ states together give a negligible contribution although the individual states may contribute large values.

This large cancellation was also noted by BS. In figure 6 we have plotted the same for Bressel potential. Here also $^3S_1$ and $^3D_1$ shows saturation while ^3P states have negligible contribution. The state $^1S_0$ gives a contribution which increases very rapidly with k_F. The $^3S_1$-$^3D_1$ states also show a tendency of saturating at a higher density.

Another interesting quantity that comes out from such a calculation is the wound integral $\int \chi^2(r)\, d^3r$. When this quantity is multiplied by the density ρ it becomes a dimensionless number κ. This essentially gives the probability of two particles undergoing strong correlations. In a finite nucleus $1-\kappa$ gives the probability of finding a particle in its shell model orbital. In modern theories of nuclear many body problem[44] it appears as a natural expansion parameter. A small value of κ means that the Brueckner-Goldstone series will converge faster. In our earlier calculations, we calculated κ using the reference wave defect and subtracting the "in-sea" Fourier components to account for the Pauli operator. Those results are shown in figure 7. It is seen that a very large contribution comes from the $^3S_1$ state. The Reid New Core potential has a bigger value for κ at all densities shown. This is expected because the presence of the hard core. In figure 8 we show the variation κ with k_F as calculated by using the exact wavefunctions. Here also the Bressel potential has a lower value for κ than Reid's. This reflects

the hardness of the Reid potential compared to Bressel's. In fact, a calculation using a "super soft" potential developed by Sprung and Srivastava[45] gives an extremely small value for κ.

CHAPTER III

FORMULATION OF AN EFFECTIVE INTERACTION

It has been the aim of nuclear physicists for a long time to calculate the properties of finite nuclei from a basic two-nucleon interaction. Although the meson theories may predict the existence of "more-than-two-nucleon" forces i.e., forces which come into play only when more than two nucleons are close together, a complete derivation of such forces is still not in a satisfactory state. In this work we would like to use, therefore, only two-nucleon forces. The main source of our knowledge of this force has been the scattering experiments and the data therefrom lend support to the idea of existence of very strongly repulsive forces at short distances or to the existence of hard cores. The extreme hard core model has, sometimes, been relaxed[31] only to be replaced by a Yukawa type singularity. Recently, Sprung and Srivastava[45] have questioned the need for the assumption of a hard core. However, their work is mainly connected with the partial wave $^1S_0$ and in the absence of a potential like theirs for other partial waves we are still forced to use potentials with infinite repulsion at short distances.

The hard-core potentials or potentials with Yukawa type of singularity do not lend themselves to be used directly in nuclear structure calculations by the highly successful

shell model or by Hartree-Fock methods. The shell model assumes the particles in a nucleus to move almost independently of one another but in actual fact, at short distances their motion will be strongly correlated. This is again, due to the presence of strong repulsion in the potential at short distances. One therefore, asks whether it is possible to derive or postulate some interaction which corrects for these correlations at short distances and then do the usual shell model or H-F calculations. One thus falls back on some kind of "as if" interactions. Examples of such interactions developed recently are those of Nestor et al.[46] and of Volkov and Manning[47]. These interactions are, however, chosen empirically with certain criteria for their justification and naturally one becomes more interested in deriving such interactions on a more fundamental basis. For instance, the G matrix obtained from a nuclear matter calculation can be treated as an effective interaction in nuclear matter because its matrix elements with respect to the H-F wavefunctions for nuclear matter (plane waves) give the same binding as obtained from a detailed calculation using Brueckner theory.

The first attempt in this direction was made by Brueckner, Gammel and Weitzner[11], (hereafter called BGW). They regarded the nuclear matter G matrix as the effective interaction in finite nuclei and noted that the important correlation structure in G matrix is contained within a

distance of about 1 fm. If $\underset{\sim}{R}$ be the coordinate of the centre of mass of the pair of particles then the density $\rho(\underset{\sim}{R})$ is the density at which the G matrix is to be calculated. Thus the effective interaction will be dependent on the position coordinate through $\rho(\underset{\sim}{R})$. This approximation should be valid only when the density does not change appreciably over the correlation distance. This is known as the local density approximation. Making this prescription BGW then write the most general non-local form of the G matrix in analogy with the scattering theory[48]. They then try to identify the different components of the force like the central and the spin-orbit force.

In a nuclear matter calculation one is interested only in the central part of the effective force because the system is symmetric in spin and isospin. However, for a symmetry energy calculation one will require the isospin-dependent part of the force. In a finite nucleus, one will require the spin-orbit, the tensor and other terms if one wishes to calculate properties other than the total binding energy of a closed-shell nucleus. With this end in view, one can write the most general non-local nucleon-nucleon interaction as

$$\langle r'|G|r\rangle = a + ic(\underset{\sim}{\sigma}^1+\underset{\sim}{\sigma}^2).\underset{\sim}{n} + m(\underset{\sim}{\sigma}^1.\underset{\sim}{n}\underset{\sim}{\sigma}^2.\underset{\sim}{n}) + (g+h)\ (\sigma^1.\underset{\sim}{X}\sigma^2.\underset{\sim}{X}) + (g-h)\ (\sigma^1.\underset{\sim}{X}\sigma^2.\underset{\sim}{X}) \qquad \text{(III-1)}$$

where

$$\underset{\sim}{n} = \frac{\hat{\underset{\sim}{r}} \times \hat{\underset{\sim}{r}}'}{|\hat{\underset{\sim}{r}} \times \hat{\underset{\sim}{r}}'|}$$

$$\underset{\sim}{X} = \widehat{\underset{\sim}{r} + \underset{\sim}{r}'} \qquad \text{.(III-2)}$$

$$\underset{\sim}{x} = \widehat{\underset{\sim}{r} - \underset{\sim}{r}'}$$

Here $\hat{\underset{\sim}{r}}$ and $\hat{\underset{\sim}{r}}'$ are unit vectors in the incoming and out going directions and the hat $\hat{\Lambda}$ indicates that $\underset{\sim}{n}$, $\underset{\sim}{X}$, and $\underset{\sim}{x}$ are normalised to unity. The angle between $\underset{\sim}{r}$ and $\underset{\sim}{r}'$ will be denoted by θ. One often prefers to write G in the SM_s representation instead of the above $\sigma_z^1\sigma_z^2$ representation. From arguments purely geometrical in nature and using traces over spins, one can show that the coefficients a, c etc. can be written as follows

$$a = \frac{1}{4}\,(G_{11}+G_{00}+G_{ss})$$

$$c = \frac{1}{\sqrt{8}}\,(e^{i\phi}G_{10}-e^{-i\phi}G_{01})$$

$$m = \frac{1}{4}\,(G_{00}-G_{ss}-2G_{1-1}e^{2i\phi}) \qquad \text{.(III-3)}$$

$$g = \frac{1}{4}\,(G_{11}-G_{ss}+e^{2i\phi}G_{1-1})$$

$$h = \frac{1}{4\cos\theta}\,(G_{11}-G_{00}-e^{2i\phi}G_{1-1})$$

We remind ourselves that we are in the singlet-triplet representation. The subscripts 1, 0, -1, s represent S_z = 1, 0, -1 for the triplet case and s for the singlet case

respectively. The object of putting two subscripts is to specify the initial and final states. The formal structure of the G matrix given by equation (III-1) is the same as the M matrix in scattering theory and one can at once use this analogy to write down expressions for a, c etc. using the expressions given by Stapp et al.[49]. For T=1, the coefficients are (interchange odd and even L for T=0):

$$a = \frac{1}{2} \sum_{\text{odd } L} \{(2L-1)\ \alpha_L^{L-1} + (2L+1)\ \alpha_L^{L} + (2L+3)\ \alpha_L^{L+1}\}\ P_L(\mu)$$

$$+ \frac{1}{2} \sum_{\text{even } L} \alpha_L (2L+1)\ P_L(\mu)$$

$$c = -\frac{1}{2} \sum_{\text{odd } L} \{(L+1)\ (2L-1)\ \alpha_L^{L-1} + (2L+1)\ \alpha_L^{L} - L(2L+3)\ \alpha_L^{L+1}\}$$

$$\times \sin\theta\ P_L'(\mu)$$

$$m = \frac{1}{2} \sum_{\text{odd } L} \{\alpha_L^{L-1} - \alpha_L^{L} + \alpha_L^{L+1} + \frac{4u}{2L+1}\}\ (2L+1)\ P_L(\mu)$$

$$+ \sum_{\text{odd } L} \{-(L+1)\ \alpha_L^{L-1} + (2L+1)\ \alpha_L^{L} - L\ \alpha_L^{L+1} + 2L(L+1)V\}$$

$$\times \frac{\mu}{L(L+1)}\ P_L'(\mu)$$

$$- \frac{1}{2} \sum_{\text{even } L} (2L+1)\ \alpha_L\ P_L(\mu)$$

$$g = \frac{1}{2} \sum_{\text{odd } L} \{-\alpha_L^{L-1} + (2L+1)\ \alpha_L^{L} + \alpha_L^{L+1} - 2u\}\ P_L(\mu)$$

$$+ \frac{1}{2} \sum_{\text{odd } L} \{(L+1)\ \alpha_L^{L-1} - (2L+1)\ \alpha_L^{L} - L\ \alpha_L^{L+1} - 2L(L+1)V\}$$

$$\times \frac{\mu}{L(L+1)} P'_L(\mu)$$

$$h = \frac{1}{2} \sum_{\text{odd } L} \{ -(L+1)\ \alpha_L^{L-1} + (2L+1)\ \alpha_L^{L} - L\ \alpha_L^{L+1} + 2V\ L(L+1) \}$$

$$\times \frac{P'_L(\mu)}{L(L+1)}$$

This set of expressions will be denoted by equation (III-4). In the above,

$$\mu = \cos\theta$$

$$u = \sqrt{(L+1)\ (L+2)}\ \alpha^{L+1} + \sqrt{L(L-1)}\ \alpha^{L-1}$$

$$V = \sqrt{(L+2)/(L+1)}\ \alpha^{L+1} - \sqrt{(L-1)/L}\ \alpha^{L-1} .$$

The superscript on α gives the total angular momentum J while the subscript gives only the orbital angular momentum L. In the cases where there is no subscript, one gets terms off-diagonal in L e.g., S-D mixture term and the superscript gives the total angular momentum. Stapp et al. gave expressions for the α's in terms of phase shifts. In fact, if S be the scattering matrix

$$\alpha = \frac{S-1}{2ik} , \quad \text{usually called the t-matrix.}$$

For the uncoupled states, α should be just one number completely determined by phase shifts. In the presence of the tensor force, it becomes a 2 x 2 matrix so that for the J=1 case

$$\alpha = \begin{pmatrix} \alpha_0^1 & \alpha^1 \\ \alpha^1 & \alpha_2^1 \end{pmatrix}$$

where the subscripts give the L value and the superscripts the J value. Terms α^1 give the S-D coupling terms. Following the notation we used for nuclear matter, one can write

$$\alpha = \begin{pmatrix} \alpha^1_{00} & \alpha^1_{02} \\ \alpha^1_{20} & \alpha^1_{22} \end{pmatrix} .$$

The second index in the subscript gives the dominant wave and the first one the subsidiary wave. The superscript, as before, gives the total angular momentum. Because the S-matrix is symmetric

$$\alpha^1_{20} = \alpha^1_{02} .$$

In the case at hand one has to make a correspondence between the α's and the nuclear G matrix. It should be noted that the α we have used here is not exactly the same as Stapp's. The parameter α used here is $\frac{\alpha}{2ik}$ for Stapp. The correspondence we were talking about can be made by looking at the central force term 'a' and its corresponding expression given by BBP. It turns out that

$$\alpha^J_L = \frac{4\pi}{k_0^2} \sum_{L'} \int \mathcal{J}_L(k_0 r)\ v^J_{LL'}(r)\ U^J_{L'L}(k_0, r)\, dr .$$

This correspondence between the M_{ij}'s of Stapp and the nuclear G matrix was also discussed and used by Bhargava[50]. BGW were the first to examine the terms containing a and c and

use them in their theory which now goes by the name of Brueckner-Hartree-Fock theory.

It was shown by BGW that whereas 'a' corresponded to the central force in the effective interaction 'c' corresponds to the spin-orbit part. Both BGW and Bhargava used c to obtain the one-body spin-orbit force of the shell model. It is of interest, therefore, to look at the other spin dependent terms. In equation (III-4) the α_L^J's correspond to expressions diagonal in L whereas α^J's corresponded to those off-diagonal in L. If the effective interaction corresponds to the following form

$$V(r) = V_c(r) + V_{LS}\ L.S + V_T\ S_{12}$$

$$+ \text{possibly a quadratic spin-orbit force}$$

then only the tensor force would have matrix elements off-diagonal in L. Therefore it is best to separate terms into diagonal and off-diagonal parts when seeking to identify the various forces. Another point to note is that the quadratic spin-orbit force which we define as

$$\underset{\sim}{\sigma}^1.\underset{\sim}{L}\underset{\sim}{\sigma}^2.\underset{\sim}{L} - \frac{1}{3}\ \underset{\sim}{\sigma}^1.\underset{\sim}{\sigma}^2 L^2 = Q_{12}$$

has diagonal matrix elements which differ from those of S_{12} by a constant multiplicative factor. Therefore it is necessary to look at the off-diagonal terms to distinguish these. In m, g, and h we denote the part containing diagonal

use them in their theory which now goes by the name of Brueckner-Hartree-Fock theory.

It was shown by BGW that whereas 'a' corresponded to the central force in the effective interaction 'c' corresponds to the spin-orbit part. Both BGW and Bhargava used c to obtain the one-body spin-orbit force of the shell model. It is of interest, therefore, to look at the other spin dependent terms. In equation (III-4) the α_L^J's correspond to expressions diagonal in L whereas α^J's corresponded to those off-diagonal in L. If the effective interaction corresponds to the following form

$$V(r) = V_c(r) + V_{LS}\ L.S + V_T\ S_{12}$$

$$+ \text{possibly a quadratic spin-orbit force}$$

then only the tensor force would have matrix elements off-diagonal in L. Therefore it is best to separate terms into diagonal and off-diagonal parts when seeking to identify the various forces. Another point to note is that the quadratic spin-orbit force which we define as

$$\underset{\sim}{\sigma}^1.\underset{\sim}{L}\underset{\sim}{\sigma}^2.\underset{\sim}{L} - \frac{1}{3}\ \underset{\sim}{\sigma}^1.\underset{\sim}{\sigma}^2 L^2 = Q_{12}$$

has diagonal matrix elements which differ from those of S_{12} by a constant multiplicative factor. Therefore it is necessary to look at the off-diagonal terms to distinguish these. In m, g, and h we denote the part containing diagonal

terms by primes as m', g', h' and off-diagonal ones by m", g", h". So,

$$h' = \frac{1}{2} \sum_{\text{odd } L} \{-(L+1)\,\alpha_L^{L-1} + (2L+1)\,\alpha_L^{L} - L\,\alpha_L^{L+1}\} \frac{1}{L(L+1)} \times \frac{P_L^{1}(\mu)}{\sqrt{1-\mu^2}}$$

$$g' = \frac{1}{2} \sum_{\text{odd } L} \{-\alpha_L^{L-1} + (2L+1)\,\alpha_L^{L} + \alpha_L^{L+1}\} \frac{P_L(\mu)}{2ik} - \frac{1}{2} \sum_{\text{even } L} (2L+1)\,\alpha_L^{L}\,P_L(\mu) - \frac{1}{2} \sum_{\text{odd } L} \{-L\,\alpha_L^{L+1} + (2L+1)\,\alpha_L^{L} - (L+1)\,\alpha_L^{L-1}\} \frac{1}{L(L+1)}\,P_L'(\mu).\mu$$

$$m' = \frac{1}{2} \sum_{\text{odd } L} \{\alpha_L^{L+1} - \alpha_L^{L} + \alpha_L^{L-1}\} (2L+1)\,P_L(\mu) + \sum_{\text{odd } L} \{-L\,\alpha_L^{L+1} + (2L+1)\,\alpha_L^{L} - (L+1)\,\alpha_L^{L-1}\} P_L'(\mu).\frac{\mu}{L(L+1)} - \frac{1}{2} \sum_{\text{even } L} (2L+1)\,\alpha_L^{L}\,P_L(\mu) \qquad .(III-5)$$

Also

$$m'' = \sum_{\text{odd } L} \{2u_L\,P_L(\mu) + 2V_L \cot\theta\,P_L^{1}(\mu)\}$$

$$g'' = \sum_{\text{odd } L} \{-u_L\,P_L(\mu) - V_L \cot\theta\,P_L^{1}(\mu)\} \qquad .(III-6)$$

$$h'' = \sum_{\text{odd } L} V_L\,P_L'(\mu)$$

With these equations in hand let us try to construct a spin-dependent central force and a quadratic spin-orbit force. We start with m', g' etc.

$$m'\underset{\sim}{\sigma}^1.\underset{\sim}{n}\underset{\sim}{\sigma}^2.\underset{\sim}{n} + (g'+h')\ \underset{\sim}{\sigma}^1.\underset{\sim}{X}\underset{\sim}{\sigma}^2.\underset{\sim}{X} + (g'-h')\ \underset{\sim}{\sigma}^1.\underset{\sim}{x}\underset{\sim}{\sigma}^2.\underset{\sim}{x}$$

$$= \frac{m'+2g'}{3}\ \underset{\sim}{\sigma}^1.\underset{\sim}{\sigma}^2 + (\frac{g'-m'}{3} - h')\ \underset{\sim}{\sigma}^1.\underset{\sim}{\sigma}^2 + (m'-g'+h')\ \underset{\sim}{\sigma}^1.\underset{\sim}{n}\underset{\sim}{\sigma}^2.\underset{\sim}{n}$$

$$+ 2h'\underset{\sim}{\sigma}^1.\underset{\sim}{X}\underset{\sim}{\sigma}^2.\underset{\sim}{X} \qquad \text{(III-7)}$$

The first term in equation (III-7) has the character of a central force. Because

$$\frac{m'+2g'}{3} = \frac{1}{3}\ [\frac{1}{2}\ \sum_{\text{odd } L}\ \{(2L+3)\ \alpha_L^{L+1} + (2L+1)\ \alpha_L^{L} + (2L-1)\ \alpha_L^{L-1}\}$$

$$\times\ P_L(\mu) - \frac{3}{2}\ \sum_{\text{even } L}\ (2L+1)\ \alpha_L\ P_L(\mu)] \qquad \text{(III-8)}$$

which we see involves only the statistical average of the various partial waves.

We now denote

$$D = \sigma^1.\underset{\sim}{\hat{r}}\sigma^2.\underset{\sim}{\hat{r}} + \sigma^1.\underset{\sim}{\hat{r}}'\sigma^2.\underset{\sim}{\hat{r}}'$$

and

$$E = \sigma^1.\underset{\sim}{\hat{r}}'\sigma^2.\underset{\sim}{\hat{r}} + \sigma^1.\underset{\sim}{\hat{r}}\sigma^2.\underset{\sim}{\hat{r}}' \ .$$

Here $\underset{\sim}{\hat{r}}$ and $\underset{\sim}{\hat{r}}'$ are unit vectors in agreement with our previous definition.

$$\therefore \quad \underset{\sim}{\sigma}^1.\underset{\sim}{X}\underset{\sim}{\sigma}^2.\underset{\sim}{X} = \frac{D + E}{2(1 + \cos\ \theta)}$$

$$\underset{\sim}{\sigma}^1.\underset{\sim}{x}\underset{\sim}{\sigma}^2.\underset{\sim}{x} = \frac{D - E}{2(1 - \cos\theta)}$$

$$\underset{\sim}{\sigma}^1.\underset{\sim}{n}\underset{\sim}{\sigma}^2.\underset{\sim}{n} = \underset{\sim}{\sigma}^1.\underset{\sim}{\sigma}^2 - \frac{D + E}{4\cos^2\theta/2} - \frac{D - E}{4\sin^2\theta/2}$$

$$= \underset{\sim}{\sigma}^1.\underset{\sim}{\sigma}^2 - \frac{D}{\sin^2\theta} + \frac{E\cos\theta}{\sin^2\theta} \qquad .(III-9)$$

We look at the last three terms of equation (III-7). We get

$$\left(\frac{g'-m'}{3} - h'\right)\underset{\sim}{\sigma}^1.\underset{\sim}{\sigma}^2 + (m'-g'+h'\cos\theta)\,\underset{\sim}{\sigma}^1.\underset{\sim}{n}\underset{\sim}{\sigma}^2.\underset{\sim}{n} + (h'-h'\cos\theta)$$

$$\times\ \sigma^1.\underset{\sim}{n}\sigma^2.\underset{\sim}{n} + 2h'\,\underset{\sim}{\sigma}^1.\underset{\sim}{X}\underset{\sim}{\sigma}^2.\underset{\sim}{X}$$

$$= \left(\frac{g'-m'}{3} - h'\cos\theta\right)\underset{\sim}{\sigma}^1.\underset{\sim}{\sigma}^2 + \frac{2h'(D+E)\sin^2\theta/2}{\sin^2\theta} + (m'-g'+h'\cos\theta)$$

$$\times\ \underset{\sim}{\sigma}^1.\underset{\sim}{n}\underset{\sim}{\sigma}^2.\underset{\sim}{n} - \frac{2h'\sin^2\theta/2}{\sin^2\theta}D + \frac{2h'\sin^2\theta/2\cos\theta}{\sin^2\theta}E$$

using (III-9)

This simplifies to

$$\left(\frac{g'-m'}{3} - h'\cos\theta\right)\underset{\sim}{\sigma}^1.\underset{\sim}{\sigma}^2 + h'E + (m'-g'+h'\cos\theta)\,\underset{\sim}{\sigma}^1.\underset{\sim}{n}\underset{\sim}{\sigma}^2.\underset{\sim}{n} \qquad (III-10)$$

$$\frac{g'-m'}{3} - h'\cos\theta = -\frac{1}{3}A\,P_L(\mu) + A\cot\theta\,\frac{P_L^1(\mu)}{L(L+1)}$$

where

$$A = \sum_{\text{odd } L}\{(L+1)\,\alpha_L^{L-1} - (2L+1)\,\alpha_L^L + L\,\alpha_L^{L+1}\} \qquad .(III-11)$$

Also

$$m'-g'+h'\cos\theta = -\frac{A\,P_L^2(\mu)}{L(L+1)} \qquad .(III-12)$$

It can be shown that (Appendix A)

$$\underset{\sim}{\sigma}^1.\underset{\sim}{L}\underset{\sim}{\sigma}^2.\underset{\sim}{L}\ P_L(\mu) = - \underset{\sim}{\sigma}^1.\underset{\sim}{n}\underset{\sim}{\sigma}^2.\underset{\sim}{n}\ P_L{}^2(\mu) - \underset{\sim}{\sigma}^1.\hat{\underset{\sim}{r}}'\underset{\sim}{\sigma}^2.\hat{\underset{\sim}{r}}\ P_L'(\mu)$$

$$+ \underset{\sim}{\sigma}^1.\underset{\sim}{\sigma}^2 \cos\theta\ P_L'(\mu)$$

so

$$\underset{\sim}{\sigma}^2.\underset{\sim}{L}\underset{\sim}{\sigma}^1.\underset{\sim}{L}\ P_L(\mu) = - \underset{\sim}{\sigma}^1.\underset{\sim}{n}\underset{\sim}{\sigma}^2.\underset{\sim}{n}\ P_L{}^2(\mu) - \underset{\sim}{\sigma}^1.\hat{\underset{\sim}{r}}\underset{\sim}{\sigma}^2.\hat{\underset{\sim}{r}}'\ P_L'(\mu)$$

$$+ \underset{\sim}{\sigma}^1.\underset{\sim}{\sigma}^2 \cos\theta\ P_L'(\mu)$$

We add and divide by 2 and call the average of L.H.S. $(\underset{\sim}{\sigma}^1.\underset{\sim}{L}\underset{\sim}{\sigma}^2.\underset{\sim}{L})_{sym}$ to get

$$\underset{\sim}{\sigma}^1.\underset{\sim}{n}\underset{\sim}{\sigma}^2.\underset{\sim}{n}\ P_L{}^2(\mu) = - (\underset{\sim}{\sigma}^1.\underset{\sim}{L}\underset{\sim}{\sigma}^2.\underset{\sim}{L})_{sym}\ P_L(\mu) - \frac{1}{2} EP_L'(\mu)$$

$$+ \underset{\sim}{\sigma}^1.\underset{\sim}{\sigma}^2 \cot\theta\ P_L{}^1(\mu)$$

$$= - (\underset{\sim}{\sigma}^1.\underset{\sim}{L}\underset{\sim}{\sigma}^2.\underset{\sim}{L})_{sym}\ P_L(\mu) + \underset{\sim}{\sigma}^1.\underset{\sim}{\sigma}^2\left(\frac{P_L{}^2(\mu)}{2}\right.$$

$$\left. + \frac{L(L+1)}{2}\ P_L(\mu)\right) - \frac{1}{2} EP_L'(\mu)$$

$$= - \left[(\underset{\sim}{\sigma}^1.\underset{\sim}{L}\underset{\sim}{\sigma}^2.\underset{\sim}{L})_{sym} - \frac{1}{3}\ \underset{\sim}{\sigma}^1.\underset{\sim}{\sigma}^2 L^2\right] P_L(\mu) - \frac{1}{2} EP_L'(\mu)$$

$$+ \frac{1}{6}\ P_L(\mu)\ L(L+1)\ \underset{\sim}{\sigma}^1.\underset{\sim}{\sigma}^2 + \frac{1}{2}\ P_L{}^2(\mu)\ \underset{\sim}{\sigma}^1.\underset{\sim}{\sigma}^2$$

$$\underset{\sim}{\sigma}^1.\underset{\sim}{n}\underset{\sim}{\sigma}^2.\underset{\sim}{n}\ (m' - g' + h' \cos\theta)$$

$$= \frac{A\ Q_{12}\ P_L(\mu)}{L(L+1)} - \left\{\frac{1}{6}\ \frac{A\ L(L+1)}{L(L+1)}\ P_L(\mu) + \frac{1}{2}\ \frac{A\ P_L{}^2(\mu)}{L(L+1)}\right\}\ \underset{\sim}{\sigma}^1.\underset{\sim}{\sigma}^2$$

$$+ \frac{1}{2} \frac{A\, P_L'(\mu)\, E}{L(L+1)} \qquad .(III-13)$$

We note that $\frac{A\, P_L'(\mu)}{L(L+1)} = -\, 2h'$ so that from (III-13) and (III-10) the coefficient of E is $-h'+h' = 0$. Thus E drops out from (III-10). The coefficient of $\sigma^1.\sigma^2$ from (III-10), (III-11) and (III-13) is

$$-\frac{1}{3} A\, P_L(\mu) + A \cot\theta \frac{P_L^1(\mu)}{L(L+1)} - \frac{1}{6} A\, P_L(\mu) - \frac{1}{2} \frac{A\, P_L^2(\mu)}{L(L+1)}$$

$$= A\left[-\frac{1}{2} P_L(\mu) + \frac{\cot\theta\, P_L^1(\mu)}{L(L+1)} - \frac{1}{2} \frac{P_L^2(\mu)}{L(L+1)}\right] = 0 \quad .$$

So in the expression (III-10) we are left with

$\frac{A\, P_L(\mu)}{L(L+1)}\, Q_{12}$ which equals the entire expression (III-10) now.

Thus the diagonal terms lead to a spin dependent central force and a Q_{12} force. But the strength of the Q_{12} force is ambiguous because S_{12} has the same matrix elements as Q_{12} in diagonal terms (except for a factor). So we look at the non-diagonal ones for the S_{12} force whose strength will then be specified. It is well known that it is the S-D coupling which is the strongest of all. So it is this one which should receive most of our attention. For the off-diagonal parts we have,

$$m''\underset{\sim}{\sigma}^1.\underset{\sim}{\sigma}^2 + (g''+h''-m'')\ \underset{\sim}{\sigma}^1.\underset{\sim}{X}\underset{\sim}{\sigma}^2.\underset{\sim}{X} + (g''-h''-m'')\ \sigma^1.\underset{\sim}{x}\sigma^2.\underset{\sim}{x}$$

$$.(III-14)$$

From (III-6) we see that

$$g'' = -\frac{1}{2} m''$$

so that $$g''-m'' = -\frac{3}{2} m''$$.

Also,

$$m'' = \sum_{\text{odd } L} 2[\{\sqrt{(L+1)\ (L+2)}\ P_L(\mu) + \sqrt{\frac{L+2}{L+1}}\ \cot\theta\ P_L^{\ 1}(\mu)\}\alpha^{L+1}$$

$$+ \{\sqrt{L(L-1)}\ P_L(\mu) - \sqrt{\frac{L-1}{L}}\ \cot\theta\ P_L^{\ 1}(\mu)\}\alpha^{L-1}] \qquad .(III-15)$$

Let us recall that summation over odd L indicates that we are dealing with the T=1 case. For the T=0 case odd should be exchanged for even. A simplification of expression (III-14) leads to a completely general expression with tensor-force-like operators in it. However, as that is very complicated we will deal only with the case J=1. In that case,

$$m'' = \sqrt{2}\ \alpha^1$$

$$h'' = -\frac{3\mu}{\sqrt{2}}\ \alpha^1 \qquad .(III-16)$$

$$g''-m''+h'' = -\frac{3}{\sqrt{2}}\ (1+\mu)\ \alpha^1$$

$$g''-m''-h'' = -\frac{3}{\sqrt{2}}\ (1-\mu)\ \alpha^1$$

Remembering that $\mu = \cos\theta$, from (III-9) and the last two

terms of (III-14) we have

$$\underset{\sim}{\sigma}^1.\underset{\sim}{X}\underset{\sim}{\sigma}^2.\underset{\sim}{X}(g"-m"+h") + \underset{\sim}{\sigma}^1.\underset{\sim}{x}\underset{\sim}{\sigma}^2.\underset{\sim}{x}(g"-m"-h")$$

$$= [-\frac{3(1+\mu)}{\sqrt{2}}\frac{D+E}{2(1+\mu)} - \frac{3(1-\mu)}{\sqrt{2}}\frac{D-E}{2(1-\mu)}]\alpha^1$$

$$= -\frac{3}{\sqrt{2}} D\ \alpha^1 \qquad .(III-17)$$

Using (III-15) and (III-16) we get from the expression (III-14)

$$\sqrt{2}\ \alpha^1(\underset{\sim}{\sigma}^1.\underset{\sim}{\sigma}^2 - 3\ \frac{\sigma^1.\hat{\underset{\sim}{r}}\sigma^2.\hat{\underset{\sim}{r}} + \sigma^1.\hat{\underset{\sim}{r}}'\sigma^2.\hat{\underset{\sim}{r}}'}{2}) \qquad .(III-18)$$

Here again $\hat{\underset{\sim}{r}}$ and $\hat{\underset{\sim}{r}}'$ are unit vectors. The term in the bracket strongly resembles the tensor force operator except for a sign.

Now although the G matrix is a non-local operator it is convenient to make a further approximation to a <u>local effective</u> force. In other words, one tries to extract a delta function $\delta(\underset{\sim}{r}-\underset{\sim}{r}')$. It is also well known that this delta function can be expanded as

$$\delta(\underset{\sim}{r}-\underset{\sim}{r}') = \sum_L \frac{(2L+1)}{4\pi}\frac{\delta(r-r')}{rr'} P_L(\cos\theta_{rr'}) \qquad .(III-19)$$

Once the local approximation is made, we can replace r=r' in (III-18) and the expression in the bracket becomes the tensor operator (with a-ve sign).

From Stapp et al. we can write

$$\sqrt{2}\ \alpha_1 \sim 4\int \mathcal{J}_0(kr)\ V_T\ \mathcal{J}_2(kr)dr \qquad (III-20)$$

in the Born approximation. This shows that we are getting in (III-18) just the matrix element of the tensor force within a numerical factor. If we do not make the Born approximation then (III-20) will be of the form

$$\int \mathcal{J}_0(kr)\ (V_{02}U_{22} + V_{00}U_{02})dr$$

The expansion (III-18) of the delta function throws a factor (2L+1) which in the coupled case should be of the form (2J+1) so that the coefficient of α^1 seems to be in error. The above analysis thus does not lead to a satisfactory extraction of the tensor force.

One, therefore, might fall back on a more unsophisticated but realistic approach for the extraction of effective forces. We have already introduced the idea of a <u>local effective</u> force; let us expand on this. This approach was first proposed by Brandow[51] and has been studied by Donnelly[52], Bhaduri and Warke[53] and Bethe[17]. We recall from nuclear matter theory that the basic relation one uses to build correlations in the interaction is

$$\langle\phi|G|\phi\rangle = \langle\phi|V|\psi\rangle \qquad \text{(III-21)}$$

We therefore see that one way to define an effective local force is to demand that

$$V_{eff}(r)\ \phi(r) = V(r)\ \psi(r) \qquad \text{(III-22)}$$

where V(r) is the realistic phenomenological two-body

interaction and $\psi(r)$ is the correlated wavefunction obtained by solving the Bethe-Goldstone equation. We can at once see that this definition of the effective force will give the correct matrix element. But, in fact, the definition is more restrictive than that. Here we are demanding that at each point the integrands of the equation (III-21) will be the same. If one uses nuclear matter wavefunctions, then equation (III-21) reduces to

$$V_{eff}(r) = \frac{V(r)\ U(k_0,r)}{j_L(k_0 r)} \qquad \text{.(III-23)}$$

The effective force thus defined will, in general, be a function of k_0, k_F and r. So this will be density-dependent through the presence of k_F, somewhat momentum dependent through the presence of k_0 while the dependence on r will give the shape. The restriction that we have put by defining equation (III-22) is now going to lead us into a difficulty. Because the zeroes of j_L do not in general coincide with those of U's we can not use the expression (III-23) for all values of r. This difficulty posed by the nodes can, however, be overcome in another way but only at some sacrifice. We can multiply the numerator and the denominator of the right hand side of (III-23) by $j_L(k_0 r)$ and multiply each of them by the weighting function $\omega(k_0)$ (which gives the probability of occurrence in the Fermi sea of a pair with relative momentum k_0) and integrate from

0 to k_F. $\omega(k_0)$ is given by

$$\omega(k_0) = \frac{24}{k_F{}^3} k_0{}^2 (1 - \frac{3}{2} \frac{k_0}{k_F} + \frac{k_0{}^3}{2k_F{}^3}) \qquad .(III-24)$$

This averaging over the Fermi sea will guarantee that the matrix element for the "average pair" will be correct. This means that the binding energy for nuclear matter will also be given correctly but the matrix elements for other values of k_0 will be inaccurate. Siemens* has found that this error is large only in the $^3S_1$ state. Thus, for the uncoupled states, the prescription is

$$V_{eff}(r) = \frac{\int_0^{k_F} v(r)\ j_L(k_0 r)\ U_L(k_0, r)\ \omega(k_0)\ k_0{}^2 dk_0}{\int_0^{k_F} j_L{}^2(k_0\ r)\ \omega(k_0)\ k_0{}^2 dk_0} \qquad .(III-25)$$

It is evident that this effective potential is still density dependent. To have a potential for the coupled states one might note that similar arguments will hold. Because of the presence of the tensor force in the coupled states, the two states differ by 2 units of angular momentum. The solution of the Bethe-Goldstone equation in this case is best represented by a 2 x 2 matrix. To be specific we take the case J=1 which has the important deuteron state in it. The other state is a dominant D and small S state. The wavefunctions

---

* Private communication from Dr. D.W.L. Sprung.

and potential matrix elements we denote by two indices, the second index giving the dominant state. So

$$V \rightarrow \begin{pmatrix} V_{00} & V_{02} \\ V_{20} & V_{22} \end{pmatrix}$$

$$U \rightarrow \begin{pmatrix} U_{00} & U_{02} \\ U_{20} & U_{22} \end{pmatrix} .$$

So the analogue of equation (III-23) in the coupled case will be

$$\begin{pmatrix} V_{00}^{eff} & V_{02}^{eff} \\ V_{20}^{eff} & V_{22}^{eff} \end{pmatrix} \begin{pmatrix} j_0 & 0 \\ 0 & j_2 \end{pmatrix} = \begin{pmatrix} V_{00} & V_{02} \\ V_{20} & V_{22} \end{pmatrix} \begin{pmatrix} U_{00} & U_{02} \\ U_{20} & U_{22} \end{pmatrix} \quad .(III-26)$$

So we will have

$$V_{00}^{eff} = \frac{V_{00}U_{00} + V_{02}U_{20}}{j_0} \qquad (III-27)$$

from the diagonal element. The off-diagonal element should lead to the tensor force. However, the off-diagonal element contains a factor of $\sqrt{8}$ which is the matrix element of S_{12} so that

$$V_T^{eff} = \frac{V_{20}^{eff}}{\sqrt{8}} = \frac{V_{20}U_{00} + V_{22}U_{20}}{\sqrt{8}\, j_0} \qquad .(III-20)$$

The subsidiary wave U_{20} is extremely important because it gives about 65% of the total $^3S_1$ attraction in V_{00}^{eff}, whereas in V_T^{eff} we find it makes only a small contribution. In the coupled case also we will be faced with the problem of nodes but it can be avoided in a similar fashion as in the uncoupled case. Remembering that the Born approximation of the effective force would give the same result as $\langle\phi|V|\psi\rangle$ we multiply both sides of equation (III-26) by

$$\begin{pmatrix} j_0 & 0 \\ 0 & j_2 \end{pmatrix}$$

from left and

then take the average over the Fermi sea. This leads to the formulae

$$V_c^{eff}(r) = V_{00}(r) \frac{\int_0^{k_F} j_0(k_0 r)\, U_{00}(k_0, r)\, \omega(k_0)\, k_0^2 dk_0}{\int_0^{k_F} j_0^2(k_0 r)\, \omega(k_0)\, k_0^2 dk_0} + V_{02}(r) \frac{\int_0^{k_F} j_0(k_0 r)\, U_{20}(k_0, r)\, \omega(k_0)\, k_0^2 dk_0}{\int_0^{k_F} j_0^2(k_0 r)\, \omega(k_0)\, k_0^2 dk_0}$$

$$V_T^{eff}(r) = \frac{1}{\sqrt{8}} \left[V_{20}(r) \frac{\int_0^{k_F} j_2(k_0 r)\, U_{20}(k_0, r)\, \omega(k_0)\, k_0^2 dk_0}{\int_0^{k_F} j_2(k_0 r)\, j_0(k_0 r)\, \omega(k_0)\, k_0^2 dk_0} \right.$$

$$+ V_{22}(r) \frac{\int_0^{k_F} j_2(k_0 r)\, U_{20}(k_0 r)\, \omega(k_0)\, k_0^2 dk_0}{\int_0^{k_F} j_2(k_0 r)\, j_0(k_0 r)\, \omega(k_0)\, k_0^2 dk_0}] \quad .(III-30)$$

Equation (III-29) would give us the effective central interaction which would include the central contribution of the tensor force. This was also done by Kuo and Brown. But whereas their procedure could include only the second order tensor contribution, this method would do it to all orders because we are dealing with a G matrix. The second advantage is that equation (III-30) gives us the non-central contribution of the tensor force to all orders. This can be looked upon as a residual tensor force.

A word about a useful check on numerical calculations may not be irrelevant. The G matrix is known to be hermitian for a given starting energy W. So one should have

$$\int_0^\infty dr\, r^2 j_{L'}(kr) \sum_{L''} V^J_{L'L''}(r)\, U^J_{L''L}(r,k_0)$$

$$= \int_0^\infty dr\, r^2 j_L(k_0 r) \sum_{L''} V_{LL''}(r)\, U^J_{L''L'}(k,r) \quad .$$

In our expansion for ψ a factor r^{-1} occurs so that instead of r^2 we need r. In the nuclear matter programme we looked for this hermiticity and quite good agreement between the two off-diagonal elements was obtained. A typical result is shown in Table 4.

CHAPTER IV

RESULTS

The aim of the present work and the methods have been outlined in Chapters II and III. In nuclear matter calculations one has to do the computation at several densities. The reason for this is to see whether the system really saturates i.e., whether it really gives maximum binding at a particular density or not. A second result to be checked is whether this particular density is really the density in the interior of a heavy nucleus. The next thing to enquire is whether the calculation with that particular potential yields the empirical value for binding energy per particle. It is well known that the empirical value for binding energy per particle is about 16 MeV and the saturation density corresponds to k_F=1.36 fm^{-1}. Calculations have been done for the Reid Soft Core and Bressel-Kerman-Rouben potential. Both these potentials fit the scattering data well. The Bressel potential also shows that for fitting the scattering data the postulate of a hard core is not necessary. Our nuclear matter calculation, however, gives completely different results for these potentials. The range of densities used in our calculation is from k_F=.7 fm^{-1} to k_F=1.6 fm^{-1}. The calculations had to be done for k_F=1.8 fm^{-1} and k_F=2.0 fm^{-1} also to investigate

the high density behaviour. For the Bressel potential, the calculation was also done for the case k_F=1.7 fm^{-1} to establish saturation. Table 3 shows that whereas the two-body calculation for Reid potential indicates saturation around 1.43 fm^{-1} giving a value of +11.31 MeV for binding energy per particle,the Bressel potential saturates at k_F=1.6 fm^{-1} giving value of +14.98 MeV per particle. We repeat that these numbers come from a two-body calculation. The trend of saturating at a higher density in the case of Bressel potential was also noted by Bhargava. However, his calculations are not very meaningful now because of the revision of the three-body cluster energy by Bethe[27]. Thus although the Bressel potential gives a value for binding energy, which is closer to the empirical value, its saturation density is unrealistic. On the other hand, the Reid potential gives a smaller binding but the two-body calculations seem to put the saturation density in the correct region. However, the minimum of the binding energy curve for this potential is very flat and the compressibility is about 174 MeV. Thus the correct saturation density can not be determined accurately without a knowledge of higher order clusters.

It has been shown by Bethe* that certain higher order clusters and diagram can yield another 1.70 MeV of binding energy. This may arise in the following way. In this

---

* Private communication from Dr. D. W. L. Sprung.

calculation we have neglected the three-body cluster energy. It has been shown in Dahlblom[54] that the three-body clusters can contribute 1.1 MeV to the binding energy. This number was obtained by direct solution of the Bethe-Faddeev equations and not by using a suppression factor 'f' as was done in the older calculations. However, Dahlblom used (see figure 8a) central or tensor force in the first or the last G-interaction and central force in all the intermediate ones. An additional contribution of .60 MeV to the binding energy comes from a third order diagram (figure 8b) which uses tensor force in all the three interactions. This was first done by Dahlblom, Fogel, Qvist åndTörn[55]. Recently, Day[56] has estimated the contribution of all four hole line diagrams. His results showed that the four body contribution is not as small as had been anticipated. The four hole line contribution is about .6 - 1.6 MeV. The dominant part of this contribution comes from the ground state correlations (figure 8c) and the hole-hole interaction (figure 8d). Thus a total contribution of 2.8 ± 1 MeV are obtained from higher order diagrams. The binding energy for the Reid potential will then be 13.5 ± 1.5 MeV. We have assumed that the errors in our calculation and in Bethe's estimate have the same magnitude as those in Day's estimate. The estimates of Bethe and those of Day are valid for k_F=1.36 fm^{-1}.
The density dependence of these contributions

may well push the saturation point to higher density. We discuss more about this point in the last Chapter.

We would like to discuss a little more about our nuclear matter calculation. We have used a combination of PSA and OPEP for higher partial waves. It has been already described in Chapter II which states are used for PSA and which for OPEP. (In fact, the states which are not done by G matrix calculation or by PSA are all done by using OPEP.) A check on this approximation can be made. A method for calculation for higher partial waves developed by Srivastava[57] and used by Sprung, Banerjee, Jopko and Srivastava[58] shows that in a typical case this method gives .7 ± .3 MeV whereas our method gives .6 MeV. This thus checks out alright. To look for more binding so as to get the empirical value one method will be to use one of the soft potentials developed by Sprung and Srivastava in $^1S_0$. This would lead to an increase of about .9 MeV in binding. However, the 'κ's' from these potentials are very small and so no further gain can be had by further softening the potential. One might use a similar potential for $^3S\text{-}^3D$ states. But such a potential is yet to be developed.

Before finishing the discussion of nuclear matter we try to see why the Bressel potential saturates at a higher density. From figures 5 and 6 one might see that the coupled state $^3S\text{-}^3D$ which contains the tensor force as the main mechanism of saturation shows the tendency of saturating

at a higher density. Also the potential energy from the $^1S_0$ state increases more rapidly with density than in the Reid case.

Using our nuclear matter results we have also calculated the effective interactions for various states at different densities and have studied their density dependence. To calculate these effective interactions we need the correlated wavefunctions as a function of r and the relative momentum k_0. From our programs for the Kallio-Day method we get the radial part of ψ (the correlated wavefunction) at 85 points in r space and for seven values of

$$k_0/k_F = .125\ (.125)\ .875 \quad .$$

Our programme could thus choose one fixed r-value and integrate over k_0 from 0 to k_F. We used an 8 point Gaussian quadrature formula. For the values of the wavefunction at the ordinates for Gaussian quadrature we used our subroutine TAINT which uses an Aitken-Lagrange type interpolation. We had to take special care to locate the zeroes of $j_L(kr)$ and had to cut the integral $\int_0^{k_F} j_L^2(kr)\ \omega(k)dk$ into subintervals to avoid the cusps particularly in $j_0(kr)$. This was also checked against the exact analytical method. The effective potential was thus obtained as a table of values at the predetermined set of 'r' values rather than as an analytical function. As expected, the potential showed the effect of correlation and was no longer singular. In

figure 9, we have plotted the effective $^1S_0$ potential derived from the two-nucleon potentials of Reid and Bressel. It is at once seen that the suppression from the highly repulsive values for small radii is very large. The Bressel potential has a discontinuity at the core edge and that characteristic has been retained by the effective potential. Both these potentials become small at large radii and attain the values corresponding to the original potential. This is however to be expected because as we go away from the origins the rapid healing of the correlated wavefunction would bring it back to its unperturbed form so that $v^{eff}(r)$ will be equal to $v(r)$. In the Bressel potential, one can note that the suppression of the square core near the origin is very considerable to give it a spiky shape. It is evident that the two potentials do not give the same effective interaction leaving an element of non-uniqueness in it. To investigate this point we used some of the soft potentials of Sprung and Srivastava. The effective interaction deduced from these $^1S_0$ potentials are shown in figure 10. The effective interactions are found to retain the shape of the original potentials and although there is a suppression in the magnitude by about 40%, this is not so considerable as in the previous case. To investigate the mechanism of this we plotted the wave defect $\chi = \phi - \psi$ for all these three types of potentials namely, Reid, Bressel and one of the soft potentials NP-2. This is shown in figure 11. Whereas in

the case of the Reid and the Bressel potential the positive peak of χ is very high, it is not so in NP-2. In the case of the Bressel potential it is also a little pushed out. The negative peaks of all the three potentials are almost the same in order of magnitude but the peaks do not occur at the same radius.

Another interesting point that comes out from this is the following. For Reid potential the two-body G matrix gives only +11.3 MeV of binding per particle so that the potential energy is about -34.2 MeV. Comparing this with the empirical value of -39 MeV we see that we get about 87.7% of the required value. Most of the remaining binding comes from ground state correlations, three-body and four-body clusters etc. It is therefore tempting to increase the effective interaction proportionately to give correct binding in finite nuclei. This approach was adopted by Nemeth and Bethe[59] in their Thomas-Fermi calculations. The overall factor by which one multiplies turns out in this case to be 1.12. The three-body and four-body clusters may behave differently in finite nuclei. But in absence of precise knowledge of their behaviour our procedure seems to be good. The overall multiplicative constant will have the added merit of preserving the exchange mixture because all states are affected equally. The effective potential for the state $^1S_0$ seems to have a very weak density dependence. In the case of the Reid

potential, the repulsive peak changes by only about 8% and the attractive one by 17% as we go from k_F=1.36 fm^{-1} to k_F=.7 fm^{-1}. In figure 9a we have plotted $V(k_F)/V_0$ as a function of k_F. V_0 is the potential at k_F=1.36 fm^{-1}. We have computed this ratio at a fixed value of the radius r (in fm) for different values of k_F. It is seen that there is some density dependence but it is really small considering the fact that k_F=.7 fm^{-1} one goes to about $\frac{1}{8}$th of normal density. The effective $^1S_0$ potential, therefore, may be treated as roughly independent of density.

The next important state that we consider is the $^3S_1$ state. Here one expects considerable density dependence through the presence of the tensor force in the coupled $^3S_1$-$^3D_1$ state of the original interaction. The calculations were done by a simple extension of the computer programme used in the uncoupled case. The effective interaction derived for Reid Soft Core potential is shown in figure 12. We have plotted the effective potential for k_F=1.36 fm^{-1} and for k_F=.7 fm^{-1}. The potential for k_F=.7 fm^{-1} comes out to be stronger than that for k_F=1.36 fm^{-1}. We looked at the density dependence of these potentials. For this purpose, the ratio of the potential at some k_F to that at 1.36 fm^{-1} was plotted against k_F holding r fixed. The unfortunate situation is that the repulsive part is seen to have a different density dependence than the attractive part. Even within the repulsive or attractive peak, the density

dependence is not simple. Figure 13 shows $V(k_F)/V_0$ plotted against k_F for various radii within the repulsive peak. V_0 is the effective potential at k_F=1.36 fm^{-1}. It is seen that the curves pass through a minimum and rise again. For different radii, the curves are different although they all look to be quadratic. A simple formula for a curve which passes through this band was attempted and can be written as

$$V(k_F) = V_0[a + b(k_F - c)^2] \quad .$$

We found

$$a = .984$$
$$b = .9$$
$$c = 1.17 \quad .$$

Here, and also in other formulae to follow, k_F is in units of fm^{-1}. Obviously this formula is an oversimplification of the actual situation but will give a reasonable average fit and simplify calculations. Figure 14 shows the density dependence at certain radii within the attractive peak. Here the curves, however, do not show a tendency of going through a minimum. The simplest reasonable fit is a linear formula

$$V = V_0[a + bk_F] \quad .$$

where

$$a = 1.699$$
$$b = -.514 \quad .$$

The same procedure has been adopted to study the density dependence of the effective potentials in other states. Figure 15 shows the remnant tensor force derived from Reid potential at two different densities and figure 16 shows the variation of $V(k_F)/V_0$ with k_F at different radii. The attractive and repulsive parts have different density dependence and simple fits to these have been obtained. In figure 17 we show the effective $^1P_1$ potential at the densities of k_F=.7 fm^{-1} and k_F=1.36 fm^{-1}. The density dependence of this potential has been shown in figure 18. A simple fit for this density dependence has also been obtained. This study has been repeated for effective potentials derived from the Bressel potential also. The effective potentials are seen to retain the discontinuity at the core boundary. The $^1S_0$ potential at normal density has been shown in figure 9. The $^3S_1$ potential at two densities and its density dependence have been shown in figures 19 and 20. In this case, the strongest density dependence comes from radii around the core edge. Figure 21 gives the residual tensor (multiplied by $\sqrt{8}$) force at two densities and figure 22 gives its density dependence. To complete the comparison, we show in figure 23, the $^1P_1$ potential and its density dependence in figure 24. For all these states we have simple fits for the density dependence and they are collected together in Appendix B. In cases where the attractive and repulsive parts have different density

dependence we have given different formulae.

One interesting point to check is the "Kuo-Brown" prescription. Kuo and Brown[60] considered the second order term $V_T \frac{Q}{e} V_T$ and showed that the "renormalization" and density dependence in the central force in S-D case comes to a great extent through the tensor force. They claimed that one could use an approximation

$$\langle V_T \frac{Q}{e} V_T \rangle \rightarrow \frac{1}{e_{eff}} \langle V_T^2 \rangle .$$

It can be shown that

$$S_{12}^2 = 8\pi^t - 2S_{12}$$

where π^t is an operator which chooses the triplet state. Therefore,

$$- V_{TL} \frac{Q}{e} V_{TL} \approx - \frac{8V_{TL}^2(r)}{e_{eff}} + \frac{2V_{TL}^2(r)\ S_{12}}{e_{eff}} .$$

It is the second term which is responsible for the "renormalization" of the tensor force. The first term is absorbed in the effective central force and is responsible for the density dependence. Kuo and Brown[60] gave an estimate for e_{eff} using the oscillator parameter $h\omega$=14 MeV and k_F=1.3 fm^{-1}. They found $e_{eff} \approx$ 220 MeV. However, it was pointed out by Law and Bhaduri[61] that Kuo and Brown had an error of factor 2 and so e_{eff} should be about 440 MeV. We checked this relation and found a qualitative agreement.

In fact e_{eff} is a strong function of r as shown in Table 13. The energy denominator e_{eff} has been calculated in Fermi units in Table 13 and in the important region of r=1 fm to r=2 fm, one can roughly use a value of 16 (~ 650 MeV).

Coming back to the effective potentials, it is seen that if these are left in the form of numerical tables, they will not be very useful for doing actual calculations in finite nuclei. It is good to try and fit some analytic forms to these. At this department, there is a centre for producing and using effective forces given in the form of gaussians. So a fit of these effective potentials with a sum of gaussians was attempted. Programmes were developed using a least square method. One criterion was to fit the potential at twenty points. Each piece of datum was given an arbitrary error of .1% and a least square fit was attempted reducing the sum of the squares of the deviation. Although these numbers do not really mean anything they give us a handle to distinguish one fit from another. Another criterion for the fit was to see whether the volume and the higher moments of the potentials could be fitted. For these we calculated the first seven Talmi integrals as these are the most important ones in a shell model calculation. The gaussian fit was now made in such a way that the errors were now distributed over both the Talmi integrals and the points of the potential table. The agreement obtained was excellent for the effective interactions obtained from the

Reid potential. For the Bressel potential case, however, it was evident that the spike could not be fitted with a finite number of gaussians. So in the region of the discontinuity a smooth interpolation was obtained. The agreement of the Talmi integrals thus calculated and the fit of the curve in other regions was reasonable. We used a five gaussian fit. However, this choice was purely accidental. One might do just as well with three or six gaussians. The gaussian potentials thus obtained have the very desirable feature of retaining all the characteristics of the original potential. So one can use them with the prescribed density factors. However, one can also study the density dependence of each of the gaussians involved in the sum. We have given in Tables 5 -- 12 the strengths of the gaussians as a function of k_F. The state for which this fit is valid and also the ranges of the gaussians have been indicated.

CHAPTER V

SUMMARY AND CONCLUSIONS

In the preceeding chapters the aim and the results of the present work have been described. Nuclear matter calculations have been done for two modern phenomenological potentials - the soft core potential of Reid and that of Bressel, Kerman and Rouben. Both these potentials fit scattering data and both saturate nuclear matter. But one important difference is at once clear from two-body calculations. The Bressel potential gives a binding of 14.98 MeV at k_F=1.6 fm^{-1} while the Reid potential gives 11.31 MeV at k_F=1.43 fm^{-1}. We reiterate that these values for binding energy and apparent saturation densities come from two-body clusters. Higher order clusters may well alter the saturation density. It is seen from estimates of Bethe and of Day that higher order clusters may contribute about 2.8 ± 1 MeV to binding energy at the normal density (k_F=1.36 fm^{-1}). (One must not forget to subtract about 20% of this contribution before adding to the two-body contribution, because of self consistency condition.) This comes from three-body clusters, ground state correlations and four-body clusters, one of which is the hole hole interaction. The higher order clusters will thus not only

increase the binding which is a welcome result especially in the Reid case. But, in the case of the Reid potential, the binding energy curve from two-body calculations, is so flat near the minimum that the higher order clusters will critically determine the saturation density. The contribution from higher order clusters will also affect the results from Bressel potential by about the same amount as Reid's. As the higher order clusters involve more hole lines they will be strongly density dependent. This is because a sum over a hole line throws in a factor of k_F^3. Another way of looking at it would be to recognise that arranging the Brueckner-Goldstone series in terms of number of hole lines means an expansion in powers of density. As the net effect is attractive, one expects physically that this would push the saturation to higher densities. However, there are also repulsive terms in higher order clusters. Day in his four-body paper has made a classification of these diagrams. He also made a careful estimate of these. He arrived at rough analytical formulae for such estimates. These formulae involve κ (which is the product of the wound integral and the density), and the potential energy U. Using the values for these parameters, as obtained from our nuclear matter calculations the net effect is really found to be strongly density dependent. It is therefore difficult to put a definite value for the saturation density for Reid Soft Core potential.

However, it is definitely better than Bressel's where even the two-body calculation shows saturation at too high a density. To investigate the cause for this, one can look at the contributions of the various partial waves to the potential energy as the density varies. The coupled ^3S-^3D states which contain the tensor force are mainly responsible for saturation mechanism. They tend to saturate at a higher density than in the case of the Reid potential. Also the variation of the $^1S_0$ state contribution to the potential energy is faster with change of density in the case of the Bressel potential. This reflects the softer core. These two together put the saturation at a higher density.

Using the wavefunctions obtained from these nuclear matter calculations effective potentials have been calculated for both these basic interactions. The effective potential has been defined in such a way as to give the correct matrix element when uncorrelated wavefunctions are used. In terms of finite nuclei, this meant that one could do shell model or Hartree-Fock calculations. This was made more restrictive by demanding that the integrand in the expression for matrix elements agree at each point of r-space. This led to the problem of zeroes so that a compromise had to be made as to give the average matrix element correctly. The effective interaction was expected to be density dependent. We can see physically why it should be so.

From the perturbation-theoretic approach we see that second and higher order terms involve energy denominators and the Pauli operator Q. As the density is increased, k_F increases so that the available phase space decreases. Although theoretically the phase space is almost infinite, the matrix elements $\langle k'|V|k\rangle$ decrease as one goes further away in k'. Secondly, the energy denominator increases. In the case of the central forces, there is a large contribution from the first order but there will also be some contribution from second order and higher orders. So in this case the density dependence will not be very strong. In the case of tensor forces, however, the first contribution comes from the second order term so that the density dependence will be strong. From these considerations, one expects the potential at lower density to be stronger than that at higher density.

The effective interactions calculated were actually found to be density dependent. To check the numerical work the matrix elements of these were computed and found to agree with original ones at the "average" relative momentum. The effective interactions were calculated for two singlet states $^1S_0$ and $^1P_1$. The density dependence of the $^1S_0$ state was so small that one could make the rough approximation that it was independent of density. The $^1P_1$ state had small but some density dependence. The main density dependent state was the $^3S_1$ state. Its density dependence at

certain value of radius was as much as 50% as one goes from normal density to $\frac{1}{8}$th density. The $^3S_1$ effective interactions from both the Reid and the Bressel potentials exhibited such strong density dependences. It was found that, in fact, the density dependence is a complex phenomenon. It varied from one point in r-space to another and that also the average value differed in the attractive region from that in the repulsive region. Approximate and simple formulae were tried to describe the average behaviour in all these states. These are collected in Appendix B.

The very weak density dependence in $^1S_0$ compared to that in $^3S_1$ leads us to believe that it is the tensor force which is the main source of density dependence. If the hard core were equally effective then $^1S_0$ should have exhibited a fair amount of density dependence too.

We have also calculated the remnant effective tensor force for both the Reid and the Bressel potential. These effective potentials show a fair amount of density dependence although not quite as strong as the $^3S_1$ state does. As before, we found the density dependence to be pretty complex varying with various points in r-space. In the case of Reid potential, the density dependence of the attractive part was approximated by a quadratic and that of the repulsive part by a straight line. Formulae have been collected in Appendix B. For the Bressel case, however, the density dependence was almost the same in repulsive and attractive

regions and a linear approximation (given in Appendix B) was made. We also looked at the Kuo-Brown prescription for the effective central and tensor force which indicated that the change in those forces would be given by the right hand side of the following relation

$$- V_{TL} \frac{Q}{e} V_{TL} \approx - \frac{8V_{TL}^2}{e_{eff}} + \frac{2V_{TL}^2}{e_{eff}} S_{12} \quad .$$

The effective energy denominator was found to be a strong function of r (Table 13) but one can claim qualitative agreement. The effective interactions for the $^1P_1$ state for both the Reid and the Bressel potentials showed some density dependence but not large. In these cases the density dependences at various radii were almost linear with k_F but different and so linear approximations were made. To make all these effective potentials readily usable we fitted them as a sum of gaussians

$$V = \sum_{i=1}^{5} c_i \, e^{-a_i r^2} \quad .$$

The strengths of these gaussians have been given as a function of density in Tables 5 -- 12. One can use these gaussians together with our density factors, or can fit simple formulae to the strengths at various densities if one so desires.

APPENDIX A

We want to derive a relation between $(\underset{\sim}{\sigma}^1.\underset{\sim}{L}\underset{\sim}{\sigma}^2.\underset{\sim}{L})P_L(\mu)$ and $(\underset{\sim}{\sigma}^1.\underset{\sim}{n}\underset{\sim}{\sigma}^2.\underset{\sim}{n})P_L{}^2(\mu)$. Recalling that $L=-i\underset{\sim}{r}X\underset{\sim}{\nabla}$, we have

$$(\underset{\sim}{\sigma}^1.\underset{\sim}{L}\underset{\sim}{\sigma}^2.\underset{\sim}{L})P_L(\mu) = - (\underset{\sim}{\sigma}^1.\underset{\sim}{r}X\underset{\sim}{\nabla})\ (\underset{\sim}{\sigma}^2.\underset{\sim}{r}X\underset{\sim}{\nabla})P_L(\mu) \quad .$$

Using the identity (31) of B.G.W. (see also Goldberger and Watson[62]) we have

$$(\underset{\sim}{\sigma}^1.\underset{\sim}{L}\underset{\sim}{\sigma}^2.\underset{\sim}{L})P_L(\mu)$$

$$= - (\underset{\sim}{\sigma}^1.\underset{\sim}{r}X\underset{\sim}{\nabla})\ (\underset{\sim}{\sigma}^2.\frac{\underset{\sim}{r}}{r} X \frac{\underset{\sim}{r}'}{r})\ \frac{d\ P_L(\mu)}{d\mu}$$

$$= - (\sigma^1.\ \frac{\underset{\sim}{r}}{r} X \frac{\underset{\sim}{r}'}{r'})\ (\sigma^2.\ \frac{\underset{\sim}{r}}{r} X \frac{\underset{\sim}{r}'}{r})\ \frac{d^2P_L(\mu)}{d\mu^2}$$

$$- \frac{d\ P_L(\mu)}{d\mu}\ (\sigma^1.\underset{\sim}{r}X\underset{\sim}{\nabla})\ (\sigma^2.\ \frac{\underset{\sim}{r}}{r} X \frac{\underset{\sim}{r}'}{r'}) \quad .$$

We use our convention of putting $\wedge$ on a vector to denote unit vector in that direction and use the summation convention of tensor algebra that a repeated index means a sum over that index. Then

$$(\sigma^1.\underset{\sim}{r}X\underset{\sim}{\nabla})\ (\sigma^2.\hat{\underset{\sim}{r}}X\hat{\underset{\sim}{r}}')$$

$$= \sigma_i^1\ \delta_{ij}\ \varepsilon_{jkL}\ r_k\ \frac{\partial}{\partial r_L}\ \sigma_\lambda^2\ \delta_{\lambda\mu}\ \varepsilon_{\mu\kappa\nu}\ \frac{r_\kappa}{|r|}\ \frac{r'_\nu}{|r|}$$

$$= \sigma_i^1 \, \delta_{ij} \, \varepsilon_{jkL} \, r_k \, \sigma_\lambda^2 \, \varepsilon_{\mu\kappa\nu} \, \frac{r'_\nu}{|r'|} \, \frac{\partial}{\partial r_L} \, \frac{r_\kappa}{|r|}$$

$$= \sigma_i^1 \, \varepsilon_{ikL} \, r_k \, \sigma_\lambda^2 \, \varepsilon_{\lambda\kappa\nu} \, \hat{r}'_\nu \, \left[\frac{\delta_{L\kappa}}{|r|} - \frac{r_\kappa r_L}{r^3}\right]$$

$$= \sigma_i^1 \, \sigma_\lambda^2 \, \hat{r}_k \, \hat{r}'_\nu \, \varepsilon_{ikL} \, \varepsilon_{\lambda L\nu} - \sigma_i^1 \, \varepsilon_{ikL} \, r_k \, \sigma_\lambda^2 \, \varepsilon_{\lambda\kappa\nu} \, \frac{r'_\nu}{r^3} \, r_\kappa r_L \, .$$

We use the relations

$$\varepsilon_{ijk} \, \varepsilon_{iLm} = \delta_{jL} \, \delta_{km} - \delta_{jm} \, \delta_{kL}$$

$$A \times B = \varepsilon_{ijk} \, A_j \, B_k \, .$$

So, the first term $= \sigma_i^1 \, \sigma_\lambda^2 \, \hat{r}_k \, \hat{r}'_\nu \, (\delta_{i\nu} \, \delta_{k\lambda} - \delta_{i\lambda} \, \delta_{k\nu})$

$$= (\sigma^1 . \hat{r}') \, (\sigma^2 . \hat{r}) - (\sigma^1 . \sigma^2) \, (\hat{r} . \hat{r}')$$

Second term $= \sigma_i^1 \, \varepsilon_{ikL} \, r_k \, r_L \, \sigma_\lambda^2 \, \varepsilon_{\lambda\kappa\nu} \, \hat{r}'_\nu \, \frac{r_\kappa}{r^3}$

$$= \sigma^1 . \, (r \times r) \, \sigma_\lambda^2 \, \varepsilon_{\lambda\kappa\nu} \, \hat{r}'_\nu \, \frac{r_\kappa}{r^3}$$

$$= 0$$

$$(\underset{\sim}{\sigma}^1 . \underset{\sim}{L} \underset{\sim}{\sigma}^2 . \underset{\sim}{L}) P_L(\mu) = - \underset{\sim}{\sigma}^1 . \hat{\underset{\sim}{n}} \underset{\sim}{\sigma}^2 . \hat{\underset{\sim}{n}} \, P_L{}^2(\mu) - (\underset{\sim}{\sigma}^1 . \hat{\underset{\sim}{r}}') \, (\underset{\sim}{\sigma}^2 . \hat{\underset{\sim}{r}}) P'_L(\mu)$$

$$+ (\underset{\sim}{\sigma}^1 . \underset{\sim}{\sigma}^2) \, (\hat{\underset{\sim}{r}} \, . \, \hat{\underset{\sim}{r}}') P'_L(\mu) \, .$$

APPENDIX B

We collect all the simple formulae for density dependence of the effective interaction for various states. These formulae are fitted with the motivation to simplify actual calculatiors. The real density dependence is a much more complex phencmenon. In the following, V_0 will indicate the effective force at k_F=1.36 fm^{-1}. For using the formulae k_F must be taken in units of fm^{-1}. The basic two-nucleon interactions from which these effective forces have been derived are also indicated.

Reid Soft Core Potential:

STATE		FORMULA
$^3S_1$	Repulsive part:	$V(k_F)=V_0(.984+.9(k_F-1.17)^2$
	Attractive part:	$V(k_F)=V_0(1.699-.514k_F)$
Residual Tensor	Repulsive part:	$V(k_F)=V_0(1.99-.73k_F)$
	Attractive part:	$V(k_F)=V_0[.99+.83(k_F-1.25)^2]$
$^1P_1$	Overall	$V(k_F)=V_0(.381+.455k_F)$.

Bressel Potential:

STATE	FORMULA
$^3S_1$	Repulsive part: $V=V_0(1.33-.243k_F)$
	Attractive part: $V=V_0(1.68-.5k_F)$
Residual Tensor	Overall: $V=V_0(1.259-.19k_F)$
$^1P_1$	Overall: $V=V_0(.483+.38k_F)$

TABLE 1

Comparison of the G matrix elements obtained by Kallio-Day method with those from reference spectrum method. For each value of k_F, the numbers in the first line are from the KD method, and those in the second line are from the RS method. The Fermi momentum k_F is in units of fm^{-1} and the G matrix elements are in fm.

k_F STATE	$^1S_0$	$^1P_1$	$^1D_2$	$^3P_0$	$^3P_1$	$^3D_2$	$^3S_1$	$^3D_1$	$^3P_2$	$^3F_2$
1.00	-5.712	.373	-.513	-1.118	2.399	- .923	-7.080	.321	-1.482	- .077
	-5.662	.369	-.513	-1.119	2.393	- .923	-7.122	.318	-1.483	-0.075
1.10	-5.201	.427	-.596	-1.144	2.610	-1.077	-6.087	.376	-1.701	- .101
	-5.164	.423	-.596	-1.144	2.601	-1.078	-6.128	.373	-1.703	- .100
1.20	-4.723	.502	-.677	-1.148	2.810	-1.222	-5.204	.427	-1.915	- .126
	-4.699	.497	-.676	-1.148	2.800	-1.221	-5.260	.433	-1.917	- .126
1.30	-4.271	.595	-.756	-1.131	3.002	-1.354	-4.416	.473	-2.119	- .153
	-4.255	.589	-.754	-1.132	2.991	-1.353	-4.465	.470	-2.122	- .153
1.40	-3.841	.706	-.832	-1.096	3.186	-1.474	-3.702	.512	-2.314	- .181
	-3.828	.699	-.831	-1.096	3.173	-1.474	-3.737	.509	-2.316	- .180

TABLE 1 - CONTINUED

1.50	-3.430	.831	-.907	-1.045	3.363	-1.580	-3.049	.545	-2.496	- .208
	-3.417	.822	-.906	-1.045	3.346	-1.580	-3.077	.542	-2.498	- .208
1.60	-3.040	.967	-.979	- .979	3.530	-1.671	-2.463	.570	-2.664	- .236
	-3.022	.955	-.979	- .977	3.510	-1.672	-2.470	.568	-2.666	- .235

TABLE 2

Test of the accuracy of the average pion mass approximation. Column (a) gives the G matrix in fm using different pion masses for T=1(nn) and T=1(np) states and then averaging. Column (b) gives that using average pion mass. These matrix-elements are not multiplied by statistical weights.

$k_F = .7$ $\Delta = .93$ $m^* = .884$

State = $^1S_0$

k_0	(a)	(b)
.0875	-27.65	-27.63
.1750	-26.40	-26.38
.2625	-24.71	-24.70
.3500	-22.83	-22.82
.4375	-20.93	-20.92
.5250	-19.08	-19.08
.6125	-17.36	-17.36

TABLE 3

Summary of Binding Energy Results (MeV)

$k_F(fm^{-1})$	Reid	Bressel
.7	- 3.35	- 3.75
.8	- 4.47	--
.9	- 5.78	- 6.43
1.0	- 7.19	--
1.1	- 8.57	- 9.67
1.2	- 9.80	--
1.3	-10.72	-12.75
1.36	-11.08	-13.51
1.4	-11.19	-13.97
1.43	-11.31	--
1.5	-11.05	-14.77
1.6	-10.21	-14.98
1.7	--	-14.50
1.8	- 5.46	-13.04

TABLE 4

Check on the hermiticity of the G matrix in the coupled S-D case

$k_F = 1.36, \quad \gamma^2 = 2, \quad m^* = .6$

k	k_0	$\langle {}^3D(k)\|G\|{}^3S(k_0)\rangle$	$\langle {}^3S(k_0)\|G\|{}^3D(k)\rangle$
.250000	.000000	-2.7531	-2.7530
.250000	.250000	-2.1422	-2.1422
.250000	.500000	-1.1371	-1.1370
.250000	.750000	- .5207	- .5205
.250000	1.000000	- .2389	- .2387
.250000	1.320434	- .0941	- .0940
.250000	1.640869	- .0393	- .0393
.250000	1.961303	- .0161	- .0160
.250000	2.281737	- .0047	- .0046
.500000	0.000000	-8.0423	-8.0428
.500000	0.250000	-6.7819	-6.7823
.500000	0.500000	-4.1922	-4.1926
.500000	.750000	-2.1152	-2.1155
.500000	1.000000	-1.0025	-1.0026
.500000	1.320434	- .3966	- .3966
.500000	1.640869	- .1648	- .1647
.500000	1.961303	- .0667	- .0663
.500000	2.281737	- .0191	- .0186

TABLE 5

Parameters of the Gaussians fitted to the effective interactions by the formula $V_{eff}(k_F) = \sum_{i=1}^{5} c_i(k_F)\, e^{-\alpha_i r^2}$. The parameters α_i (in fm^{-2}) give the range of the gaussians while c_i's give the strength in MeV. Reid Soft Core potential has been used in deriving the effective force. The Fermi momentum k_F is in units of fm^{-1}

State = $^1S_0$

$\alpha_1 = 4.0$ $\alpha_2 = 2.56$ $\alpha_3 = 6.4 \times 10^{-1}$ $\alpha_4 = 4.0 \times 10^{-2}$ $\alpha_5 = 1.6 \times 10^{-1}$

k_F	$c_1 \times 10^{-3}$	$c_2 \times 10^{-3}$	$c_3 \times 10^{-1}$	$c_4 \times 10^{2}$	c_5
.7	2.78603848	-1.3880526	-8.04985268	-1.43324171	-1.75478351
.9	2.59647841	-1.28986101	-7.43827972	-1.42889979	-1.83124995
1.1	2.55874304	-1.27083148	-7.10055152	-1.40718883	-1.90538816
1.36	2.63463627	-1.31262774	-6.8240139	-1.38250401	-1.97448823
1.40	2.65426473	-1.32342739	-6.78759891	-1.37886194	-1.98367688

TABLE 6

SAME AS TABLE 5

State = $^3S_1$

$\alpha_1 = 4.0$ $\alpha_2 = 3.6 \times 10^{-1}$ $\alpha_3 = 4.0 \times 10^{-2}$ $\alpha_4 = 1.0$ $\alpha_5 = 1.6 \times 10^{-1}$

k_F	$c_1 \times 10^{-3}$	c_2	$c_3 \times 10^{1}$	$c_4 \times 10^{-2}$	$c_5 \times 10^{1}$
.7	1.69306276	-7.64189677	-1.09576487	-4.24064230	-7.6319631
.9	1.47348187	-5.30050549	-1.23409665	-3.60165609	-2.5681249
1.0	1.42668013	-3.66726921	-1.28919054	-3.44552054	-1.7073057
1.1	1.40091185	-1.72528595	-1.30590170	-3.34336304	-2.05639657
1.2	1.38622227	0.30274847	-1.29027073	-3.26972050	-3.24808028
1.3	1.36951196	2.06108148	-1.26651573	-3.19848310	-4.64167726
1.36	1.34831179	2.77291840	-1.25987848	-3.13769487	-5.25591491

TABLE 7

SAME AS TABLE 5

Residual tensor force from Reid potential for ^3S-^3D states

$\alpha_1 = 3.24$ $\alpha_2 = 2.56$ $\alpha_3 = 6.4 \times 10^{-1}$ $\alpha_4 = 4.0 \times 10^{-2}$ $\alpha_5 = 1.6 \times 10^{-1}$

k_F	$c_1 \times 10^{-3}$	$c_2 \times 10^{-3}$	$c_3 \times 10^{-1}$	$c_4 \times 10^{1}$	c_5
.7	1.50508475	-1.21995237	-7.46562360	-2.34191268	-5.06248089
.8	1.36574440	-1.10991387	-6.76214538	-2.44713877	-5.20225333
.9	1.27967308	-1.04341821	-6.30220964	-2.50632911	-5.38028264
1.0	1.22477976	-1.00271993	-5.97910612	-2.50776004	-5.58716025
1.1	1.18990384	- .978588982	-5.75696224	-2.45642314	-5.79926458
1.2	1.16621568	- .963345419	-5.63402174	-2.39015644	-5.97521187
1.3	1.15280387	- .956391243	-5.57389023	-2.31721931	-6.11573581
1.36	1.14132891	- .948368063	-5.60093774	-2.24413611	-6.16770444

TABLE 8

SAME AS TABLE 5

State $^1P_1$

$\alpha_1 = 1.96$ $\alpha_2 = 3.6 \times 10^{-1}$ $\alpha_3 = 6.4 \times 10^{-1}$ $\alpha_4 = 4.0 \times 10^{-2}$ $\alpha_5 = 1.6 \times 10^{-1}$

.7	3.11113730	-4.68665069	1.59101631	3.01179913	6.23910522
.9	3.60083462	-4.64759574	1.57708558	3.01774203	5.85523457
1.0	3.86977643	-4.62106120	1.56811532	3.02284178	5.59641199
1.2	4.46589450	-4.55447185	1.54586532	3.03969579	4.98335269
1.3	4.77300296	-4.52079569	1.53420925	3.04674581	4.71990500
1.36	4.95193717	-4.50164620	1.52750537	3.04982334	4.58613963
1.40	5.07596384	-4.48735898	1.52251673	3.05193614	4.48986638

TABLE 9

Same as Table 5 but Bressel potential has been used in place of Reid potential

State = $^1S_0$

$\alpha_1 = 3.24$ $\alpha_2 = 2.56$ $\alpha_3 = 3.6 \times 10^{-1}$ $\alpha_4 = 4.0 \times 10^{-2}$ $\alpha_5 = 1.6 \times 10^{-1}$

k_F	$c_1 \times 10^{-3}$	$c_2 \times 10^{-3}$	$c_3 \times 10^{-1}$	$c_4 \times 10^{1}$	c_5
.7	6.44387754	-4.83640353	-1.61633621	-1.68497683	-1.85853140
.9	5.94168730	-4.45228486	-1.50698654	-1.68134577	-1.98443116
1.1	5.70463100	-4.26646106	-1.46790201	-1.66557246	-2.06194449
1.3	5.61739618	-4.19221334	-1.45736006	-1.65717953	-2.09588505
1.36	5.61076764	-4.18457343	-1.45544106	-1.65512569	-2.10276045
1.40	5.60955173	-4.18198105	-1.45419301	-1.65379101	-2.10690455

TABLE 10

SAME AS TABLE 9

State = $^3S_1$

$\alpha_1 = 3.24$ $\alpha_2 = 2.56$ $\alpha_3 = 3.6 \times 10^{-1}$ $\alpha_4 = 4.0 \times 10^{-2}$ $\alpha_5 = 1.6 \times 10^{-1}$

k_F	$c_1 \times 10^{-3}$	$c_2 \times 10^{-3}$	$c_3 \times 10^{-1}$	$c_4 \times 10^{1}$	$c_5 \times 10^{1}$
.7	6.56169314	-4.99689549	-3.46308365	-1.72534804	-7.48379615
.9	5.63339148	-4.26547177	-2.79582298	-1.80011659	-5.71433203
1.1	5.22015836	-3.93521316	-2.25039978	-1.84435212	-6.72518304
1.3	4.99012779	-3.74518321	-1.76166103	-1.78540955	-10.2237017
1.36	4.92881054	-3.69349518	-1.63965810	-1.76531797	-11.3037038

TABLE 11

SAME AS TABLE 9

Residual Tensor force derived from Bressel potential for ^3S-^3D states

$\alpha_1 = 4.0$ $\alpha_2 = 1.96$ $\alpha_3 = 3.6 \times 10^{-1}$ $\alpha_4 = 4 \times 10^{-2}$ $\alpha_5 = 1.6 \times 10^{-1}$

k_F	$c_1 \times 10^{-2}$	$c_2 \times 10^{-2}$	$c_3 \times 10^{-1}$	$c_4 \times 10^{1}$	c_5
.7	10.9509999	-7.21904792	-1.85662963	-2.71850686	-4.39857826
.9	9.40229539	-6.16483135	-1.60812320	-2.88145759	-4.83497743
1.1	8.76144643	-5.71849344	-1.49441542	-2.81615864	-5.32784663
1.3	8.41204248	-5.46082066	-1.51061123	-2.67711328	-5.60916321
1.36	8.36548860	-5.42126036	-1.52532900	-2.66224502	-5.64991732
1.40	8.29289424	-5.36734856	-1.55456547	-2.63125928	-5.64447998

TABLE 12

SAME AS TABLE 9

State = $^1P_1$

$\alpha_1 = -4.0$ $\alpha_2 = 3.24$ $\alpha_3 = 6.4 \times 10^{-1}$ $\alpha_4 = 4.0 \times 10^{-2}$ $\alpha_5 = 1.6 \times 10^{-1}$

k_F	$c_1 \times 10^{-3}$	$c_2 \times 10^{-3}$	$c_3 \times 10^{-1}$	$c_4 \times 10^{1}$	c_5
.7	-6.69217753	6.73037597	-4.37222406	4.36532326	5.08726025
.9	-7.03585353	7.07464423	-4.43705939	4.34264561	5.14563504
1.1	-7.37872492	7.41789471	-4.47685396	4.32991971	5.16576466
1.3	-7.75146528	7.79116712	-4.53054134	4.32579420	5.17099760
1.36	-7.86907055	7.90900268	-4.55382452	4.3238869	5.17373262
1.40	-7.94603870	7.98613045	-4.56997107	4.32259727	5.17570352

TABLE 13

Study of the effective energy denominator for the residual tensor force*. Reid Soft Core potential $k_f^\circ = 1.36$ fm^{-1}

$$e_{eff} = \frac{2v_T^2}{\Delta V_T}; \quad \Delta V_T = V_T^{eff} - V_T$$

Radius (fm)	V_T(fm^{-2})	V_T^{eff}(fm^{-2})	e_{eff}(fm^{-2})
.24	-84.4585	.8100	167.31
.54	-12.0330	-1.3909	27.21
1.04	- 1.4562	-1.4025	78.97
1.24	- .8198	- .8882	- 23.07
1.34	- .6411	- .7007	- 16.48
1.54	- .4165	- .4436	- 12.80
1.84	- .2406	- .2419	- 90.00
2.04	- .1737	- .1703	+ 17.71
2.24	- .1278	- .1240	+ 8.60

* Near r=1 fm and r=2 fm the curves for $V_T(r)$ and $V_T^{eff}(r)$ cross each other resulting in a change of sign and large energy denominators.

BIBLIOGRAPHY

(1) R. Jastrow, Phys. Rev. 81, 165 (1951)

(2) See, for example, G. E. Brown - "Unified Theory of Nuclear Models and Forces" - North Holland Publishing Company - Amsterdam (1967)

(3) K. A. Brueckner and C. A. Levinson, Phys. Rev. 97, 1344 (1955)

K. A. Brueckner, ibid. 97, 1353 (1955)

(4) J. Goldstone, Proc. Roy. Soc. (London) A293, 267 (1957)

(5) See, for example, - "The Quantum Mechanics of Many Body Systems", D. J. Thouless - Academic Press (1961)

(6) A. G. W. Cameron, Can. J. Phys. 35, 1021 (1957)

(7) K. A. Brueckner and J. L. Gammel, Phys. Rev. 109, 1023 (1958)

(8) S. A. Moszkowski and B. L. Scott, Ann. Phys. (New York) 11, 65 (1960)

(9) H. S. Köhler, Ann. Phys. (New York) 16, 375 (1961)

(10) H. A. Bethe, B. H. Brandow and A. G. Petschek, Phys. Rev. 129, 225 (1963)

(11) K. A. Brueckner, J. L. Gammel and H. Weitzner, Phys. Rev. 110, 431 (1958)

(12) R. J. McCarthy and H. S. Kohler, Nucl. Phys. A99, 65 (1967)

(13) R. L. Becker, A. D. MacKellar and B. L. Morris, Phys. Rev. 174, 1264 (1968)

(14) R. A. Berg and L. Wilets, Phys. Rev. 101, 201 (1956)

(15) Y. Hara, Progr. Theoret. Phys. (Kyoto) 24, 1179 (1960)

(16) K. Kumar, K. J. LeCouteur and M. K. Roy, Nucl. Phys. 42, 529 (1963)

(17) H. A. Bethe, Phys. Rev. 167, 879 (1968)

(18) K. A. Brueckner and K. S. Masterson, Phys. Rev. 128, 2267 (1962)

(19) M. Razavy, Phys. Rev. 130, 1091 (1963)

(20) K. E. Lassila, M. H. Hull, Jr., H. M. Ruppel, F. A. McDonald and G. Breit, Phys. Rev. 126, 881 (1962)

(21) T. Hamada and I. D. Johnston, Nucl. Phys. 34, 383 (1962)

(22) G. E. Brown, G. T. Schappert and C. W. Wong, Nucl. Phys. 56, 191 (1964)

(23) R. Rajaraman, Phys. Rev. 131, 1244 (1963)

(24) H. A. Bethe, Phys. Rev. 138, B804 (1965)

(25) P. C. Bhargava and D. W. L. Sprung, Ann. Phys. 42, 222 (1967)

(26) M. W. Kirson, Ph.D. thesis, Cornell University, (1966)

(27) H. A. Bethe, Phys. Rev. 158, 941 (1967)

(28) N. Azziz, Nucl. Phys. 85, 15 (1966)

(29) T. Dahlblom, private communication

(30) See, for example, D. W. L. Sprung - "Proceedings of the Third International Conference on Atomic Masses in Winnipeg, 1967, (University of Manitoba Press, 1968) pp. 37-57

(31) R. Reid, Ann. Phys. 50, 411 (1968)

(32) A. Kallio and B. D. Day, Nucl. Phys. A124, 177 (1969)

(33) H. S. Köhler, Nucl. Phys. A128, 273 (1969)

(34) C. N. Bressel, A. K. Kerman and B. Rouben, Nucl. Phys. A124, 624 (1969)

(35) G. Dahl, E. Ostgaard and B. H. Brandow, Nucl. Phys. A124, 481 (1969)

(36) B. Day, Rev. Mod. Phys. 39, 719 (1967)

(37) R. Rajaraman and H. A. Bethe, Rev. Mod. Phys. 39, 745 (1967)

(38) See, for example, reference 10

(39) N. M. Hugenholtz, Physica 23, 533 (1957)

(40) L. D. Faddeev, Sov. Phys. (JETP) 12, 1014 (1961)
Sov. Phys. (DOKLADY) 6, 384 (1961)

(41) B. Day, Phys. Rev. 151, 826 (1966)

(42) E. C. Ridley, Proc. Cambridge Phil. Soc. 53, 442 (1957)

(43) L. N. G. Filon, Proc. Roy. Soc. (Edinburgh) 49, 38 (1928)

(44) B. H. Brandow, Phys. Rev. 152, 863 (1966)

(45) D. W. L. Sprung and M. K. Srivastava, Nucl. Phys. (to be published)

(46) C. W. Nestor, Jr., K. T. R. Davies, S. J. Krieger and M. Baranger, Nucl. Phys. A113, 14 (1968)

(47) M. R. Manning and A. B. Volkov, Phys. Letts. 26B, 60 (1967)

(48) See, for example, L. Wolfenstein, Phys. Rev. 96, 1654 (1954)
L. Wolfenstein and J. Ashkin, Phys. Rev. 85, 947 (1952)

(49) H. P. Stapp, T. J. Ypsilantis and N. Metropolis, Phys. Rev. 105, 302 (1957)

(50) P. C. Bhargava, Ph.D. thesis, McMaster University, (1966)

(51) B. H. Brandow, Proceedings of the International School of Physics "Enrico Fermi", Course 36, Varenna, 1965

(52) I. J. Donnelly, Nucl. Phys. A111, 201 (1968)

(53) R. K. Bhaduri and C. S. Warke, Phys. Rev. Letts. 20, 1379 (1968)

(54) T. Dahlblom, preprint

(55) T. Dahlblom, K. G. Fogel, B. Qvist and A. Törn, Nucl. Phys. 56, 177 (1964)

(56) B. D. Day, preprint

(57) M. K. Srivastava, Nucl. Phys. (to be published)

(58) D. W. L. Sprung, P. K. Banerjee, A. M. Jopko and M. K. Srivastava, Nucl. Phys. (to be published)

(59) J. Nemeth and H. A. Bethe, Nucl. Phys. A116, 241 (1968)

(60) T. T. S. Kuo and G. E. Brown, Phys. Letts. 18, 54 (1965) Nucl. Phys. 85, 40 (1966)

(61) J. Law and R. K. Bhaduri, Can. J. Phys. (to be published)

(62) M. L. Goldberger and K. M. Watson, "Collision Theory", John Wiley and Sons, Inc., New York (1964)

FIGURE CAPTIONS

Figure 1. This is a schematic figure to illustrate the gap Δ. E^R is the reference spectrum. E is the spectrum of occupied states. Δ is an average measure of the separation between the actual energies of the occupied states and the reference spectrum.

Figure 2. This figure illustrates Δ'. $\mathbf{U}(k)$ is the potential energy as a function of relative momentum k. The intermediate states are assumed to have zero potential energy. $\mathbf{U}(k)$ for occupied states is approximately a quadratic function.

Figure 3. Variation of Λ with k_F. The Fermi momentum k_F is given in units of fm^{-1}. The line indicated by 'a' corresponds to the Bressel potential while 'b' corresponds to the Reid potential.

Figure 4. Variation of m* with k_F. k_F is in units of fm^{-1}. The solid line corresponds to the Bressel potential and the broken line to Reid's.

Figure 5. Average potential energy in MeV due to certain two-body states as a function of Fermi momentum (in fm^{-1}). Reid potential.

Figure 6. Same as figure 5. Bressel potential.

Figure 7. Variation κ with Fermi momentum k_F (in fm^{-1}) calculated from reference wavefunctions but correcting for the "in-sea" states. The solid line corresponds to the Reid Soft Core and the broken line to the Reid Hard Core (also called new core) potential.

Figure 8. Variation of κ with k_F (in fm^{-1}) using exact wavefunctions from KD method. The line 'a' corresponds to the total value of κ for Reid Soft Core while 'b' corresponds to that for Bressel potential. The line 'c' gives the contribution of the dominant S state in $^3S-^3D$ for Reid potential and 'd' gives that for Bressel potential.

Figures 8a, 8b, 8c, 8d. Certain higher order diagrams (described in text) which give some contribution to the binding energy. Figure 8d is known as the hole-hole interaction and is included in Day's treatment of four-body diagrams.

Figure 9. Effective potential (in fm^{-2}) for the state $^1S_0$ is plotted against the radius r (in fm). Curve (a) corresponds to the effective potential derived from Reid potential while (b) corresponds to that from Bressel potential. The right hand scale (also in fm^{-2}) is to be used for the attractive part of (a). These curves correspond to the Fermi momentum k_F=1.36 fm^{-1}.

Figure 9a. Variation of $\frac{V}{V_0}$ with Fermi momentum k_F. V corresponds to the effective potential at a certain density (determined by k_F) and V_0 is that at k_F=1.36 fm^{-1}. Curve 'a' corresponds to a radius r=.24 fm, 'b' to r=.30 fm, 'c' to r=1.84 fm and 'd' to r=.89 fm. Curves 'a' and 'd' correspond to the repulsive and the attractive peaks respectively.

Figure 10. Effective interaction (in fm^{-2}) from super soft potentials of Sprung and Srivastava. r is in units of fm. Curve (a) corresponds to the effective force derived from the potential called PP-2, (b) from SSC, (c) from PP-1 and (d) from NP-2.

Figure 11. Plot of the wave defect χ obtained from three potentials against r (in fm). Curve (a) corresponds to Reid potential, (b) to Bressel potential and (c) to NP-2 of Sprung and Srivastava.

Figure 12. Effective potential (in fm^{-2}) for the state $^3S_1$ plotted against r (in fm). Curve (a) corresponds to k_F=1.36 fm^{-1} and (b) to k_F=.7 fm^{-1}. The right hand scale (also in fm^{-2}) is to be used for the attractive part of the potential. Reid potential has been used.

Figure 13. The ratio $\frac{V}{V_0}$ for the effective $^3S_1$ potential of figure 12 is plotted against k_F (in fm^{-2}) for

Figure 13. cont'd.
different values of radius r. The values of r chosen lie in the repulsive part of the potential. Curve (a) corresponds to r=.4 fm, (b) to r=.3 fm, and (c) to r=.2 fm. The broken line is for r=.49 fm. Here again V corresponds to potential at a certain density and V_0 that at k_F=1.36 fm^{-1}. The analytical formula given in the text tries to fit curve (b).

Figure 14. Same as figure 13, but for those values of r which are in the attractive region. Curve (a) for r=.79 fm, (b) for r=.94 fm, (c) for 1.09 fm, (d) for r=1.19 fm and the broken line for r=1.34 fm.

Figure 15. Effective residual tensor force (in fm^{-2}) is plotted against r (in fm). Curve (a) corresponds to k_F=.7 fm^{-1} and (b) to k_F=1.36 fm^{-1}. Reid potential.

Figure 16. The ratio $\frac{V}{V_0}$ for the residual tensor force of figure 15 is plotted against k_F (in fm^{-1}). V and V_0 have the same meaning as before. The upper 4 curves correspond to repulsive part of the potential. (a) corresponds to r=.30 fm, (b) to r=.28 fm, (c) to r=.22 fm and (d) to r=.16 fm. The broken line is the fitted curve. The lower four lines correspond to the attractive

Figure 16. cont'd.

part of the potential. (e) to r=.99 fm, (f) to r=.79 fm, (g) to r=.74 fm and (h) to .69 fm. The broken line is the fitted curve.

Figure 17. Effective $^1P_1$ potential (in fm^{-2}) from Reid potential is plotted against r (in fm). Curve (a) is for k_F=1.36 fm^{-1} and (b) for k_F=.7 fm^{-1}.

Figure 18. The ratio $\frac{V}{V_0}$ for the $^1P_1$ potential of figure 17 is plotted against k_F (in fm^{-1}). Curve (a) corresponds to r=.84 fm, (b) to r=.64 fm, (c) to r=.3 fm and (d) to r=.22 fm. The broken line is the fitted curve.

Figure 19. Effective $^3S_1$ potential (in fm^{-2}) from Bressel potential is plotted against r (in fm). The lower scale is for the attractive part only. Curve (a) corresponds to k_F=.7 fm^{-1} and (b) to k_F=1.36 fm^{-1}.

Figure 20. The ratio $\frac{V}{V_0}$ for the ^3S_L potential of figure 19 is plotted against k_F (in fm^{-1}). The lower 2 curves are for the repulsive peak and the upper 2 for attractive peak. Curve (a) corresponds to r=.7189 fm, (b) to r=.806 fm, (c) to r=.663 fm and (d) to r=.5617 fm. The broken lines are fitted curves for these two regions.

Figure 21. The effective residual tensor force (in fm^{-2}) from Bressel potential is plotted against r

Figure 21. cont'd.

(in fm). The curve (a) is for k_F=.7 fm^{-1} and (b) for k_F=1.36 fm^{-1}. The potential still contains a factor of $\sqrt{8}$ which is the matrix element of S_{12}.

Figure 22. The ratio $\frac{V}{V_0}$ for the effective tensor force of figure 21 is plotted against k_F (in fm^{-1}). Curve (a) is for r=.6632 fm, (b) for r=.5995 fm, (c) for r=1.155 fm. The broken line is the fitted curve.

Figure 23. Effective $^1P_1$ potential (in fm^{-2}) from Bressel potential is plotted against r (in fm). Curve (a) is for k_F=1.36 fm^{-1} and (b) for k_F=.7 fm^{-1}.

Figure 24. The ratio $\frac{V}{V_0}$ for the $^1P_1$ potential of figure 23 is plotted against k_F. Curve (a) is for r=.784 fm, (b) for r=.7189 fm, (c) for r=.5278 fm and (d) for r=.3924 fm. The broken line is the fitted st. line.

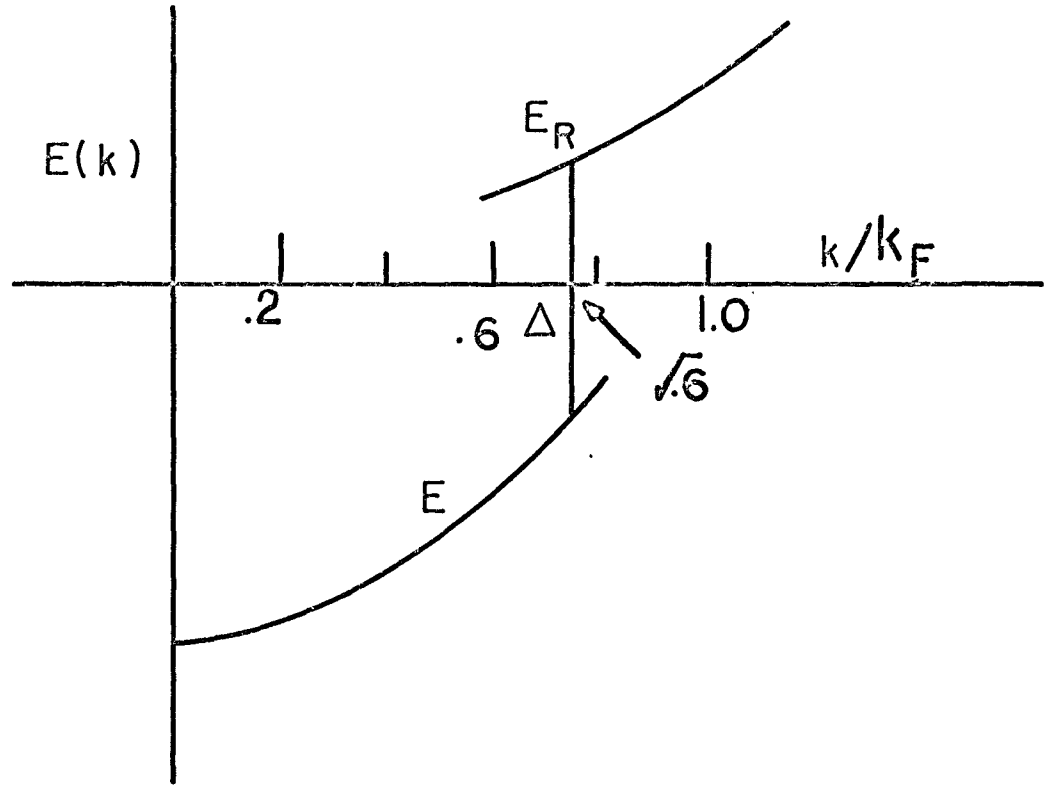

Figure 1

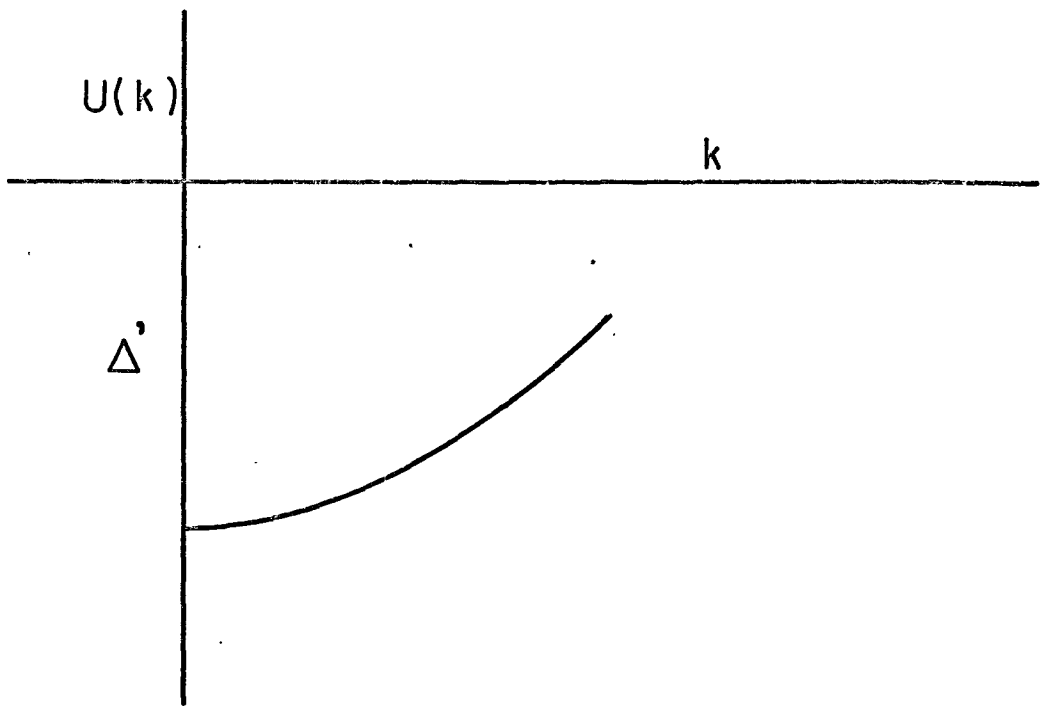

Figure 2

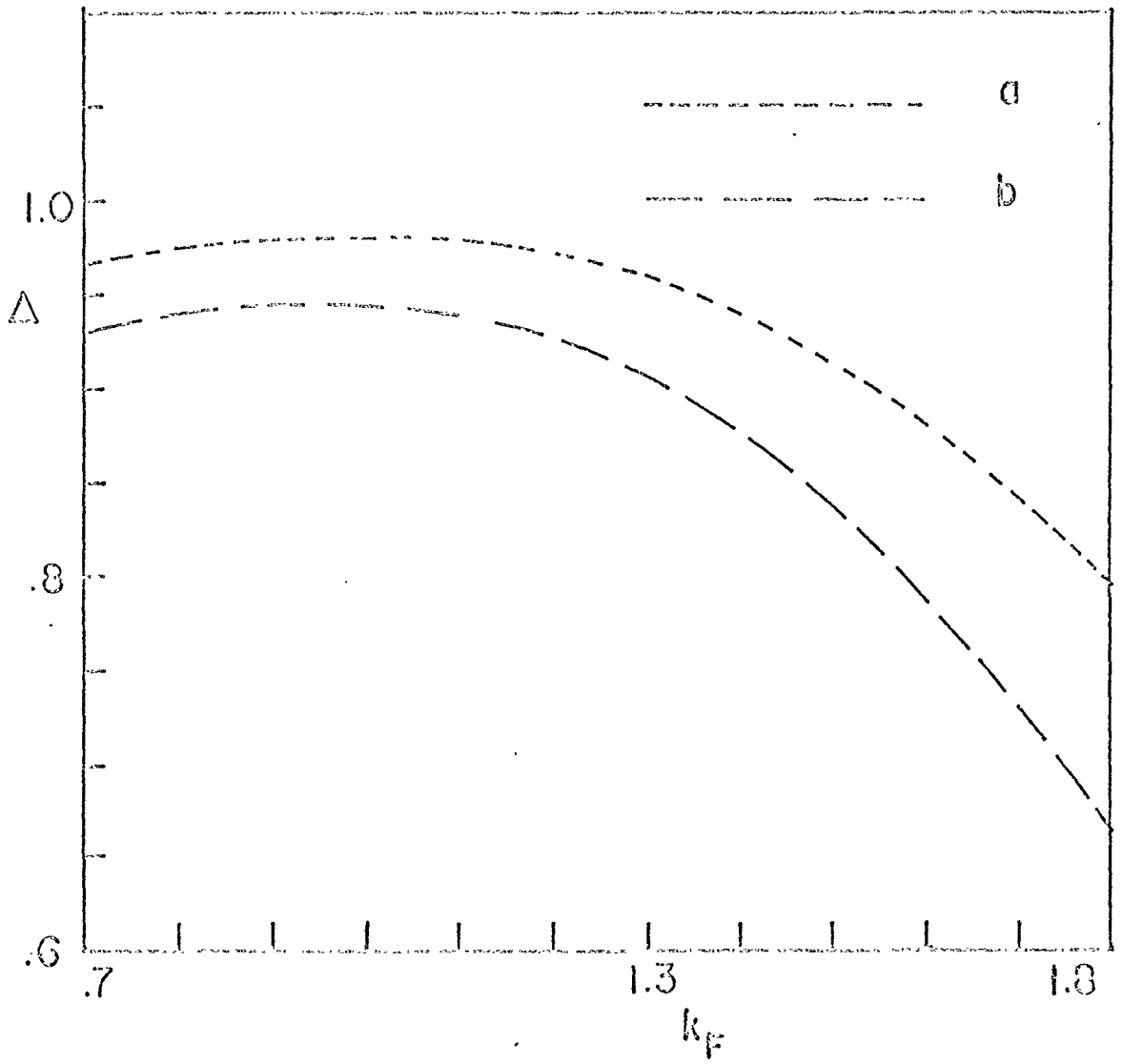

Figure 3

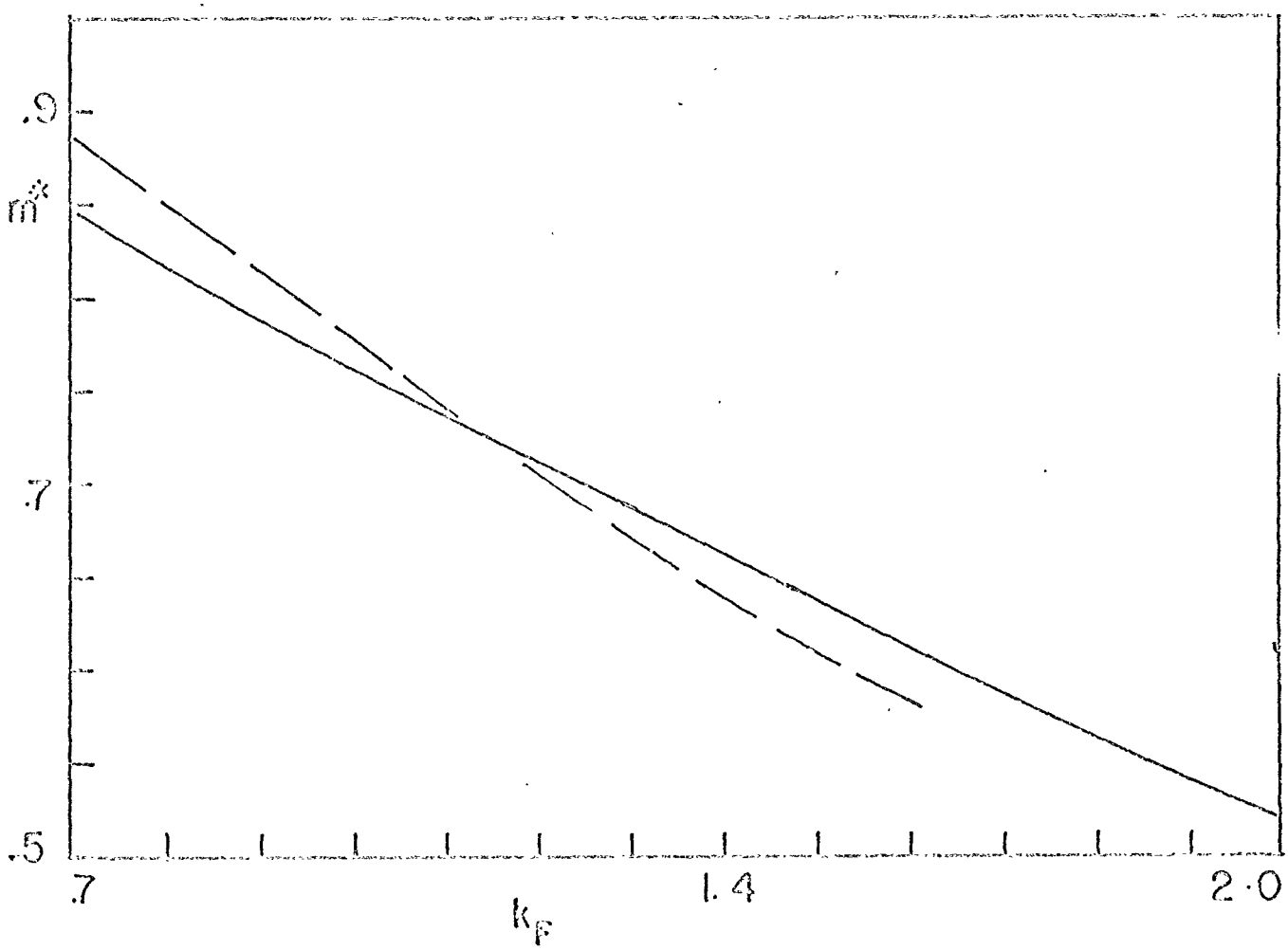

Figure 4

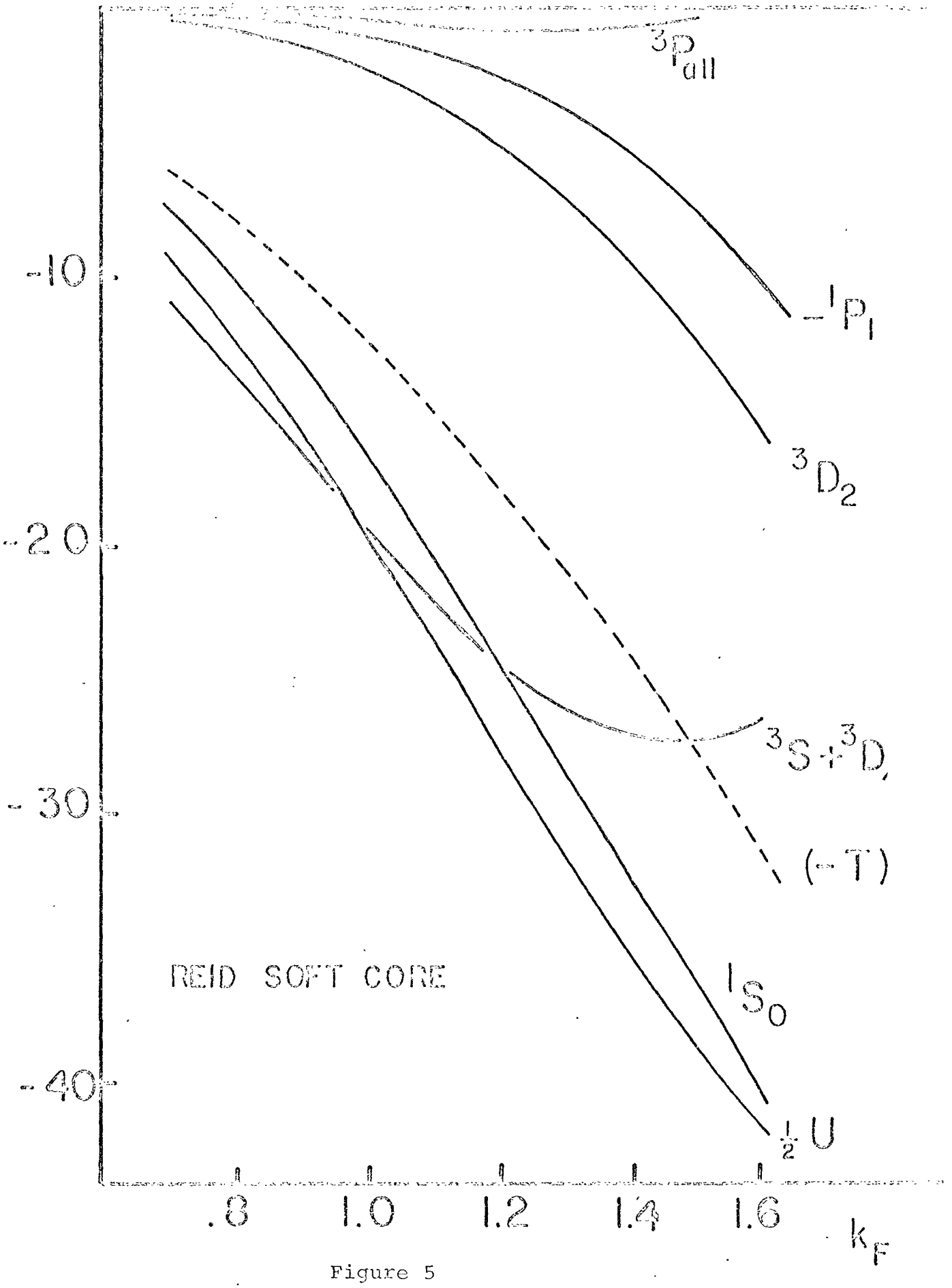
$^3P_{all}$
$^1P_1$
$^3D_2$
$^3S+^3D_1$
(-T)
$^1S_0$
$\frac{1}{2}U$
REID SOFT CORE
-10
-20
-30
-40
.8
1.0
1.2
1.4
1.6
k_F

Figure 5

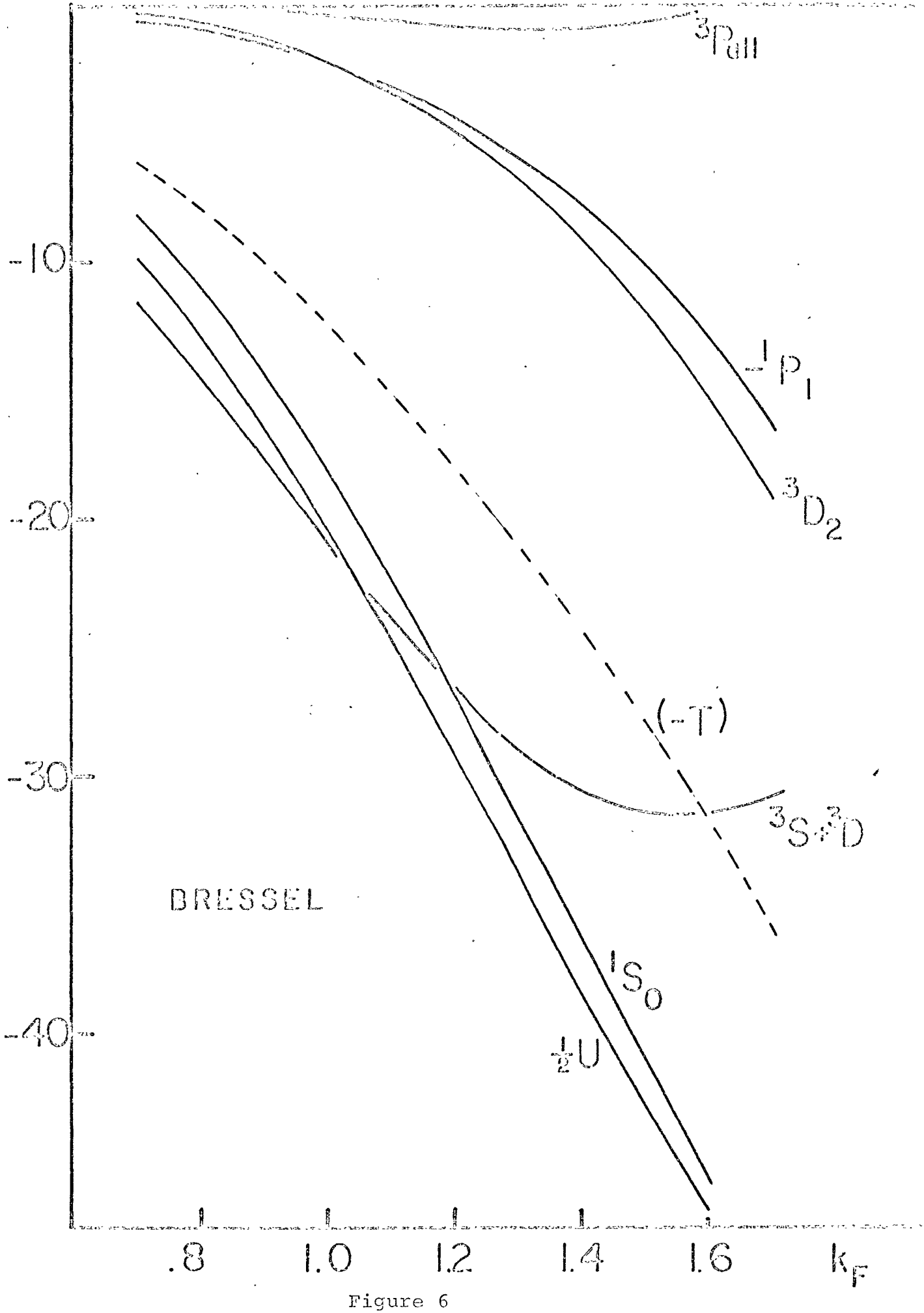
$^3P_{III}$
$^1P_1$
$^3D_2$
(-T)
$^3S+^3D$
BRESSEL
$^1S_0$
$\frac{1}{2}U$
-10
-20
-30
-40
.8
1.0
1.2
1.4
1.6
k_F

Figure 6

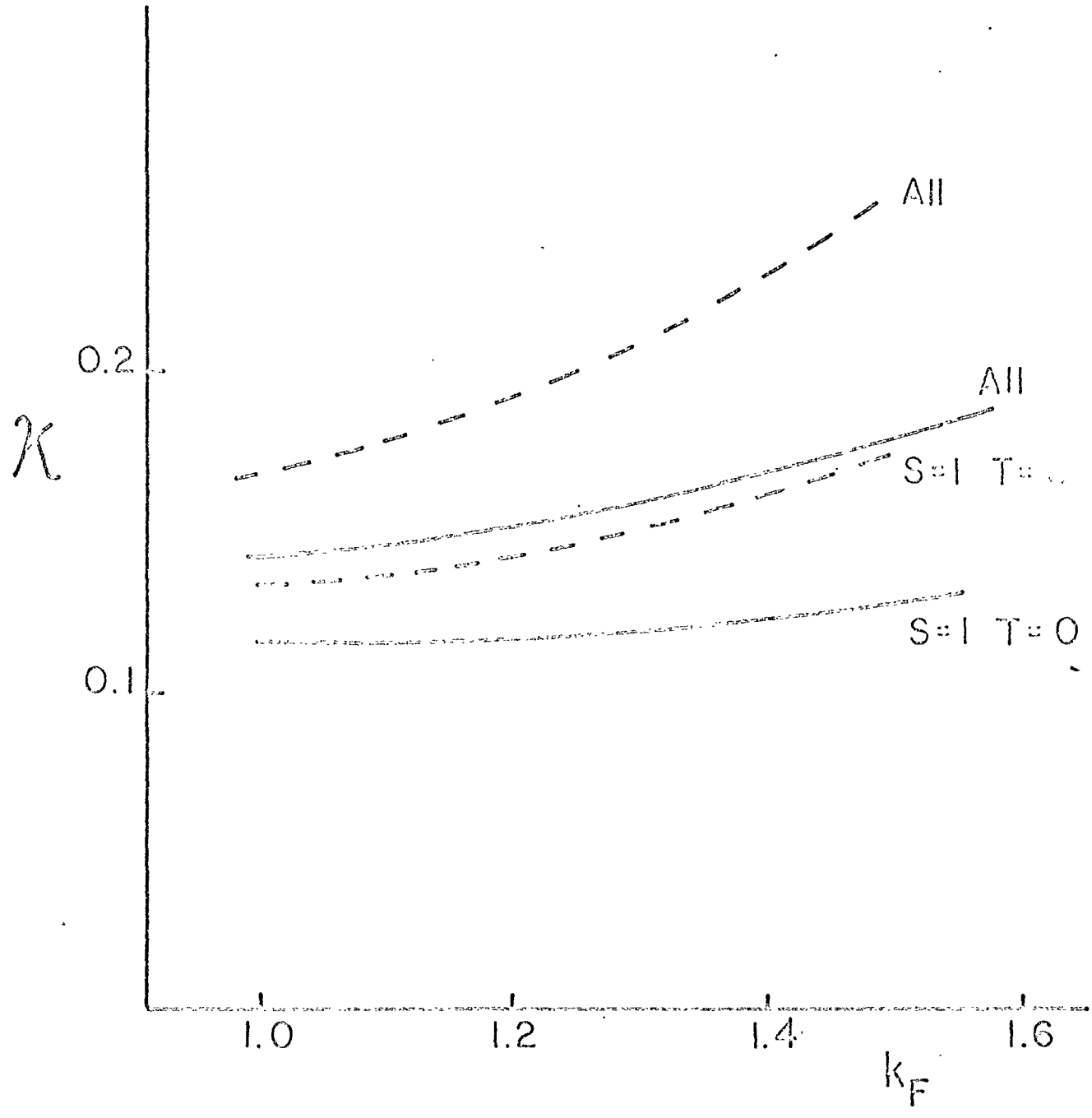

Figure 7

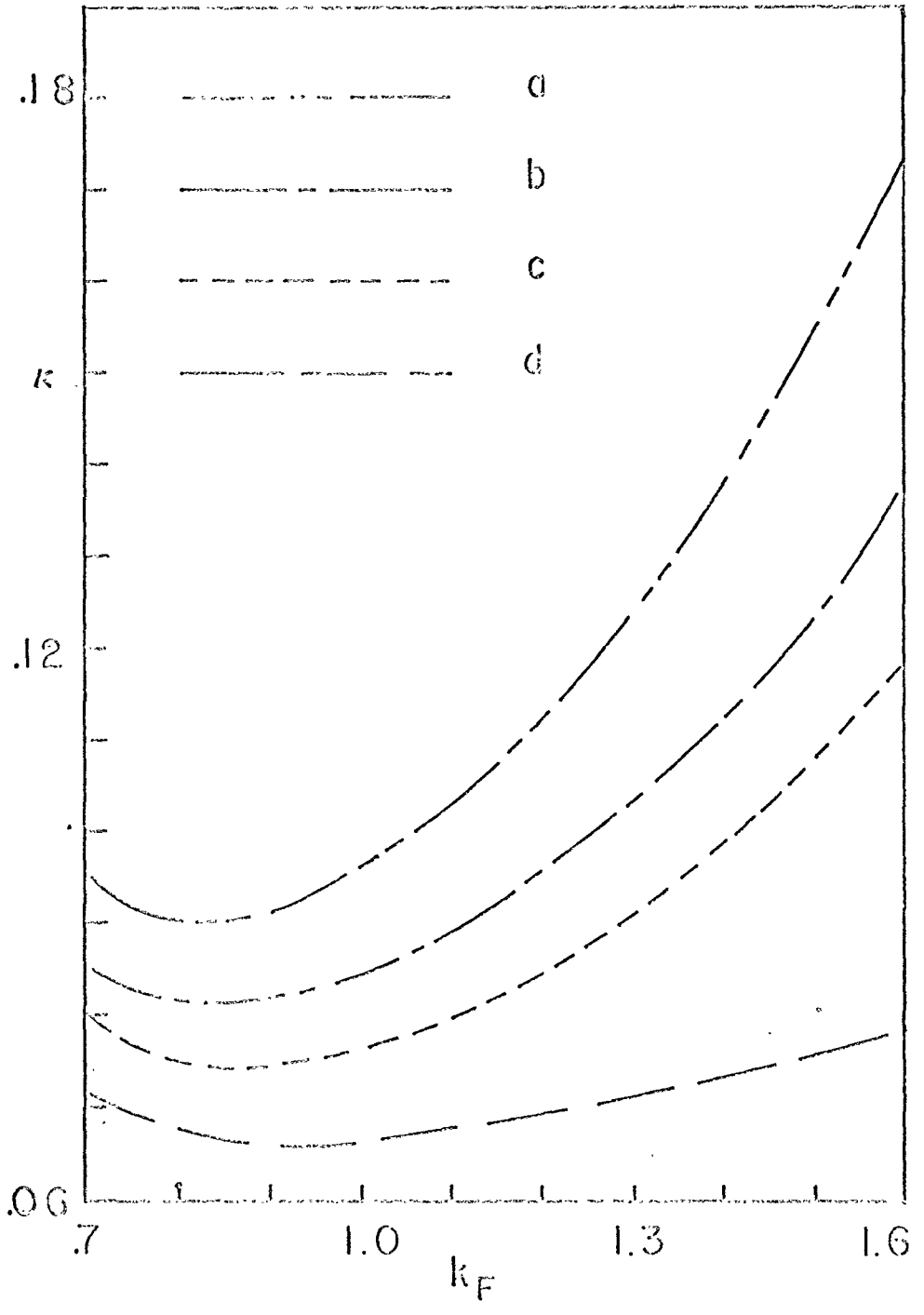

Figure 8

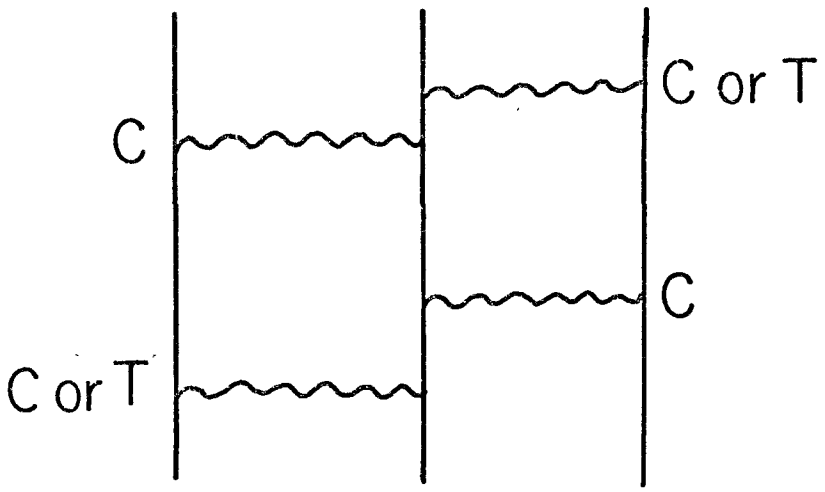

Figure 8a

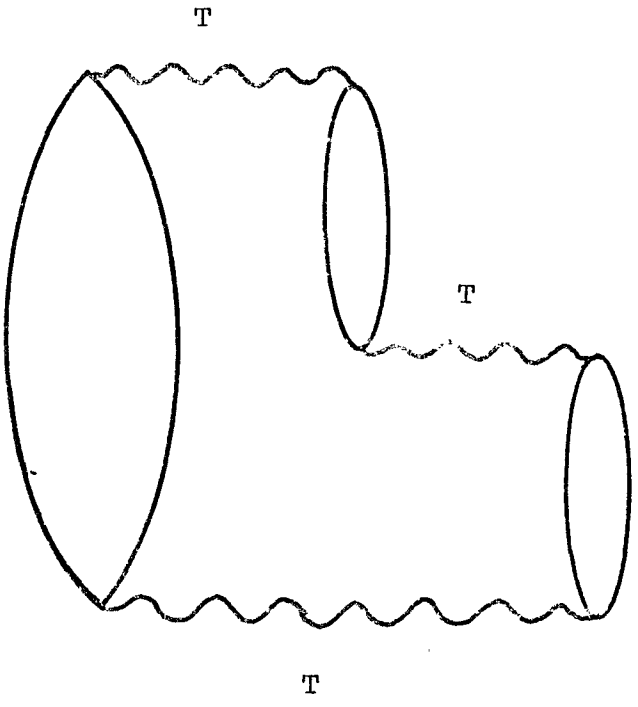

Figure 8b

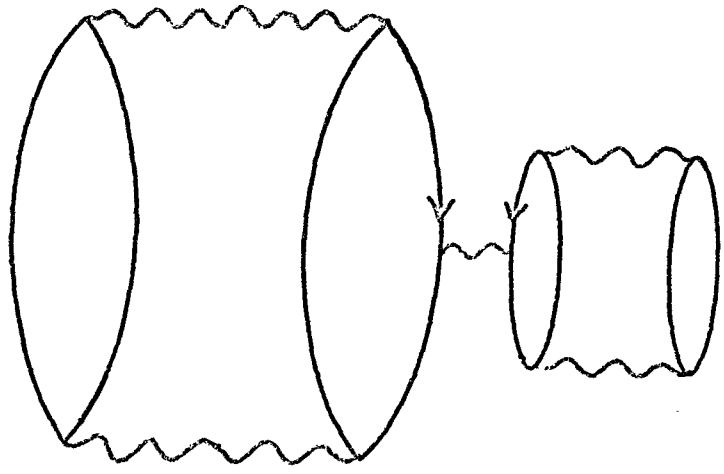

Figure 8c

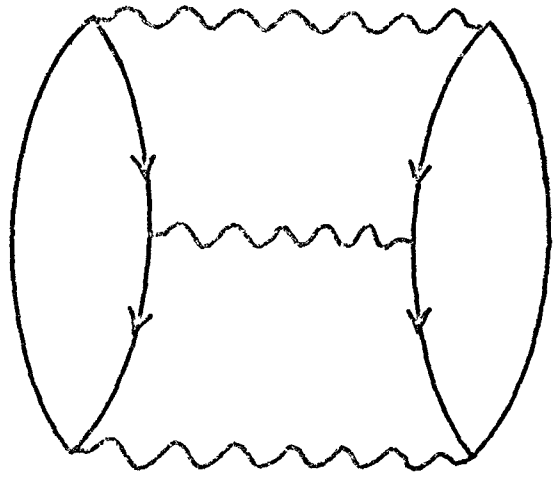

Figure 8d

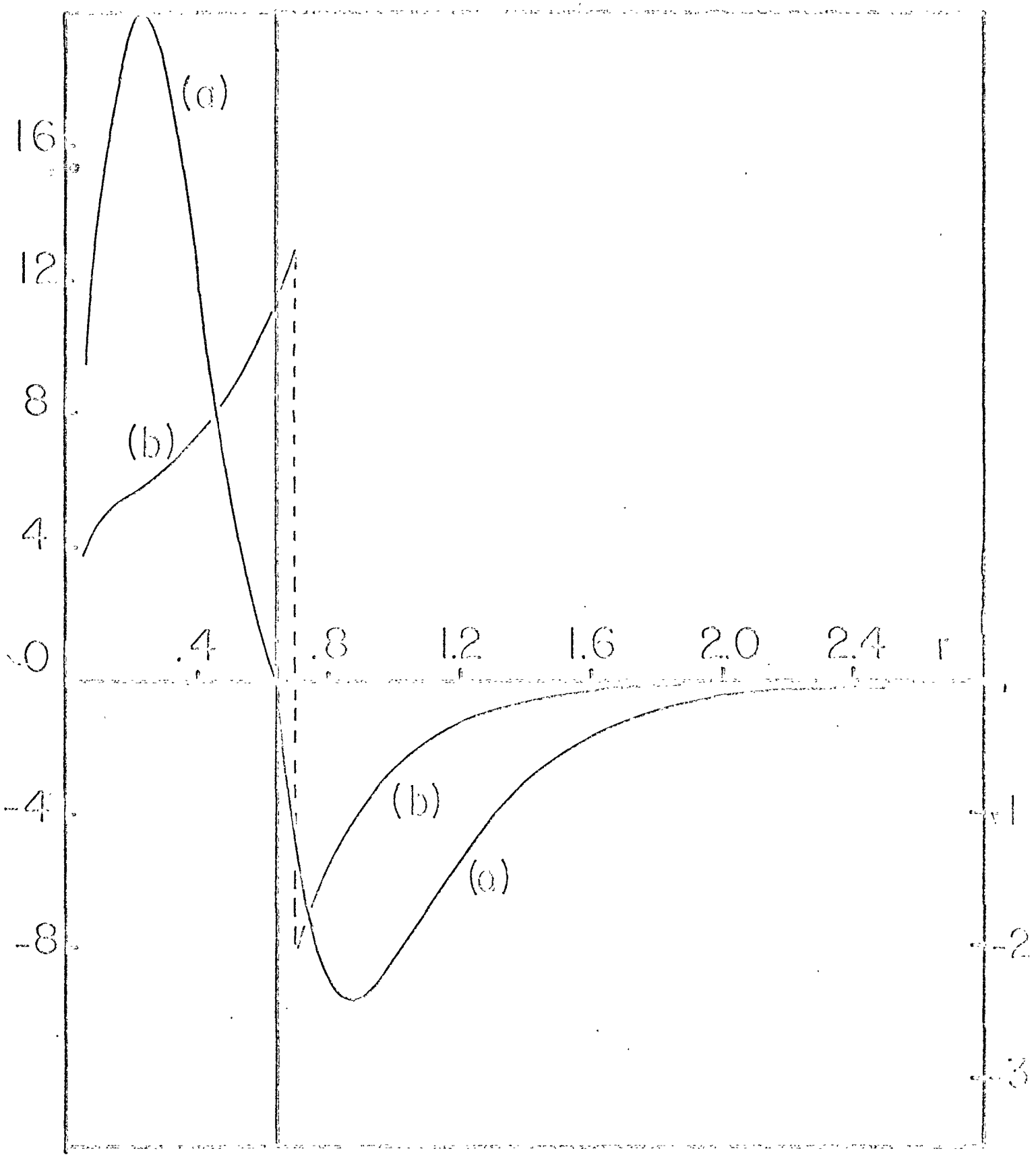

Figure 9

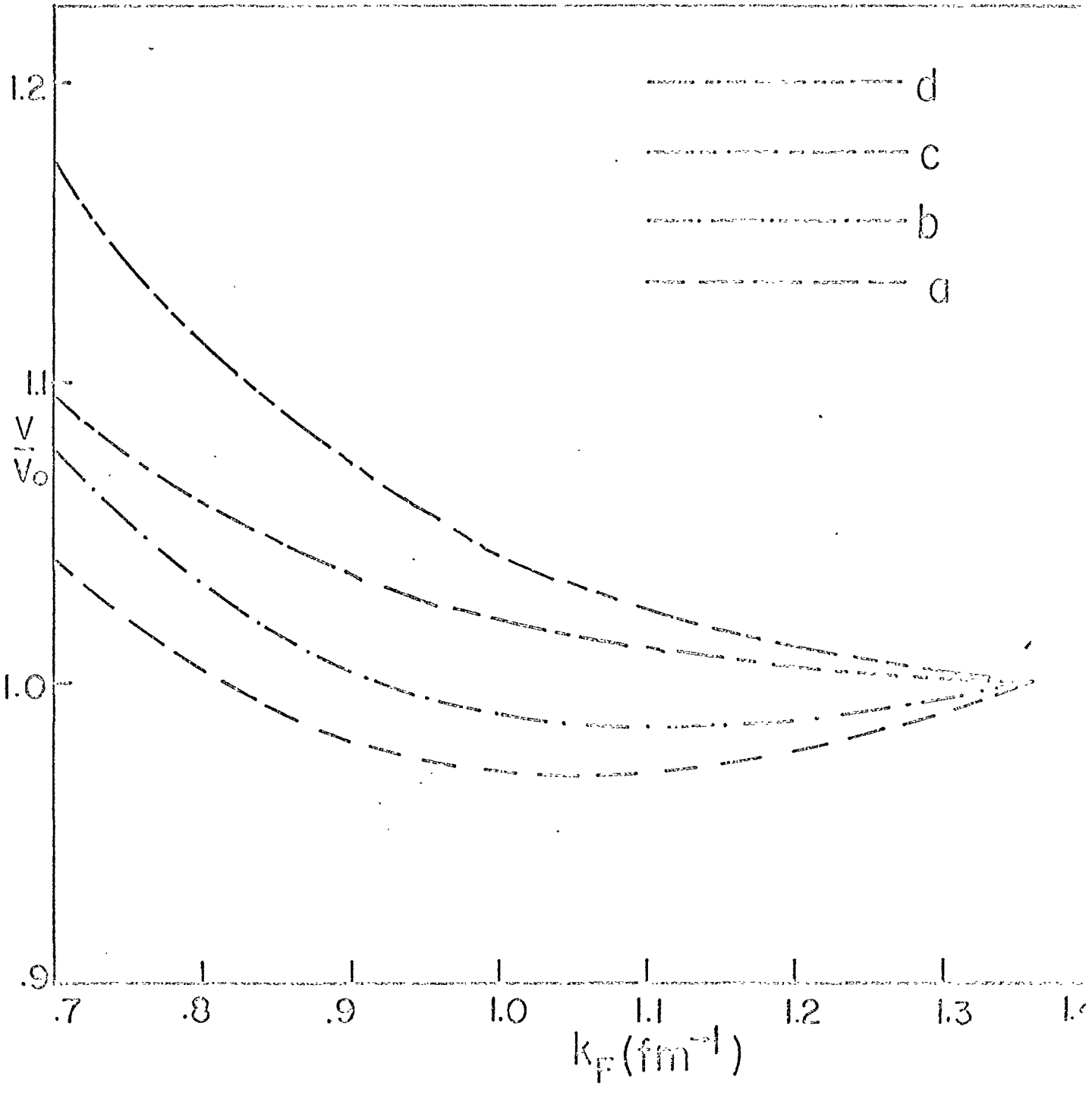

Figure 9a

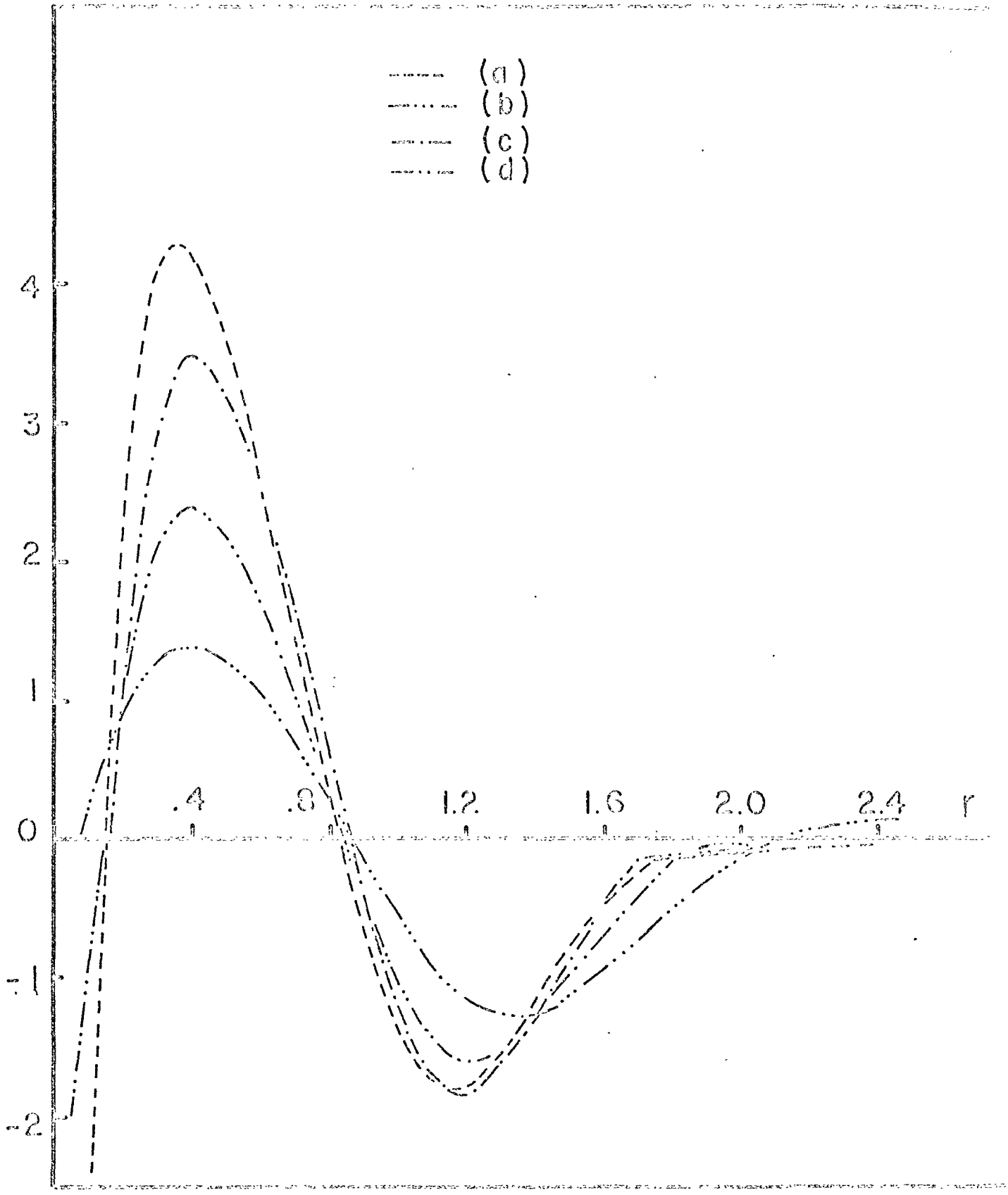

Figure 10

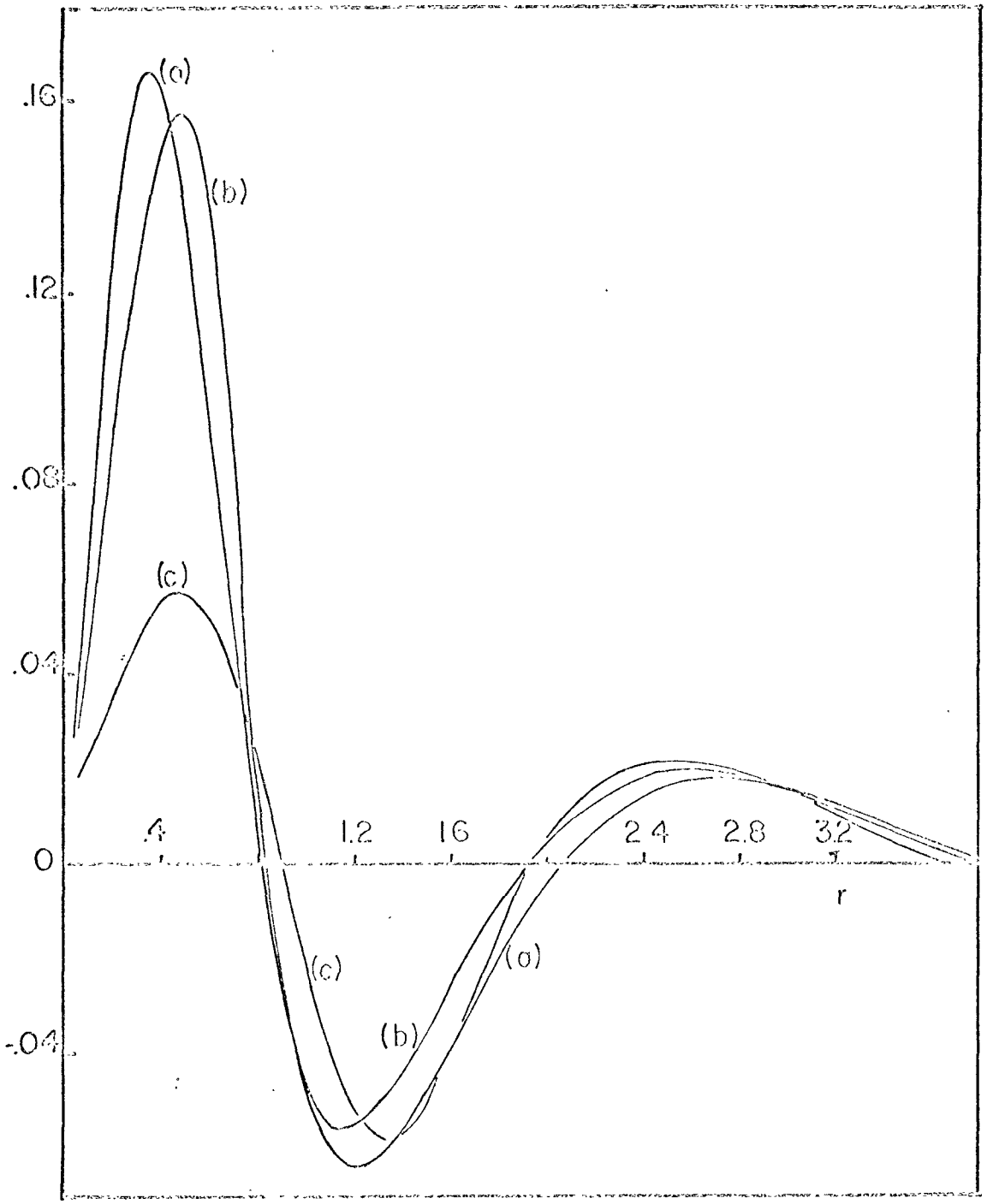

Figure 11

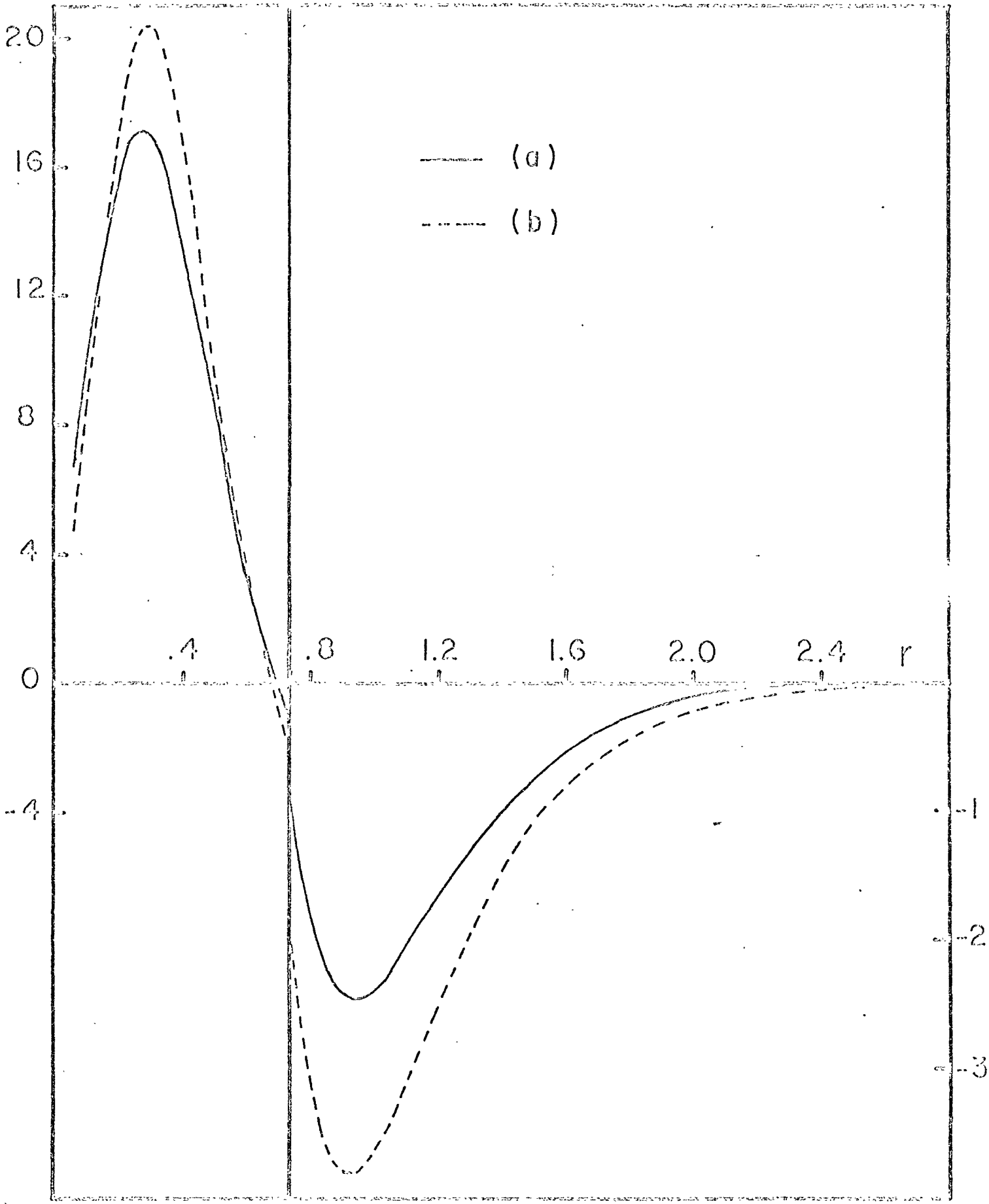

Figure 12

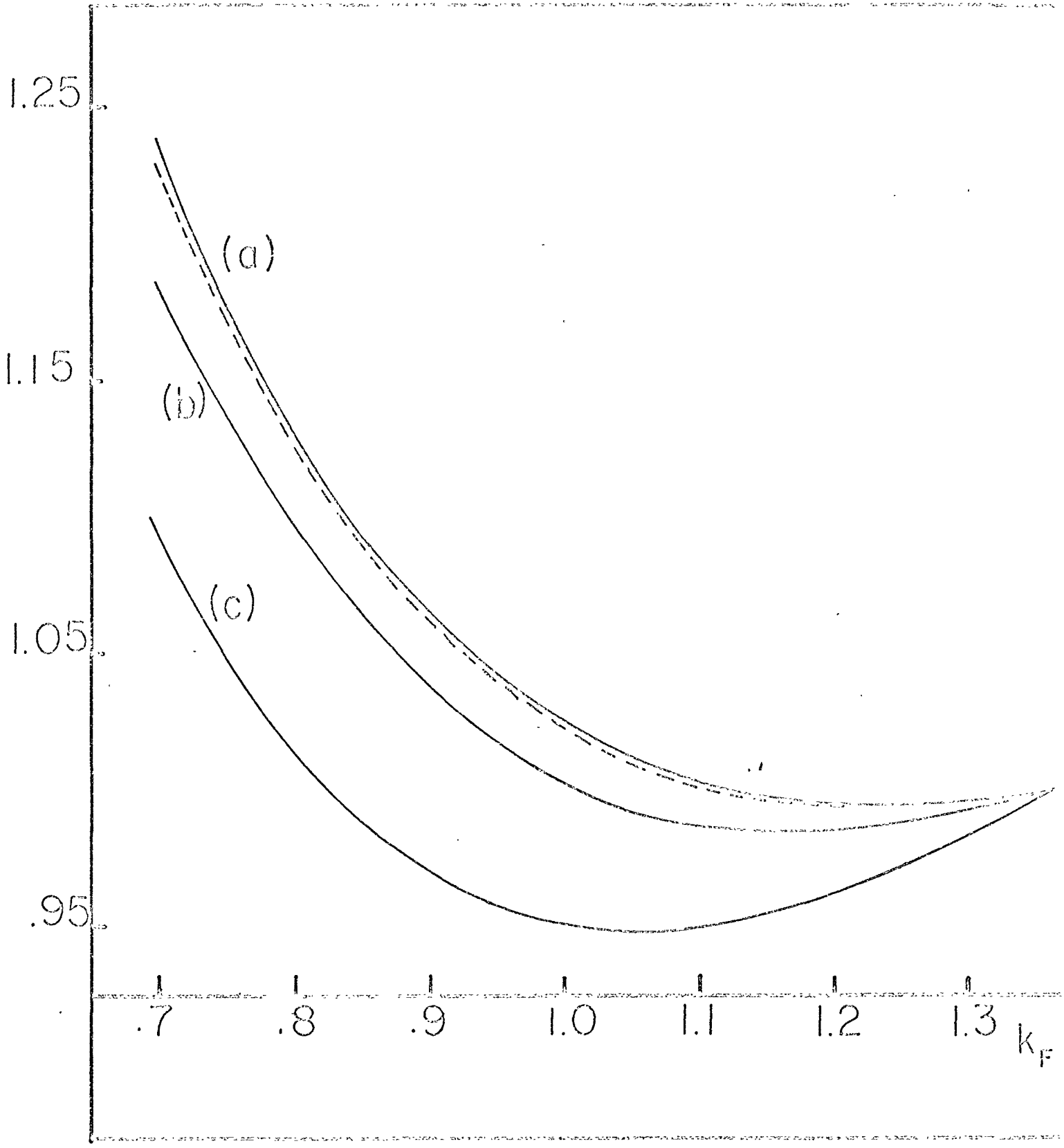

Figure 13

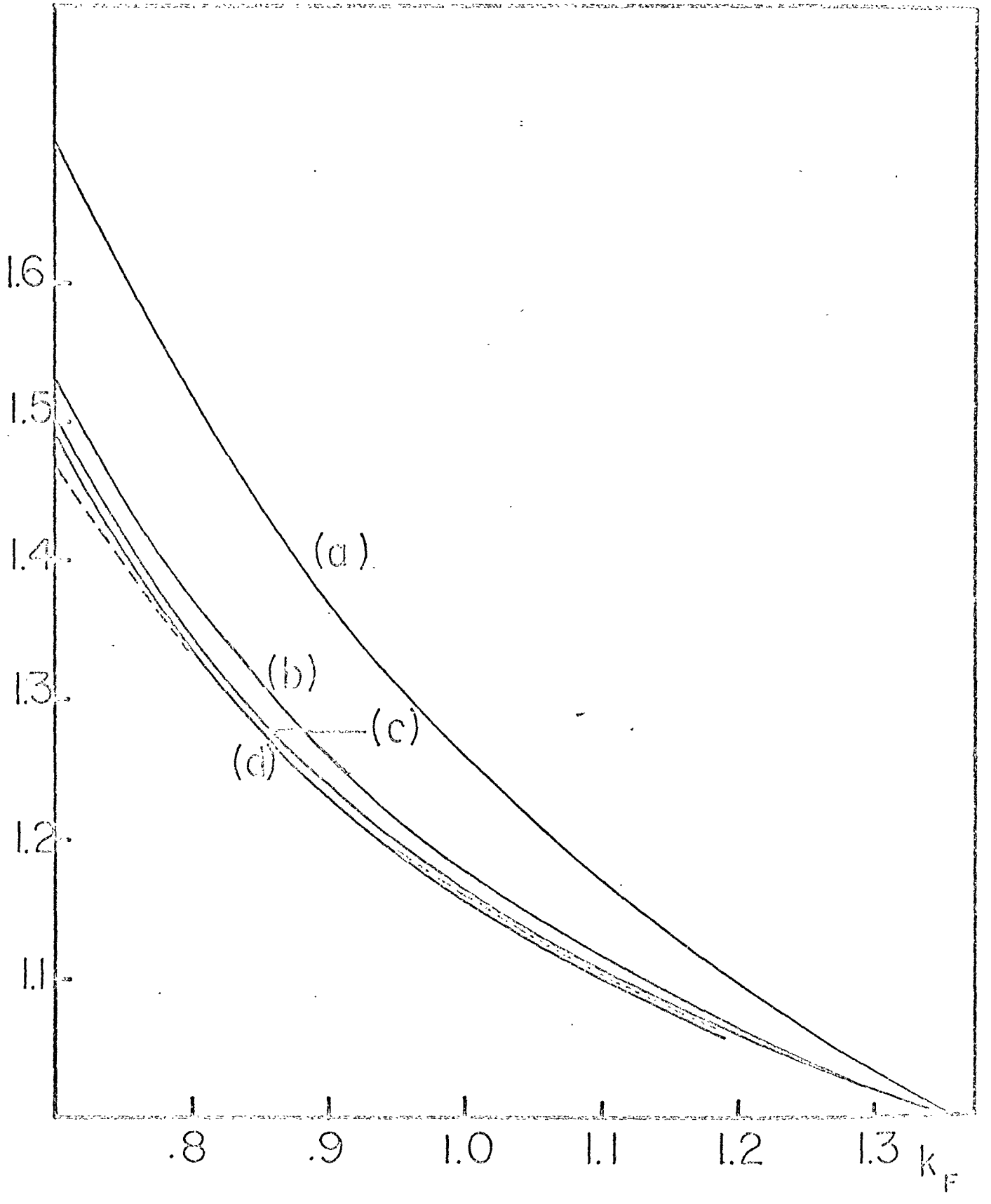

Figure 14

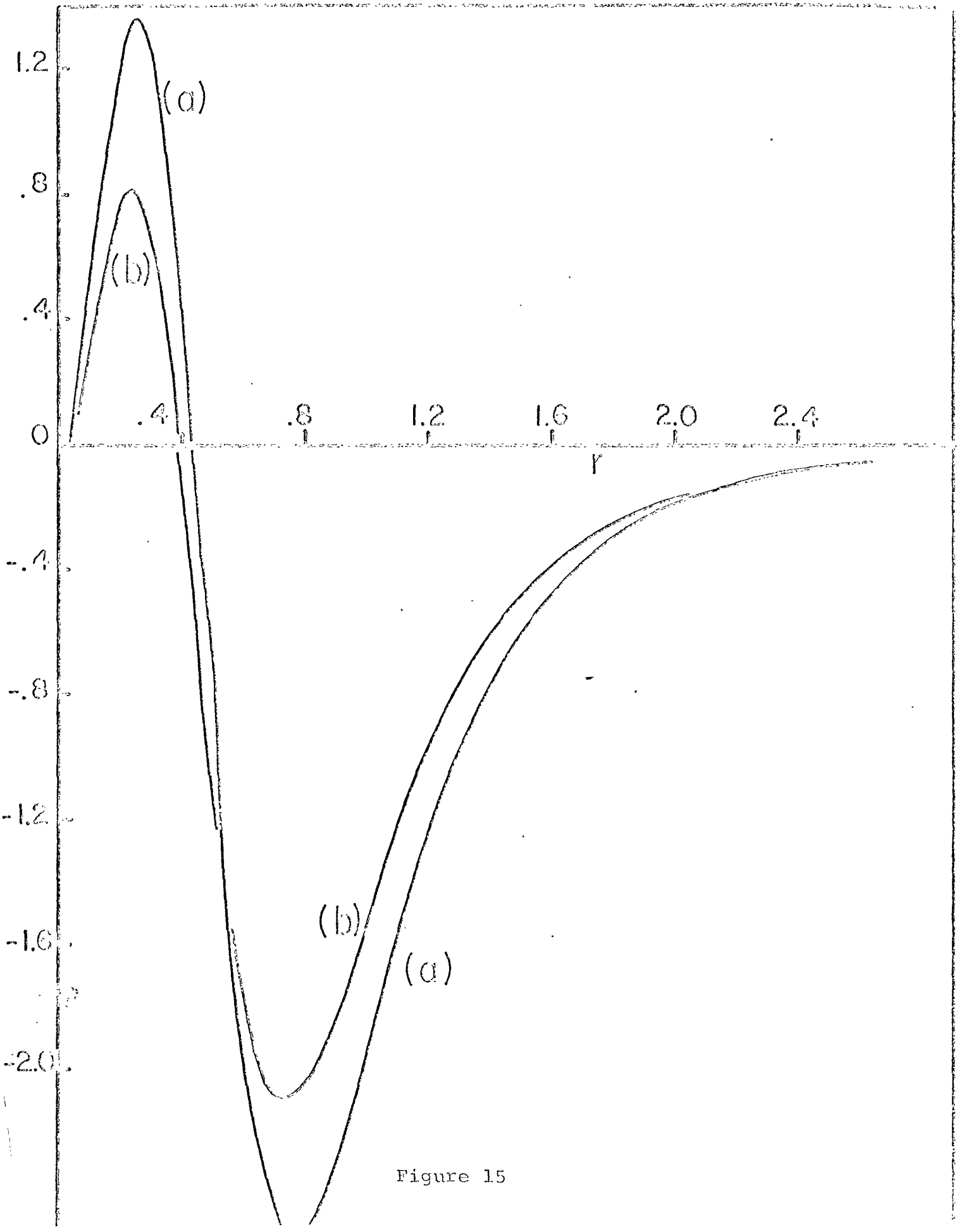

Figure 15

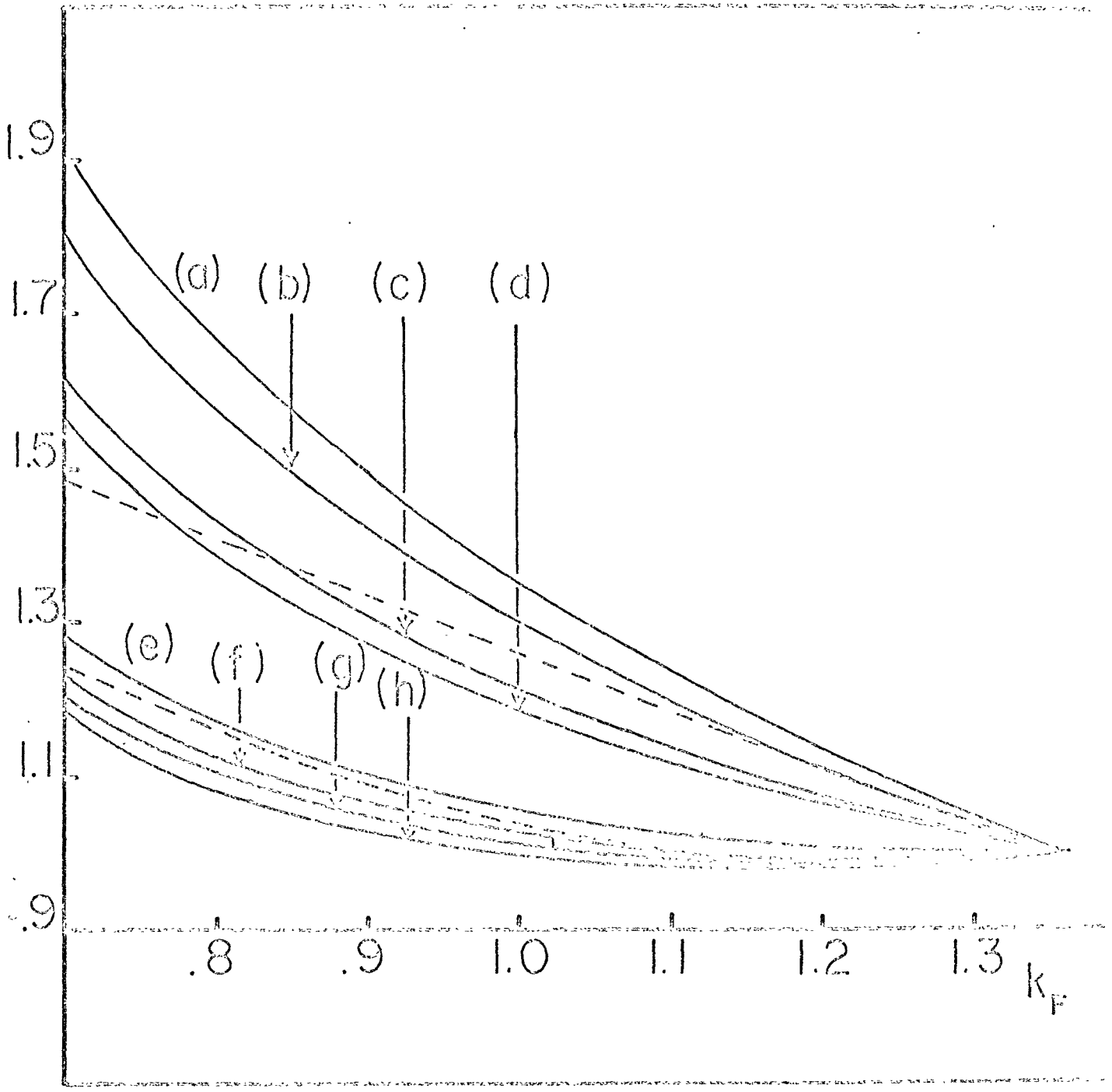

Figure 16

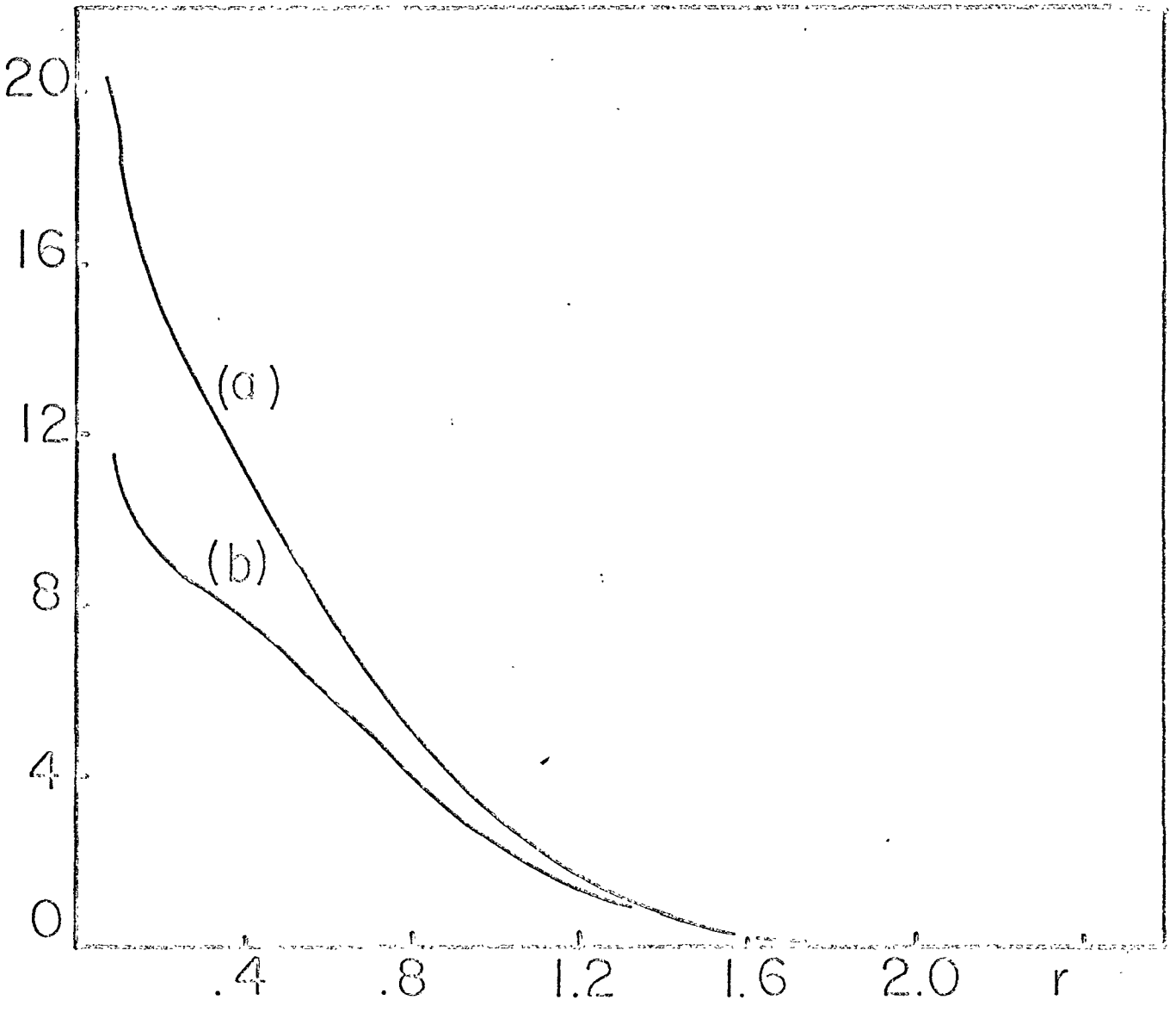

Figure 17

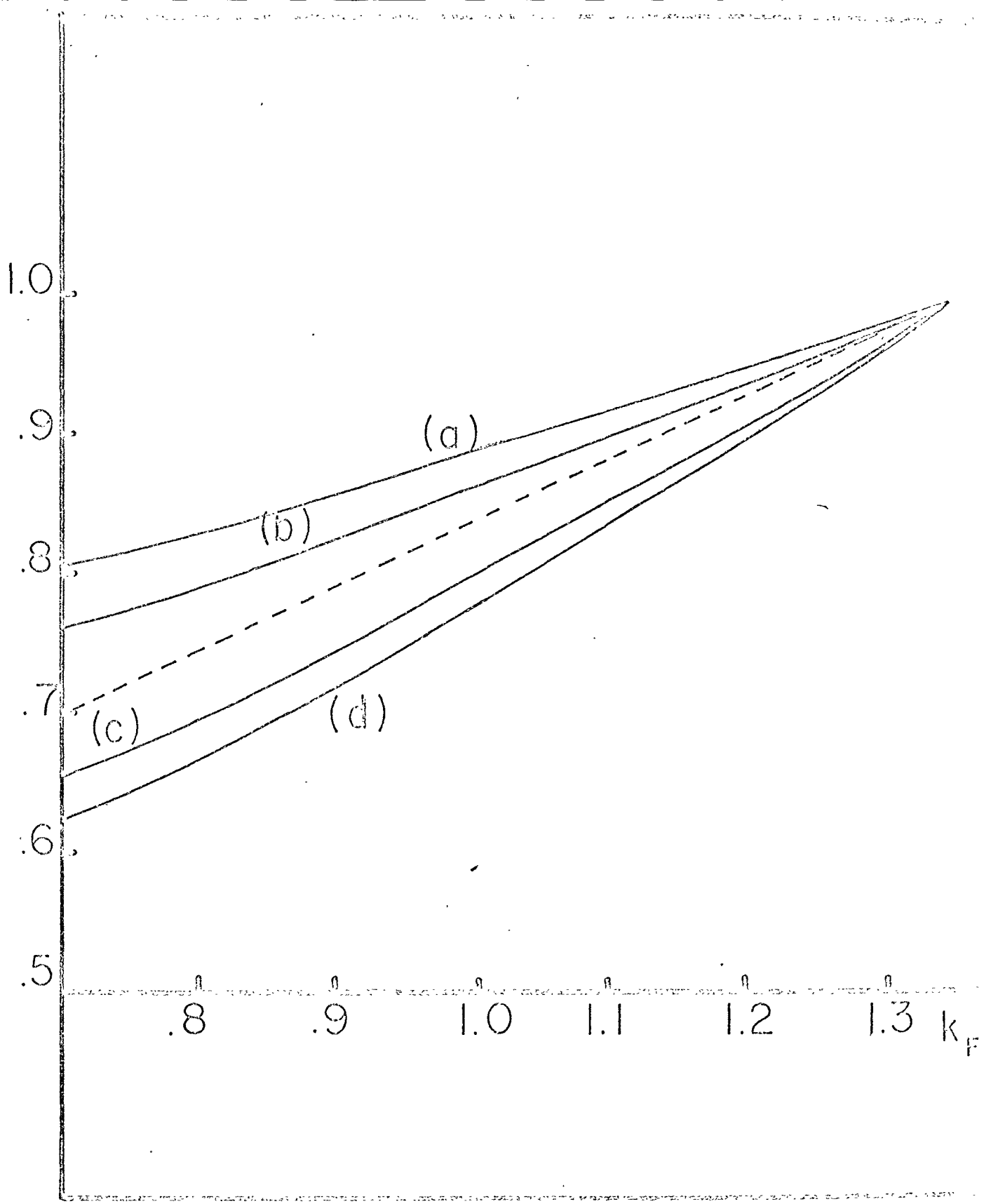

Figure 18

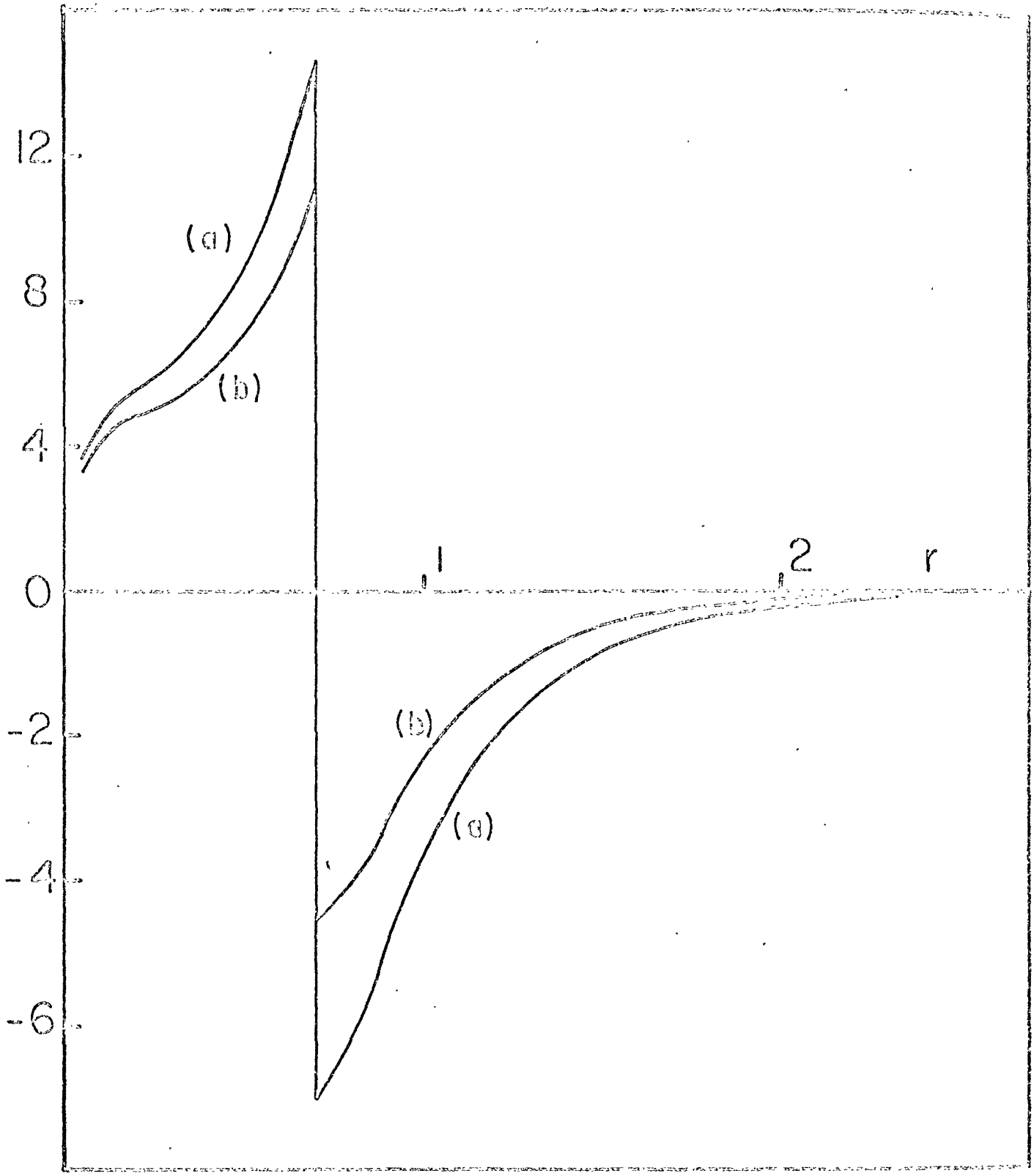

Figure 19

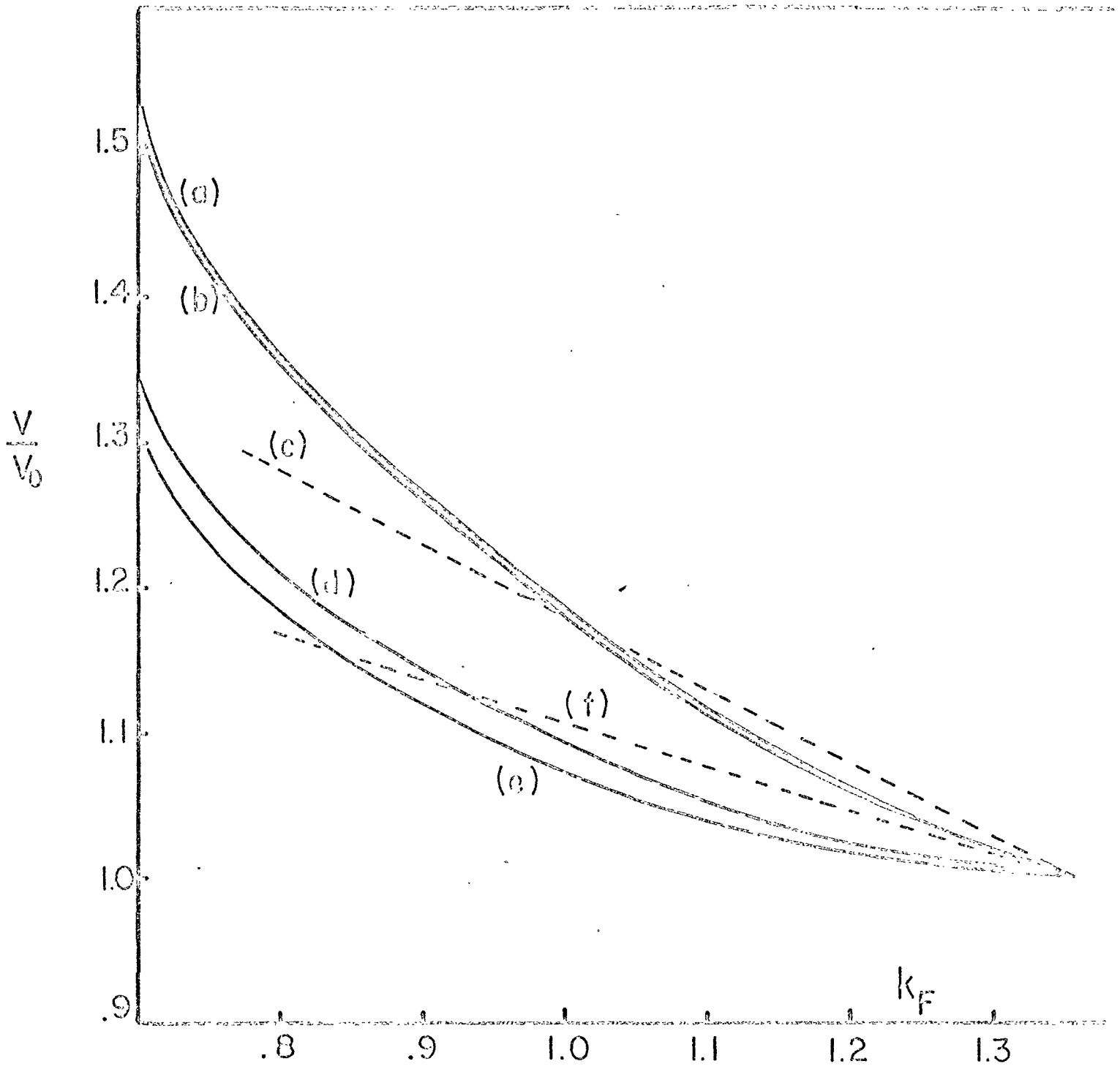

Figure 20

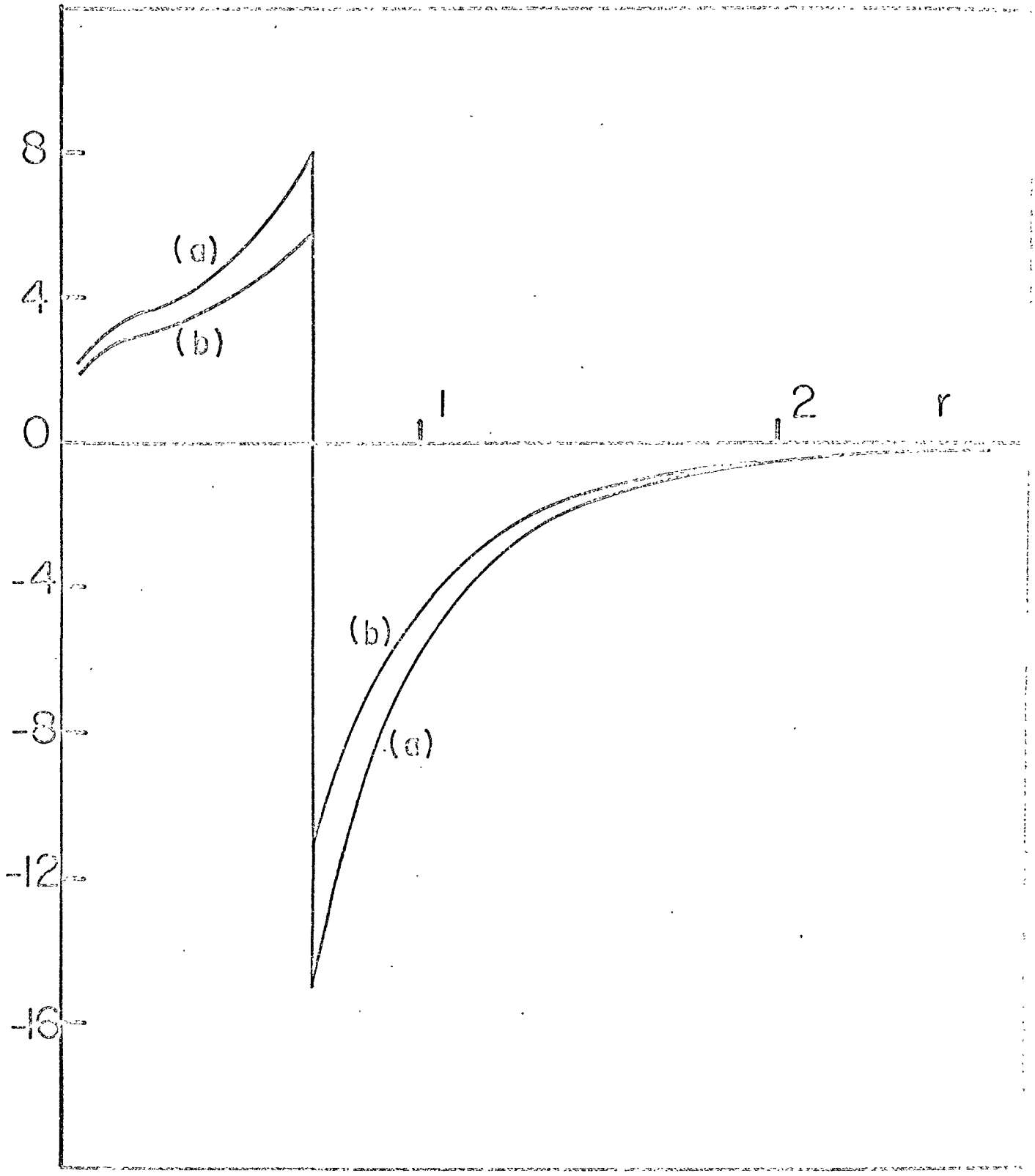

Figure 21

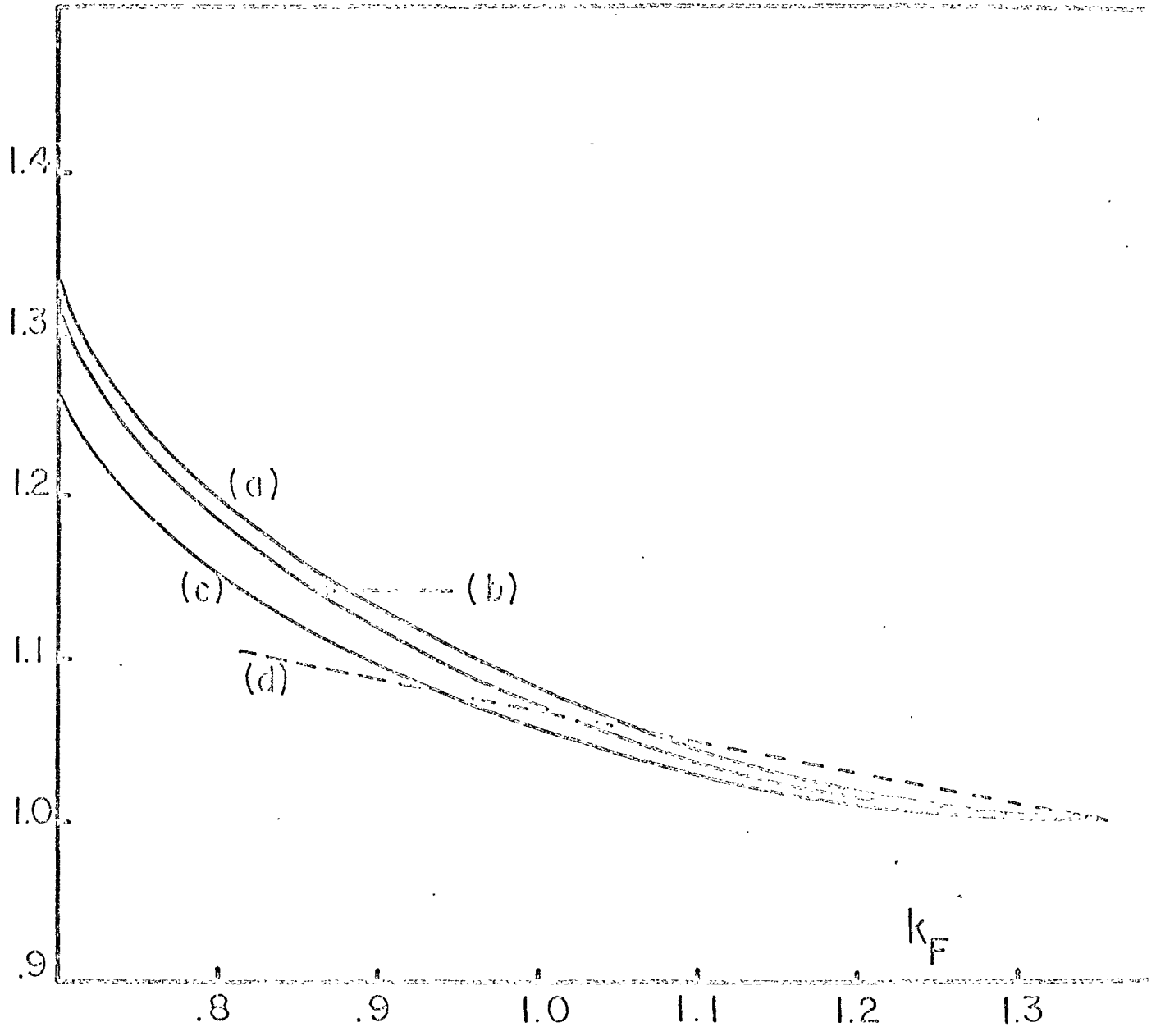

Figure 22

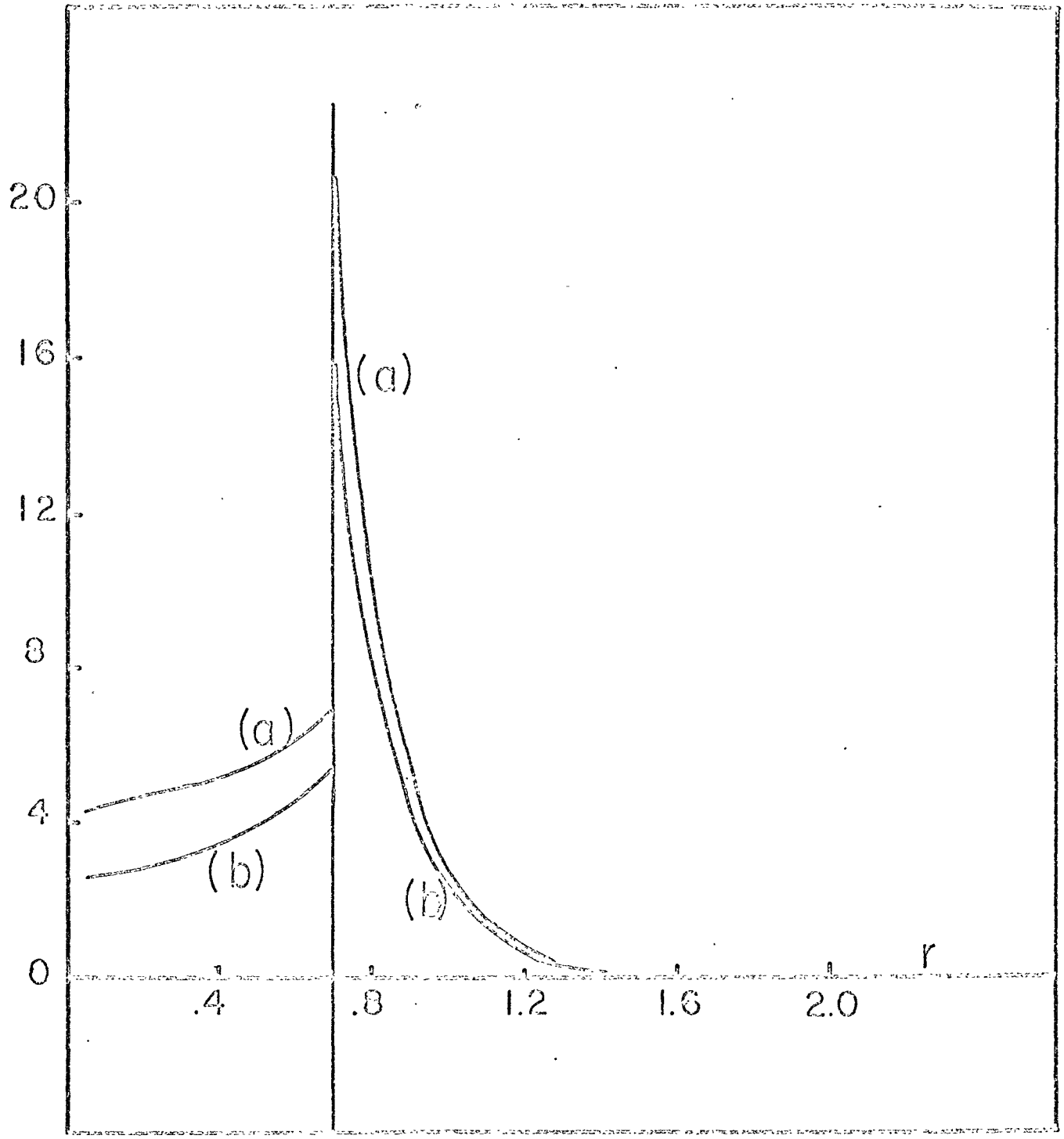

Figure 23

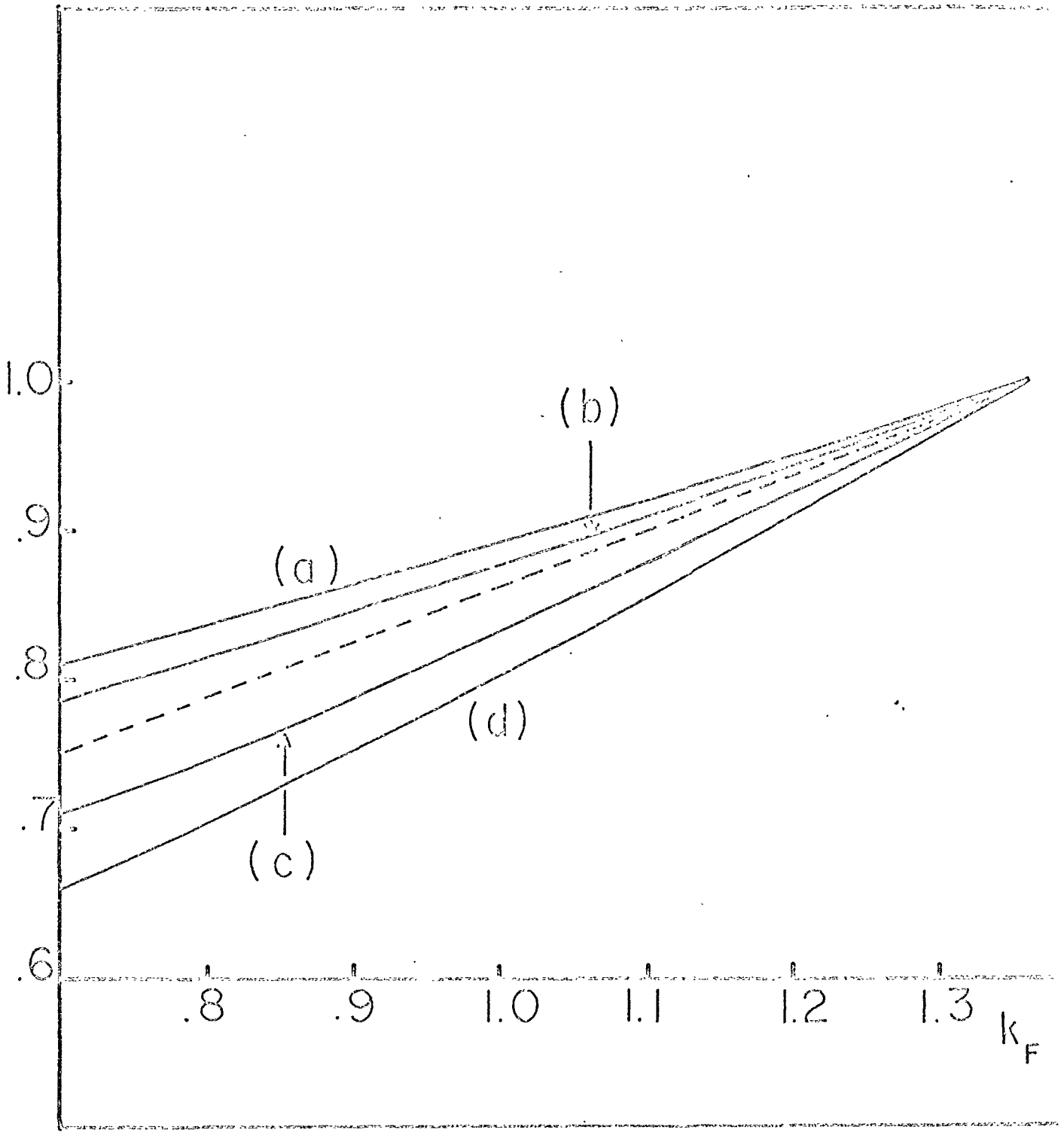

Figure 24